universität
wien

# DIPLOMARBEIT

## An *in vivo* RNAi Approach to study Gene Function in Hematopoiesis

Verfasserin

Marie-Theres Tazreiter

angestrebter akademischer Grad

Magistra der Naturwissenschaften (Mag. rer. nat.)

| Wien, 2011 | |
|---|---|
| Studienkennzahl | A490 |
| Studienrichtung | Diplomstudium Molekulare Biologie |
| Betreuer | Prof. Dr. Josef M. Penninger |

# Abstract

Hematopoiesis is a developmental process in which hematopoietic stem cells give rise to a variety of blood cell types with different morphologies and diverse functions [Tavian et al., 2010]. The hematopoietic compartment is a highly dynamic system composed of relatively short-lived cells of which millions are newly generated by the bone marrow every day and thus needs to be tightly regulated by a fine balance between proliferation, differentiation and apoptosis [Dingli and Pacheco, 2010]. Consequently, deregulation of hematopoietic differentiation or homeostasis builds the basis for various hematopoietic disorders such as lymphomas, leukemias or autoimmune diseases [Kondo et al., 2003].

Using blood cell-specific RNAi silencing in *Drosophila* larvae, a screen of evolutionarily conserved genes for hematopoiesis identified 356 genes implicated in blood cell homeostasis in the fly [Elling et al., unpublished]. The genes causing the strongest phenotypes, namely "fly leukemia" characterized by marked overproliferation of macrophage-like plasmatocytes and formation of melanotic tumors, included amongst others the protease inhibitor Papilin, two transcriptional co-regulators called Symplekin and Ssrp1 as well as several genes involved in the regulation of endocytosis: the small GTPase Rab5a, the SNARE protein Stx7 and the two HOPS/CORVET complex subunits Vps16 and Vps33a. In order to characterize the relevance of these identified factors in the mammalian hematopoietic system *in vivo*, we applied a bone marrow chimeric approach to test the hematopoietic potential of bone marrow cells with down-regulated expression of either of these genes.

The knock-down of three of the analyzed genes, namely Symplekin, Rab5a and Vps16, resulted in an increase of either mature or immature myeloid cells in lethally-irradiated recipient mice, while promoting a decreased percentage of lymphoid B- or T-cells, indicating an impairment of lineage decision in favor of the myeloid lineage. Moreover, the down-regulation of the same genes in bone marrow cells was associated with an elevated percentage of innate natural killer cells in the spleens of transplanted mice. Analysis of the hematopoietic compartment of Papilin mutant mice revealed that these mice harbor decreased numbers of granulocytes in the peripheral blood which correlated with a significant reduction in the percentage of c-kit$^+$ myeloid precursor cells in the bone marrow. These data indicate that the conserved factors identified to regulate proliferation and homeostasis of blood cells in the fruit fly *Drosophila melanogaster* directly translate into conserved mammalian genes involved in hematopoiesis.

# Zusammenfassung

Hämatopoiese beschreibt den entwicklungbiologischen Vorgang der Differenzierung hämatopoetischer Stammzellen zu den verschiedenen Blutzellytpen [Tavian et al., 2010]. Aufgrund der Kurzlebigkeit von Blutzellen, müssen täglich mehrere Millionen Blutzellen neu vom Knochenmark gebildet werden. Dieser hohe "Turnover" erfordert ein stetiges Gleichgewicht zwischen den Prozessen Wachstum, Differenzierung und Zelltod, um die Homöostase des dynamischen Blutsystems zu garantieren [Dingli and Pacheco, 2010]. Eine Störung dieses Gleichgewichts kann verschiedene hämatologische Erkrankungen wie Lymphome, Leukämien oder Autoimmunerkrankungen zur Folge haben [Kondo et al., 2003].

Anhand eines blut-spezifischen, RNAi-basierenden Screens in der *Drosophila* Larve wurden 356 konservierte Gene identifiziert, die an der Regulation der Blutbildung in der Fruchtfliege beteiligt sind [Elling et al., unveröffentlicht]. Die fehlende Expression einiger dieser Gene in den Blutzellen der Larve führte zur Entstehung einer sogenannten "Fliegenleukämie", die sich durch eine stark vermehrte Bildung von Makrophagen-ähnlichen Plasmatozyten und das Auftreten von stark pigmentierten Tumoren, sogenannten "melanotic tumors", auszeichnet. Zu den Genen, die zu einem besonders starken Phänotyp in der Fliege führten, zählen der Proteaseinhibitor Papilin, zwei transkritionelle Koregulatoren namens Symplekin und Ssrp1, und mehrere Faktoren, die an der Regulation der Endozytose beteiligt sind, nämlich die kleine GTPase Rab5a, das SNARE Protein Syntaxin 7 sowie zwei Untereinheiten des HOPS/ CORVET-Komplexes namens Vps16 und Vps33a. Durch die Analyse von Knochenmarkchimären, haben wir getestet, ob die genannten Gene auch bei der Blutbildung in Säugetieren eine Rolle spielen. In unseren Versuchen wurde die Expression des jeweils zu untersuchenden Gens in Vorläuferzellen aus dem Knochenmark hinunterreguliert. Anschließend wurde die Fähigkeit dieser Vorläuferzellen in die verschiedenen Blutzelllinien zu differenzieren durch deren Transplantation in Mäuse getestet.

Vorläuferzellen, die eine verminderte Expression von entweder Symplekin, Rab5a oder Vps16 aufwiesen, entwickelten sich bevorzugt zu reifen oder unreifen myeloiden Blutzellen, während diese Vorläuferzellen seltener zu B- oder T-Lymphozyten differenzierten. Dies ist ein Hinweis darauf, dass die sogenannte "lineage decision" beeinträchtigt sein könnte. Außerdem förderte die Herabregulation der selben Gene eine vermehrte Bildung von natürlichen Killerzellen in der Milz der Rezipienten. Weiters konnten wir zeigen, dass die Granulozytenpopulation im peripheren Blut von Papilin Knockout-Mäusen vermindert ist. Dieser Befund korrelierte mit einem niedrigeren Prozentsatz von myeloiden Vorläuferzellen im Knochenmark dieser Mäuse im Vergleich zu Wildtyp-Mäusen. Unsere Resultate deuten darauf hin, dass die konservierten

Gene, die ursprünglich als Regulatoren für die Blutbildung und Homöostase in Fruchtfliegen identifiziert wurden, auch eine Rolle in der Regulation der Hämatopoiese in Säugetieren spielen.

# Contents

# 1 Introduction

## 1.1 The fruit fly *Drosophila melanogaster* as model organism to study hematopoiesis

In the last decade, the fruit fly *Drosophila melanogaster* has become a powerful tool to study basic molecular mechanisms. First, the full genomic sequence of the fly genome was resolved in the year 2000 [Adams et al., 2000], revealing that more than half of the *Drosophila* proteins share similarities with mammalian proteins [Rubin et al., 2000]. Moreover, it was shown that not only proteins involved in core biological processes, such as metabolism, transport and cell structure are conserved among insects and vertebrates [Lopez-Bigas et al., 2008], but *Drosophila* orthologs have also been identified for more than 60% of genes implicated in a diverse set of human disease [Fortini et al., 2000]. On the other hand, the discovery of new potent techniques such as targeted gene knock-down by RNA interference [Fire et al., 1998] and the generation of stable transgenic RNAi lines, enabling tissue- and time-specific knock-down of individual genes [Kennerdell and Carthew, 2000], paved the way for the model organism *Drosophila* to become a strong and reliable genetic tool to study conserved gene function.

Interestingly, despite the phylogenetic distance of arthropods and vertebrates of about 964 million years [Hedges et al., 2004], the development of the hematopoietic system in *Drosophila melanogaster* and mammals displays an eminent functional similarity [Evans et al., 2003]. Analogous to vertebrates, hematopoiesis in the developing fly can be divided into two spatially and temporally distinct phases. The first wave of hematopoiesis occurs in the early embryo, when blood cell progenitors, so called prohemocytes, differentiate from the head mesoderm and populate the embryo [Tepass et al., 1994]. During the second hematopoietic phase, hemocytes are derived from a specialized mesodermal organ, the so called lymph gland, that only exists during the larval stages of development [Shrestha and Gateff, 1982]. Upon the onset of metamorphosis, the lymph gland degenerates and differentiated hemocytes are released into the hemolymph. These two hemocyte populations, originating from the embryonic and the larval stage, persist throughout metamorphosis

and form the cellular components of the blood in the adult fly [Holz et al., 2003]. Although the existence of hematopoietic stem cells in the *Drosophila* lymph gland has been demonstrated by lineage tracing experiments [Minakhina and Steward, 2010], to date no evidence for an imaginal organ harboring hematopoietic stem cells in adult fly equivalent to the bone marrow in mammals has been identified [Holz et al., 2003; Krzemien et al., 2010]. Analogously, the hematopoietic precursors in vertebrates are generated at two distinct times and locations in the embryo [Dzierzak and Speck, 2008]: Primitive hematopoiesis occurring in the extra-embryonic yolk sac gives rise to the first blood cell progenitors, which are basically of erythroid nature [Godin and Cumano, 2002]. Definitive hematopoiesis in the mesodermal aorta/gonad/mesonephros (AGM) region provides the long-lived hematopoietic stem cells, which subsequently seed the fetal liver and the bone marrow and generate the mature blood cell lineages of the mammalian immune system [Medvinsky et al., 2011].

Due to the phylogenetic distance between arthropods and vertebrates, the blood cell types in the fly are less diverse and primarily comprise the innate branch of immunity [Evans et al., 2003]. Notably, the tracheal system maintains the oxygen supply in insects and thus no erythroid lineage exists. Furthermore, no cell type that is equivalent to the lymphoid lineage can be found in *Drosophila* [Williams, 2007]. Subsequently, prohemocytes develop into cells that closely resemble the mammalian myeloid lineage and can be classified into three terminally differentiated types: plasmatocytes, crystal cells and lamellocytes (Figure1.1) [Meister, 2004]. *Plasmatocytes* function as phagocytic cells, that constitute 90-95% of all blood cells in the fly and share several similarities with vertebrate macrophages or monocytes. During development these cells play a critical role in morphogenesis by eliminating apoptotic cells and secreting and remodeling the extracellular matrix [Lanot et al., 2001], while in the course of an immune response plasmatocytes are responsible for phagocytosis of invading bacteria or fungi [Lemaitre and Hoffmann, 2007]. Additionally, these macrophage-like cells stimulate the humoral immune response by secreting antimicrobial peptides [Dimarcq et al., 1997] and cytokine-like molecules [Agaisse et al., 2003]. The other two cell types, namely crystal cells and lamellocytes, do not have known homologs in mammals. *Crystal cells*, the second most abundant blood cell population, functions in innate immune responses as well as wound healing processes. This cell type is characterized by crystalline inclusions storing large amounts of prophenoloxidase [Rizki et al., 1980; Waltzer et al., 2002] that catalyzes the humoral production of melanin, which in turn, together with its biosynthetic byproducts, is cytotoxic to pathogens [Reumer et al., 2010]. The third hemocyte lineage is presented by the *lamellocytes*, which are large, flat and adherent cells nearly absent in normal larvae.

Upon parasitisation differentiation of these immune cells is massively induced, which then function in the encapsulation and neutralisation of invading parasites too large to be phagocytosed by plasmatocytes [Meister, 2004].

Importantly, several transcription factors and signaling pathways controlling hematopoiesis are highly conserved between *Drosophila* and vertebrates [Evans et al., 2007] (Figure 1.1). For instance, the transcription factor Serpent (Srp) that was identified as central determinant of hemocyte fate, belongs to the conserved GATA family of zinc finger transcription factors [Rehorn et al., 1996]. Similarly, the orthologous factors GATA-1, GATA-2 and GATA-3 in the mouse have fundamental roles in cell fate determination and hematopoietic development [Bresnick et al., 2010]. Moreover, Srp interacts with two other conserved factors, namely U-shaped (Ush) and Lozenge (Lz), to further control hemocyte differentiation [Fossett et al., 2003]. The friend-of-GATA (FOG) homolog Ush acts together with Srp to repress crystal cell fate [Fossett et al., 2003], whereas in the mouse, FOG-1 regulates together with GATA-1 erythropoiesis and megakaryopoiesis [Tsang et al., 1997]. On the other hand, Srp works in concert with Lz to promote crystal cell differentiation [Fossett et al., 2003]. Lz shares significant similarities with human AML-1/Runx1 [Daga et al., 1996], which also interacts with GATA-1 in the mouse [Elagib et al., 2003] and is often mutated in acute myeloid leukemia (AML) [Renneville et al., 2008]. The factors that confer plasmatocyte lineage differentiation and block crystal cell development are known as Glial-cell-missing (Gcm and Gcm2) proteins [Alfonso and Jones, 2002]. Although there are two homologous Gcm proteins found in mammals, no known hematopoietic function has yet been identified, though they have been indicated in controlling differentiation of the placenta, thymus, and kidney [Hartenstein, 2006].

Functional similarity among flies and vertebrates can be seen also in regard to the hematopoietic microenvironment. The larval lymph gland harbors a signaling cell population in the so-called posterior signaling center (PSC) controlling blood cell differentiation [Lebestky et al., 2003]. This signaling cells functionally resemble the stromal cells in mammalian bone marrow. Moreover, the most important conserved signal transduction pathways regulating hematopoietic development include for instance the Notch pathway, which plays a critical role in lineage specification and crystal cell development [Lebestky et al., 2003]. Interestingly, not only cells of the PSC express the Notch ligand Serrate (Ser), its murine homolog Jagged-1 is also present on stromal cells in the bone marrow in mice [Lindsell et al., 1995]. Furthermore, the generation of hematopoietic stem cells (HSCs) from endothelial cells and the differentiation of the myeloid lineage in mammals is controlled by Notch-1 [Kumano et al., 2001, 2003]. Another conserved signaling route through the PDGF/VEGF receptor,
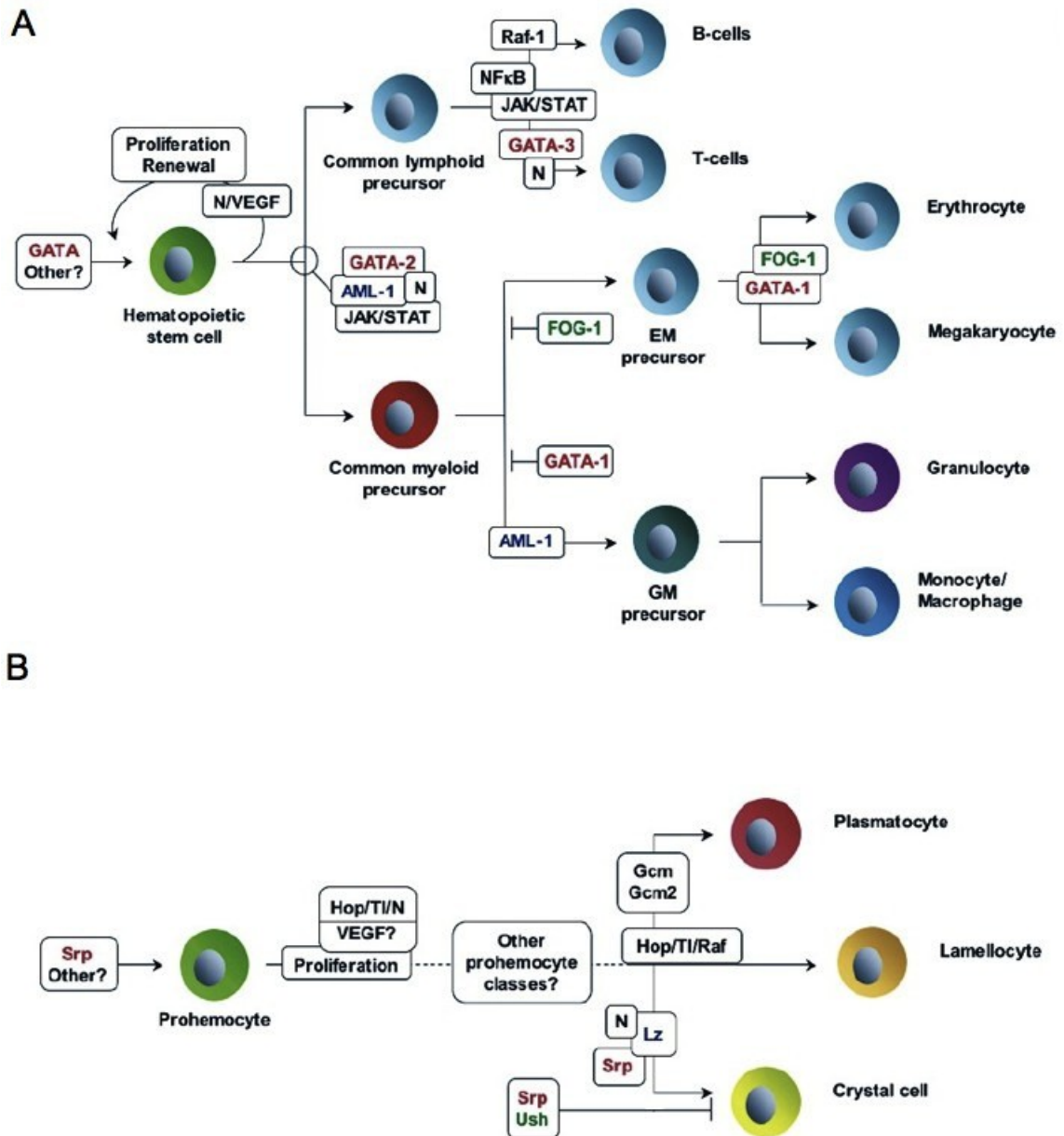
**Figure 1.1:** Hematopoiesis in mice (A) and *Drosophila* (B). Conserved proteins and pathways regulating hematopoiesis are highlighted in green and red. Scheme was adapted from Evans et al., 2003. Abbreviations: Erythrocyte/Megakaryocyte precursor (EM precursor); Granulocyte/Monocyte/Macrophage precursor (GM precursor); Serpent (Srp); Lozenge (Lz); U-shaped (Ush); Glial-cell-missing (Gcm/Gcm2); Notch (N); Hopscotch (Hop); Toll (Tl).

known as PVR in *Drosophila*, mediates hemocyte survival and migration in the fly [Cho et al., 2002], whereas it promotes B cell development and inhibits dendritic cell maturation in vertebrates [Hattori et al., 2001; Gabrilovich et al., 1996]. Moreover, increased expression of either receptor or ligand of the PDGF pathway is associated with various hematologic malignancies [Gerber and Ferrara, 2003; Birk et al., 2008]. Additionally, JAK/STAT signaling, known to be involved in hematopoietic development in mammals, also modulates hemocyte proliferation and differentiation [Hou et al., 2002]. As a final example, the Toll pathway was identified to control hemocyte proliferation by activating the NF-κB homolog Relish [Qiu et al., 1998]. Although the Toll pathway primarily mediates innate immune responses in vertebrates [Barton and Kagan, 2009; Silverman and Maniatis, 2001], dysfunction of factors downstream of the Toll-like receptor, such as NFκB or its inhibitor IκB, is related to several cancers including leukemias and lymphomas [Wong and Tergaonkar, 2009].

In summary, numerous functional and molecular processes directing hematopoiesis are conserved between *Drosophila melanogaster* and mammals. This strengthens the idea of identifying novel regulators of blood cell formation and homeostasis in the fly, which might highlight yet unknown orthologous players and mechanisms in mice and even humans. Importantly, several recent genome-wide screens in *Drosophila melanogaster* were successful in identifying novel conserved genes involved in obesity, pain sensitivity as well as regulation of heart function [Pospisilik et al., 2010; Neely et al., 2010a,b], confirming the fruit fly as a useful model organism for such studies.

## 1.2  An *in vivo* high-throughput screen to identify novel regulators of hematopoiesis in *Drosophila melanogaster*

In order to identify conserved genes required for blood cell formation and homeostasis, a blood cell specific RNA interference (RNAi) screen was conducted in the fly [Elling et al., unpublished]. For conditional knock-down of the selected target genes, 8800 different lines of the Vienna global *Drosophila* RNAi library [Dietzl et al., 2007] were crossed to the hemocyte specific hemolectin-GAL4 (hml-GAL4) driver line, which expresses the transcriptional activator GAL4 in the lymph gland as well as in circulating plasmatocytes and crystal cells throughout all larval stages [Goto et al., 2003]. GAL4 subsequently induces gene silencing by dsRNA expression controlled by the UAS promoter. The resultant progeny of the first generation was then screened for increased or decreased numbers of plasmatocytes or crystal cells and for the presence

of melanotic tumors or giant cells in third instar (L3) larvae. Plasmatocytes were visualised by using the UAS-GFP reporter line, while crystal cells could be detected as black dots after heating the larvae to 60°C for 10 minutes [Duvic et al., 2002]. The primary screen identified 620 lines that were positive for one or more of the above stated phenotypes. Retesting of these primary hits reduced the number to a total set of 356 genes (Figure 1.2).
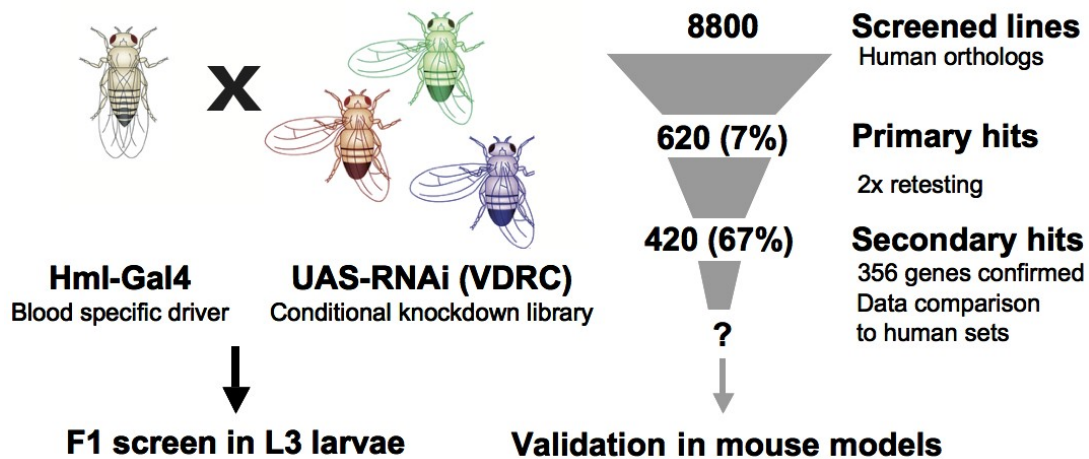


**Figure 1.2:** Schematic for genome-wide RNAi Screen for regulators of hematopoiesis in *Drosophila* larvae. Virgin Hml-Gal4 females were crossed to UAS-RNAi transgenic males and the cell number of plasmatocytes and crystal cells in late L3 larvae of the F1 progeny was determined. A total of 8800 lines were screened, identifying 620 lines as primary hits. The secondary screen confirmed 420 hits, representing 356 genes.

Amongst the identified candidates, the majority of genes caused general cell loss upon deficiency, whereas only a small number of the hits led to marked overproliferation of hemocytes. The overrepresentation of the phenotype of decreased hemocyte numbers might be due to the fact that many of the identified genes encode ribosomal proteins or factors involved in oxidative phosphorylation or other core housekeeping functions, which are essential for cell survival. Importantly, known regulators of blood cell development and homeostasis, such as Notch and its ligand Serrate, VEGF/PDGF Receptor (PVR), U-shaped or lesswright, were identified, thereby validating the screening strategy. The identified genes were categorized according to their assigned function by cluster analysis, revealing that more than 100 of the 356 identified genes are novel and do not connect to any cluster. Moreover, these genes do not have any assigned function in hematopoiesis. The large interaction networks mainly group genes mediating housekeeping functions such as ribosomal proteins or cell cycle regulators. Figure 1.3 shows a cluster analysis of all genes causing overproliferation of plasmatocytes. Furthermore, genes additionally causing increase of the crystal cell compartment and melanotic tumor formation are marked. Interestingly,

gene ontology (GO) term analysis showed a significant enrichment of a small group of genes involved in endocytosis which are highlighted in the cluster analysis (genes in red circle; Figure 1.3).

To select promising candidates for further validation in a mammalian model system, we focused on the small set of genes causing overproliferation of plasmatocytes mainly for two reasons. First, plasmatocytes are the only hemocyte type showing functional similarities to a mammalian blood cell type, namely macrophages or monocytes, respectively. Second, we reasoned that it would be technically easier to model an increase in cell number than to look for the decrease of any blood cell type, since the expression of the candidate genes is more or less abundant in all mammalian hematopoietic lineages, not solely in the plasmatocyte-like macrophages. Primarily based on a high score in the screen, the expression of the gene in the murine blood system and hematopoietic tissues and the assigned molecular function, we selected the following candidates for the follow-up study in mice: Papilin (Ppn), Structure specific recognition protein 1 (Ssrp1), Symplekin (Sympk), and four genes involved in endocytosis, namely the Ras-related protein Rab5a, Syntaxin 7 (Stx7) and the two vacuolar protein sorting proteins Vps16 and Vps33a, which are highlighted in blue in the cluster analysis (Figure 1.3).

## 1.3 Candidate genes

### 1.3.1 Structure specific recognition protein 1

The murine S̲tructure s̲pecific r̲ecognition p̲rotein 1 (Ssrp1) is highly conserved to its fruit fly homolog with 49% identity in the amino acid sequence (http://www.ebi.ac.uk /Tools/sss/ncbiblast). In mice, the factor is also known as T160 and was first isolated in a screen for DNA-binding components of a putative V-(D)-J-recombinase from a mouse pro-B cell line [Shirakata et al., 1991]. The protein was identified to bind to DNA containing recombination signal sequences (RSS) with its carboxy terminal high-mobility group (HMG) homology region. However, recombinase activity has not been demonstrated so far. Independently, the human homolog, SSRP1, was found to interact specifically with DNA modified by cis-diamminedichloroplatinum(II) (cis-DDP or cisplatin) and consequently it was suggested to be involved in DNA repair [Toney et al., 1989]. Further characterization of murine Ssrp1 revealed that the protein is highly expressed in tissues containing fast proliferating cells including the spleen, thymus, lymph nodes, bone marrow, testis and the ovary. Additionally, it was shown that Ssrp1 colocalizes with replication foci in the nucleus of mid to late

**Figure 1.3:** Cluster analysis of all genes associated with plasmatocyte overproliferation. Potential interactions between genes were visualized using Cytoscape. Nodes represent individual genes and lines represent putative associations. Round nodes represent all genes causing plasmatocyte overproliferation. Genes causing additional phenotypes such as increased number of crystal cells or induction of melanotic tumors are indicated by squares nodes or thicker border lines, respectively. Genes highlighted in red mark already known regulators of hematopoiesis in *Drosophila*, while blue highlighted genes were selected for validation in mice. The red circle distinguishes genes with the GO term endocytosis. Interaction data were derived from DroID, STRING and BioGRID, and include direct experimental interaction evidence from D. mel. as well as genetic and interolog links, text mining and pathway based association.

S phase cells, suggesting a role in cellular DNA replication [Hertel et al., 1999].

At the same time, human SSRP1 was identified to form a heterodimer with p140/ hSpt16, the human homolog of the yeast Spt16/Cdc68 [Orphanides et al., 1999]. This complex, known as the FACT complex (facilitates chromatin transaction) is involved in a wide range of cellular processes, including initiation of transcription, transcriptional elongation, DNA replication as well as DNA repair [Formosa, 2008]. During transcription, binding of the FACT complex to the nucleosome leads to destabilization of the histone octamere, triggering the delocalization of one H2A/H2B dimer upon Pol-II passage and thereby facilitates elongation [Belotserkovskaya and Reinberg, 2004]. Additionally, FACT harbors a histone chaperon activity and is able to mediate histone core deposition onto DNA [Belotserkovskaya et al., 2003]. The ability of FACT to overcome nucleosomal barriers [Jimeno-Gonzalez et al., 2006], as well as its capability to enhance binding of the TATA binding protein to a TATA site in a nucleosome [Biswas et al., 2004], plays an important role in transcription initiation. During DNA replication, FACT is recruited to replication origins by the replicative helicase complex (MCM), where it promotes initiation of DNA synthesis and progression of the MCM helicase [Tan et al., 2006].

Several lines of evidence implicate Ssrp1 in DNA damage repair: Upon UV irradiation, FACT forms a complex with casein kinase 2 (CK2), causing the selective phosphorylation of p53 at Ser-392 and thereby enhancing its activity [Keller et al., 2001; Keller and Lu, 2002]. Interestingly, Ssrp1 appears to have functions independent of Spt16 as well: It was shown that mammalian Ssrp1 functions as a transcriptional coregulator by directly interacting with other activators of transcription such as serum response factor (SRF) or the p53 homolog p63 [Spencer et al., 1999; Zeng et al., 2002a]. More recently, gene expression profiling after siRNA mediated knock-down of Ssrp1 or Spt16 revealed that the expression of a subset of genes is regulated by Ssrp1, independent of Spt16 [Li et al., 2007]. In light of the diverse cellular functions of Ssrp1, it is not surprising that the targeted disruption of Ssrp1 in the mouse results in early embryonic lethality soon after implantation [Cao et al., 2003]. Taken together, the intriguing expression profile of Ssrp1, especially in hematopoietic tissue, as well as its function as a transcriptional co-regulator, suggested that the factor might be a suitable candidate for addressing its role in hematopoiesis.

## 1.3.2 Symplekin

Symplekin derives its name from the Greek word 'συμπλέκειν', which stands for "to tie together", because it was initially found to be associated with the cytoplasmic plaque domain of tight junctions in the zonula occludens of polarized epithelial cells

in humans [Keon et al., 1996]. Interestingly, Symplekin was also shown to localize primarily to the nucleoplasm in cells that do not form tight junctions, such as fibroblasts, endothelial cells and most importantly lymphocytes in the lymph node [Keon et al., 1996]. Functionally, Symplekin acts as a scaffold in a large protein complex that is required for 3'-end cleavage and polyadenylation of eukaryotic messenger RNA precursors [Takagaki and Manley, 2000]. Additionally, Symplekin was identified to be essential for cytoplasmic polyadenylation as well as maturation of histone mRNAs, which are not polyadenylated [Barnard et al., 2004; Kolev and Steitz, 2005]. Moreover, Symplekin is implicated in the modulation of gene expression by two mechanisms: First, the polyadenylation machinery interacts with the preinitiation complex at the promoter as well as with the C-terminal domain (CTD) of the RNA polymerase II itself, thereby coupling RNA processing to transcription initiation, elongation as well as termination [Calvo and Manley, 2003]. On the other hand, Symplekin has been shown to directly interact with the transcription factor heat shock factor 1 (HSF1) in a stress-dependent manner, thereby inducing the transcription of stress response genes [Xing et al., 2004]. Moreover, the tight junction protein cooperates with the Y-box transcription factor ZONAB/DbpA in regulating the expression of Cyclin D1, thereby promoting proliferation of epithelial cells [Kavanagh et al., 2006]. Finally, the finding that the Symplekin/ZONAB complex represses the expression of AML-1/Runx1, a gene often mutated in human leukemias [Buchert et al., 2009], prompted us to validate its function in the hematopoietic system in mice.

### 1.3.3  Candidates involved in endocytosis: Rab5a, Syntaxin 7, Vps16 and Vps33a

Endocytosis is the regulated process by which cells internalize macromolecules from the environment into transport vesicles derived from the plasma membrane [Kumari et al., 2010]. This transport vesicles or endosomes subsequently deliver their cargo to lysosomes for degradation or recycle it back to the cell surface. Endocytosis can be categorized into two different mechanisms [Conner and Schmid, 2003]: Phagocytosis, which is the uptake of larger particles, and Pinocytosis, where smaller molecules are internalized. *Phagocytosis* is primarily restricted to specialized immune cells, such as macrophages, monocytes and neutrophils, which clear various pathogens or engulf dead cells. *Pinocytosis* on the other hand occurs in all cells and is mediated by four distinct mechanisms: macropinocytosis, clathrin-mediated endocytosis (CME), caveolae-mediated endocytosis, and clathrin- and caveolae-independent endocytosis [Conner and Schmid, 2003]. The candidates identified in the fly screen

primarily function in the pathway of the classical clathrin-mediated endocytosis, in which Rab GTPases act as the key regulators.

Rab5 is a member of the Rab (Ras-like proteins in brain) family of proteins, which represents the largest subgroup within the Ras superfamily consisting of more than 70 members in humans [Jiang and Ramachandran, 2006]. Displaying the typical characteristics of a small GTPase, Rab5 acts as a molecular switch by cycling between a cytoplasmic GDP-bound inactive and a GTP-bound active membrane-associated state [Stenmark et al., 1994]. Applying an affinity chromatography-based approach, more than 20 putative interacting proteins for Rab5 were identified [Christoforidis et al., 1999a; Stenmark, 2009]. These Rab5 binding partners can be classified into two groups. The first class represents regulatory proteins, which primarily modulate the status of guanine-nucleotide binding of Rab5 and include guanine nucleotide exchange factors (GEFs), GTPase-activating proteins (GAPs) and GDP dissociation inhibitors (GDIs). Particularly, Rabex-5 which forms a regulatory complex with Rabaptin-5 was identified to catalyze GDP-GTP exchange on Rab5 [Horiuchi et al., 1997], whereas RabGAP-5 was shown to specifically active the intrinsic GTPase activity of Rab5 [Haas et al., 2005]. Additionally, GDI binds to inactive GDP-associated Rab5 in the cytoplasm and acts as a chaperon, recycling the small GTPase back to the membrane [Ullrich et al., 1994]. Once activated, Rab5 fulfills its function by interacting with the second class of binding partners, namely the effector proteins. One of the recruited effectors is the Class III phosphatidylinositol (PI) 3-kinase hVPS34, which binds to Rab5 via the adaptor protein p150 [Christoforidis et al., 1999b] and generates phosphatidylinositol 3-phosphate (PI3P) at the membrane of early endosomes. These PI3P binding sites are recognized by two other Rab5 effectors that predominantly mediate vesicle docking and early endosome fusion: Namely early-endosome antigen 1 (EEA1) [Simonsen et al., 1998] and Rabenosyn-5 [Nielsen et al., 2000]. In summary, Rab5 acts as a central element in the tightly regulated process of endocytosis: On one hand the small GTPase functions as a timer by cycling between an active membrane-associated and an inactive cytoplasmic state, thereby imposing temporal and spatial regulation to vesicular transport. On the other hand, Rab5 operates as a molecular scaffold that sequentially recruits a network of effector proteins, enabling a coordinated progression of the individual steps of endocytosis.

Another protein identified in the screen and involved in endocytosis is Syntaxin 7. In humans, 15 different syntaxins have been identified that all belong to the SNARE family of proteins (soluble N-ethylmaleimide-sensitive factor-attachment protein receptors) [Teng et al., 2001; Strömberg et al., 2009]. Together with other

SNAREs, cytoplasmic NSF (N-ethylmaleimide-sensitive factor) and SNAP (soluble NSF-attachment protein) proteins, the transmembrane syntaxin proteins mediate membrane fusion in diverse vesicular transport processes along the exocytic and the endocytic pathway [Teng et al., 2001]. When first identified, Syntaxin 7 (Stx7) was shown to be ubiquitously expressed in various rat tissues and its subcellular localization with the early endosome was revealed [Wong et al., 1998; Prekeris et al., 1999]. Later, it was found that Stx7 also localizes to late endosomes and it was implicated in the mediation of endocytic trafficking from early to late endosomes and lysosomes [Nakamura et al., 2000]. Furthermore, Syntaxin 7 forms two types of trans-SNARE complexes with Vti1b and syntaxin 8 and either VAMP7 or VAMP8, thereby triggering either heterotypic late endosome to lysosome fusion or homotypic fusion of late endosomes, respectively [Antonin et al., 2000; Pryor et al., 2004]. More recently, human STX7 was shown to be differentially expressed in malignant melanoma and lymphoma, whereas a decreased expression of the SNARE protein correlated with more aggressive tumors [Strömberg et al., 2009].

Interestingly, human STX7 was identified to interact with the heteromeric Class C Vps complex, consisting of hVPS11, hVPS18, hVPS16 and hVPS33a [Kim et al., 2001]. Vps18 and Vps33 are the mammalian homologs of the *Drosophila* eye color genes deep orange (dor) and carnation (car), respectively, which are implicated in vesicle trafficking to lysosomes [Sevrioukov et al., 1999]. In combination with other factors, this class C Vps core tetramer can form two different complexes, namely HOPS (homotypic fusion and protein sorting) [Nakamura et al., 1997] and CORVET (class C core vacuole/ endosome tethering) [Peplowska et al., 2007]. These large multimeric tethering complexes are best studied in yeast where they coordinate Rab and SNARE function at the endosome and vacuole (the yeast lysosome) and thereby provide specificity to vesicle fusion. In human cells, the HOPS complex was identified to interact with Rab5 and to function as a GEF for Rab7 thereby mediating the Rab5 to Rab7 conversion during early to late endosome progression [Rink et al., 2005]. Moreover, immunohistochemistry as well as *in vitro* binding assays showed that the mammalian tethering complex associates with actin filaments as well as microtubules, suggesting that the HOPS complex may coordinate the attachment and movement of endosomes along the cytoskeleton [Richardson et al., 2004]. Interestingly, missense mutations in Vps33a in the mouse results in a phenotype that is similar to the human Hermansky–Pudlak syndrome (HPS), which is a organelle biogenesis disorder characterized by albinism, bleeding, and in most cases pulmonary fibrosis due to defects of melanosomes, platelet-dense granules, and lysosomes [Suzuki et al., 2003].

Taken together, Rab5, Syntaxin 7, Vps16 and Vps33 all have important regulatory functions in various steps along the endocytic pathway. Importantly, endocytosis does not only control pivotal physiological processes such as nutrient uptake, liquid and protein homeostasis of the plasma membrane, cell adhesion and immune surveillance, it also mediates intercellular communication and signal transduction [Sorkin and Zastrow, 2009]. Indeed, cell signaling is not simply regulated by controlling the number of receptors available at the cell surface for activation, endosomes are recognized as highly flexible scaffolds for sequential assembly of unique signaling complexes that mediate spatiotemporal regulation of various signaling pathways [Zastrow and Sorkin, 2007]. More recently, it has become clear that endosomes are essential in such diverse processes as cell migration, polarization and even cytokinesis, by acting as multifunctional platforms for the assembly of unique molecular machineries [Gould and Lippincott-Schwartz, 2009]. Therefore, it will be interesting to determine whether the repression of either of the selected genes interferes with blood cell homeostasis in mice and if even similar effects can be observed by inhibiting these various regulators along the vesicular trafficking pathway.

## 1.3.4 Papilin

Papilin was first discovered as a large extracellular matrix (ECM) glycoprotein with O-linked, sulfated glycosaminoglycan chains that is secreted by cultured *Drosophila melanogaster* cells and primarily localizes to the basement membrane of embryos [Campbell et al., 1987]. Homologs of the extracellular matrix protein have been determined in nematodes, mouse and human. The papilin found in *Mus musculus* shows a protein identity of 39% to its *Drosophila* homolog (http://www.ebi.ac.uk/Tools /sss/ncbiblast). Moreover, Papilin contains a distinctly conserved domain, the so called "papilin cassette", consisting of a set of thrombospondin type 1 domains (TSR) separated by a cysteine-rich spacer region. Additionally, this domain shares homology with the noncatalytic portion of the ADAMTS (A Disintegrin And Metalloprotease with Thrombospondin type 1 motifs) family of secreted metalloproteases [Fessler et al., 2004]. Interestingly, papilin harbors multiple copies of domains similar to other protease inhibitors, such as the Kunitz domains of BPTI (Bovine Pancreatic Trypsin Inhibitor) type, and was shown to non-competitively inhibit an ADAMTS metalloproteinase *in vitro* [Kramerova et al., 2000]. Furthermore, in *Drosophila* papilin is expressed in head mesoderm derived hemocytes, which subsequently give rise to the extracellular matrix [Kramerova et al., 2003; Wood and Jacinto, 2007]. Thus, papilin is not only expressed throughout development in the ECM, it also seems to be essential for embryogenesis in *Drosophila* and *Caenorhabditis elegans* since its repres-

sion in the embryo by RNAi is lethal [Kramerova et al., 2000]. Taken together, these results suggest a possible regulatory role for papilin in development, organogenesis and angiogenesis by modulating the activity of ADAMTS metalloproteinases.

## 1.4 Project outline

The similarity of hematopoietic development in the fruit fly *Drosophila melanogaster* and mammals, considering its spatiotemporal regulation and the molecular factors controlling blood cell differentiation [Waltzer et al., 2010], suggest that several basic mechanisms of hematopoiesis are conserved during evolution between insects and vertebrates. Based on this knowledge, an *in vivo* RNAi screen in developing hemocytes in fly larvae was applied to identify novel conserved regulators of hematopoietic differentiation and homeostasis [Elling et al., unpublished]. In this survey the down-regulation of certain genes resulted in a marked overproliferation of macrophage-like plasmatocytes in third instar *Drosophila* larvae. The screen identified not only known regulators of hematopoiesis in the fruit fly but it also uncovered novel genes, which have not been implicated in hematopoiesis so far. The aim of this study therefore, was to select promising hits of the screen and evaluate the relevance of this novel candidate genes in the mammalian hematopoietic system. In order to do this, we first analyzed if the knock-down of these genes promotes proliferation and growth of a murine B-cell line *in vitro*. Furthermore, we established down-regulation of the selected genes in mouse bone marrow precursor cells and analyzed their potential to repopulate lethally irradiated hosts *in vivo*. This bone marrow chimeric approach showed that indeed three out of six of the identified genes influence hematopoiesis by promoting the abundance of the myeloid lineage while interfering with the reconstitution of the lymphoid lineage.

# 2 Results

## 2.1 Candidate genes are expressed in hematopoietic tissues in the mouse

To select promising candidate genes, expression profiles from published gene annotation resources (http://biogps.gnf.org) [Wu et al., 2009] and data in the literature was used as a reference. Since these data are sometimes incomplete and misleading, we confirmed mRNA expression of the selected candidates by RT-PCR. Importantly, all genes are expressed in hematopoietic tissues in the mouse, such as the bone marrow, spleen and thymus, as well as in the mouse pro-B cell line Ba/F3 (Figure 2.1).
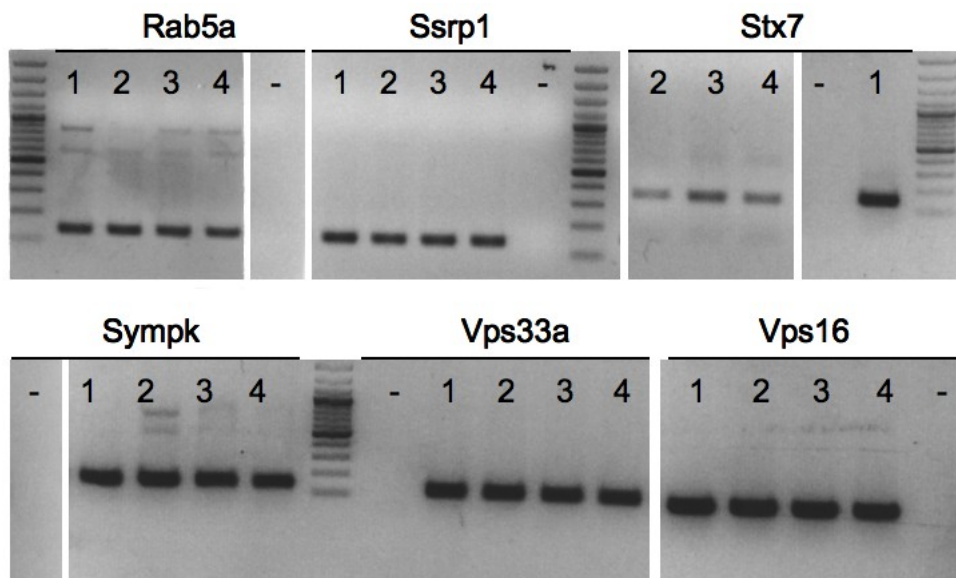


**Figure 2.1:** Candidate genes are expressed in hematopoietic tissues in mice. Total mRNA was isolated from BaF/3 cells (lane 1), thymus (lane 2), spleen (lane 3) as well as bone marrow (lane 4). Expression of indicated mRNA was determined by RT-PCR. Lanes marked with (-) show negative $H_2O$ control.

## 2.2 Knock-down of candidate genes does not effect cell proliferation *in vitro*

Considering the fact that knock-down of the selected genes caused massive over-growth of plasmatocytes in *Drosophila* larvae, it was tempting to test whether their repression would promote proliferation of a hematopoietic cell line *in vitro*. Therefore we decided to use the mouse pro-B cell line Ba/F3, which expresses all the candidate genes (Figure 2.1), to generate cells stably expressing a short hairpin RNA (shRNA), which selectively down-regulates gene expression. For each gene, three independent small hairpin RNAs (shRNAs) were cloned into the modified retroviral vector MSCV-LMP (http://www.openbiosystems.com/RNAi/RetroviralCloningVectors) (Figure 2.2A), hereafter referred to as pMIG. The miR30 styled shRNAs were first amplified from a 97 nucleotide long, single stranded DNA template by PCR (Figure 2.2B) and after subsequent restriction digest, ligated into the linearized pMIG vector. The incorporation of the gene specific hairpin into the backbone of the mir-30 microRNA improves its processing by endogenous Drosha and Dicer and promotes active loading into the RISC complex, thereby ensuring a more efficient knock-down [Zeng et al., 2002b].

**A**                                                **B**
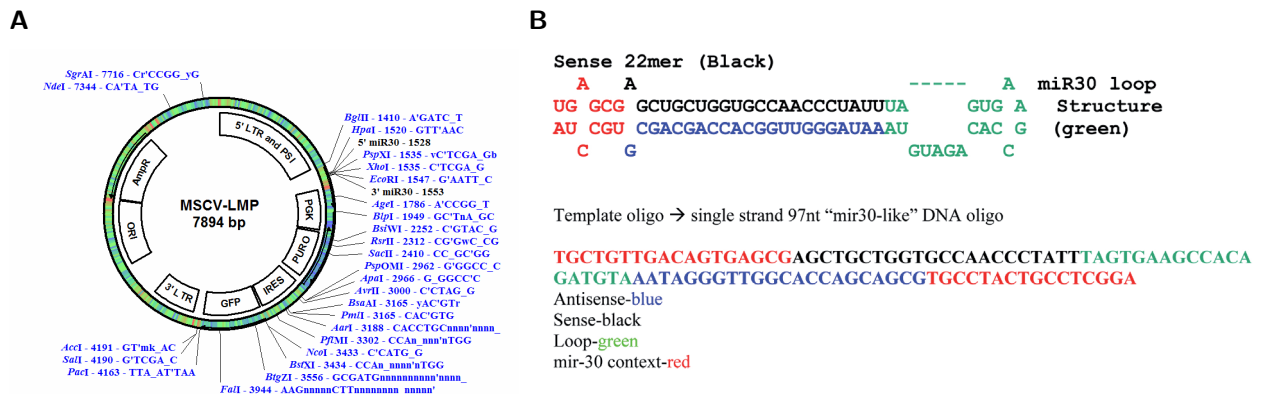


**Figure 2.2:** (A) Vector map of MSCV-LMP. In the modified vector, named pMIG, the PGK promoter driving the expression of the puromycin resistance was inactivated.The miR30-based gene-specific shRNAs are inserted into the miR30 backbone using the restriction sites XhoI and EcoRI. (B) Schematic design of miR-30-styled shRNAs. In the upper picture the final preprocessed structure of the sense (back) and antisense (blue) target sequences inserted in the backbone of the miR-30 microRNA is shown. Below the sequence of the corresponding single stranded DNA oligonucleotide used for PCR amplification is shown. Sequences in red or green represent the flanking miR-30 nucleotides or the miR-30 loop structure, respectively.

After successful cloning of all constructs, the mRNA levels of the targeted genes were determined in the stable Ba/F3 cell lines to verify efficient knockdown. In all cases, at least one of the three hairpins was capable of decreasing the endogenous transcript levels more than 60% from the baseline (Figure 2.3). In fact, most knock-down cell lines showed a remaining mRNA expression of about 30%, except for Rab5a and Stx7 were transcript levels could even be reduced to more than 90% from baseline levels. For each gene, the hairpin showing the most potent knock-down efficacy was used for further analysis.
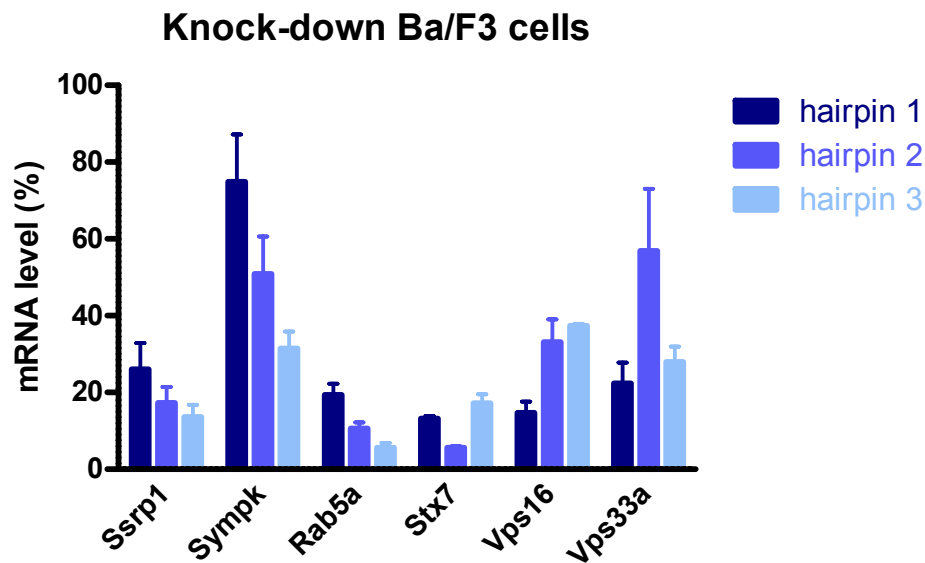


**Figure 2.3:** Knock-down efficiency of three individual hairpins. Total mRNA was isolated from mouse Ba/F3 cells stably expressing a gene-specific shRNAs targeting the indicated genes. Expression levels of mRNA were determined by qRT-PCR relative to ß-actin levels. Data are shown as percentage of the remaining transcript levels compared to the control cell line stably transfected with the empty vector pMIG (mean values ± SD).

In order to analyse the effect of the knock-down on proliferation, we compared the growth rate of the knock-down cell lines to wild-type cells or cells harboring the empty vector. No significant increase in cell growth could be detected for all cell lines tested (Figure 2.4). The lack of an obvious growth advantage might have several reasons. For instance, plasmatocytes closely resemble macrophages or monocytes of the myeloid lineage in vertebrates, thus the functionality of the identified genes might not readily be applicable to mouse Ba/F3 cells, which is an immortalized lymphoid pro-B cell line [Palacios and Steinmetz, 1985]. Additionally, important factors of the microenvironment such as signaling molecules and cell to cell interaction, which might contribute to the observed phenotype *in vivo* are not recapitulated in an *in vitro* system. Thus, we decided to analyze the effect of gene repression in the hematopoietic system *in vivo*.
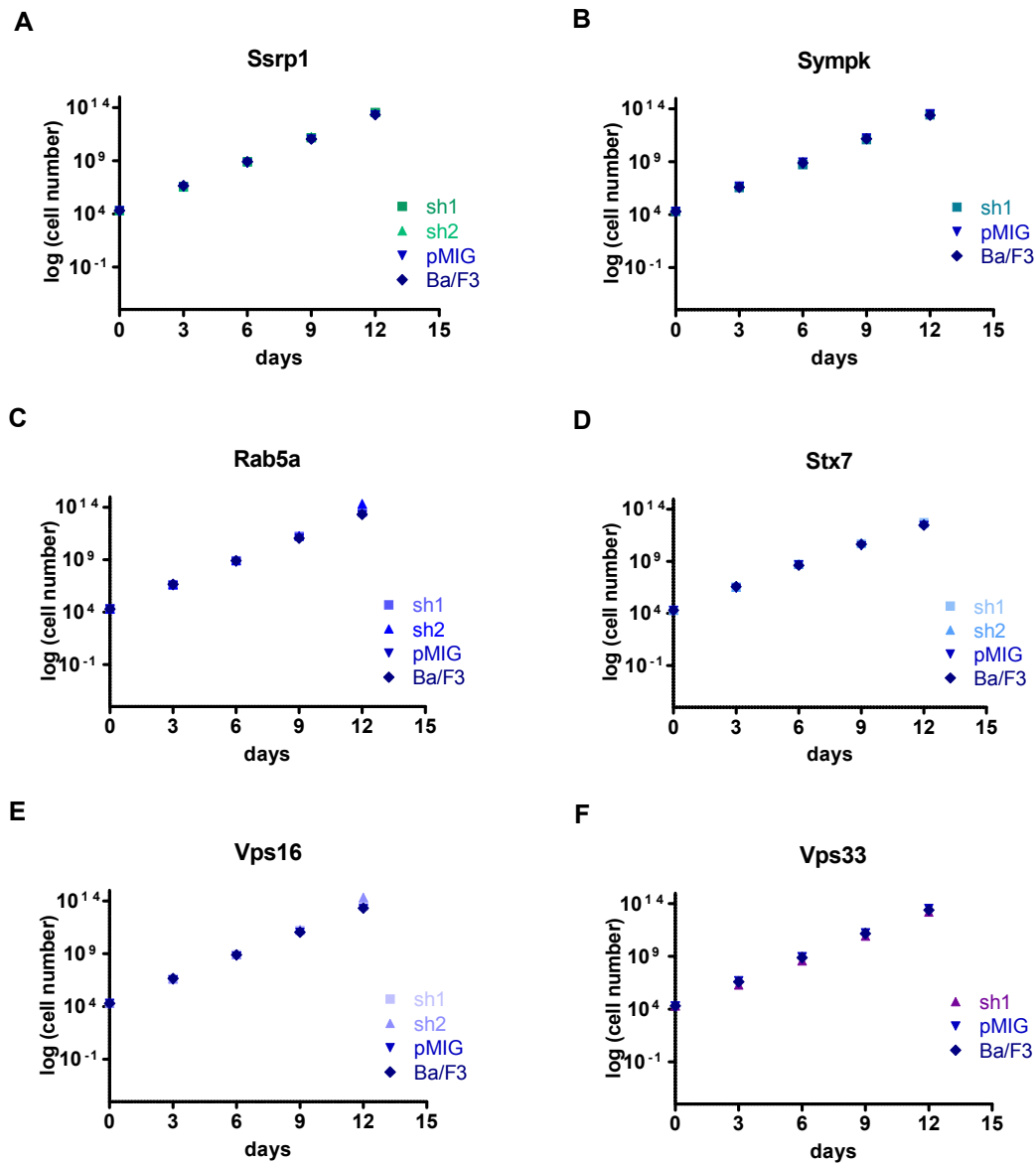
**Figure 2.4:** *In vitro* proliferation of the stable knock-down cell lines is similar to wild-type cells. Mouse pro-B cells (Ba/F3) stably expressing the indicated shRNAs, growing under standard conditions, were counted and split all 3 days for 2 weeks. Exponential growth is shown as logarithmic function of the cell number on the indicated days for cells stably expressing shRNAs (sh) against Ssrp1 (A), Sympk (B), Rab5a(C), Stx7 (D), Vps16 (E) and Vps33a (F). Wild-type and only GFP-expressing (pMIG) Ba/F3 cells serve as negative controls. For Ssrp1, Rab5a, Stx7 and Vps16 proliferation of cell lines expressing the two most potent shRNAs was validated (sh1 and sh2).
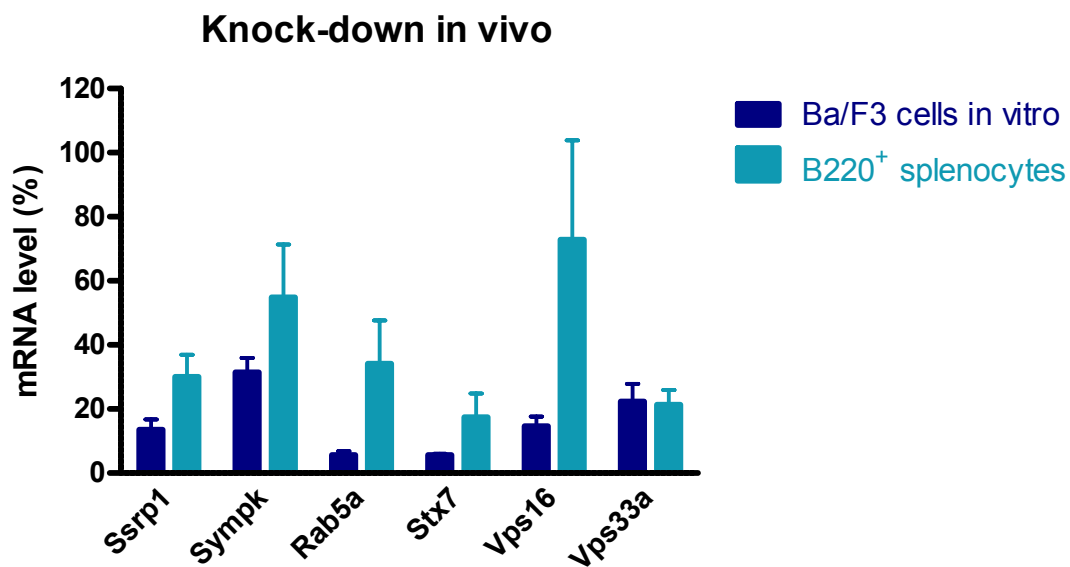
## 2.3 Generation of bone marrow chimeras

The "gold standard" for studying the molecular function of potential oncogenes and tumor suppressor genes involves the generation of transgenic and knock-out mice harboring the altered, oncogenic lesion in the germline. Nevertheless their production is time-consuming and laborious. Therefore, we took advantage of a faster chimeric approach, where knock-down of the candidate genes is established in isolated bone marrow cells *in vitro*. These cells are subsequently transplanted into recipient mice previously depleted of hematopoietic cells by irradiation (Figure 2.5). The gene silencing constructs were introduced into bone marrow cells with retroviruses, derived from an ecotropic packaging cell line (Plat-E). All the retroviral constructs contained an internal ribosome entry site (IRES) followed by the green fluorescent protein (GFP) next to the gene specific shRNA (Figure 2.2A), allowing us to distinguish transduced and wild-type cells.
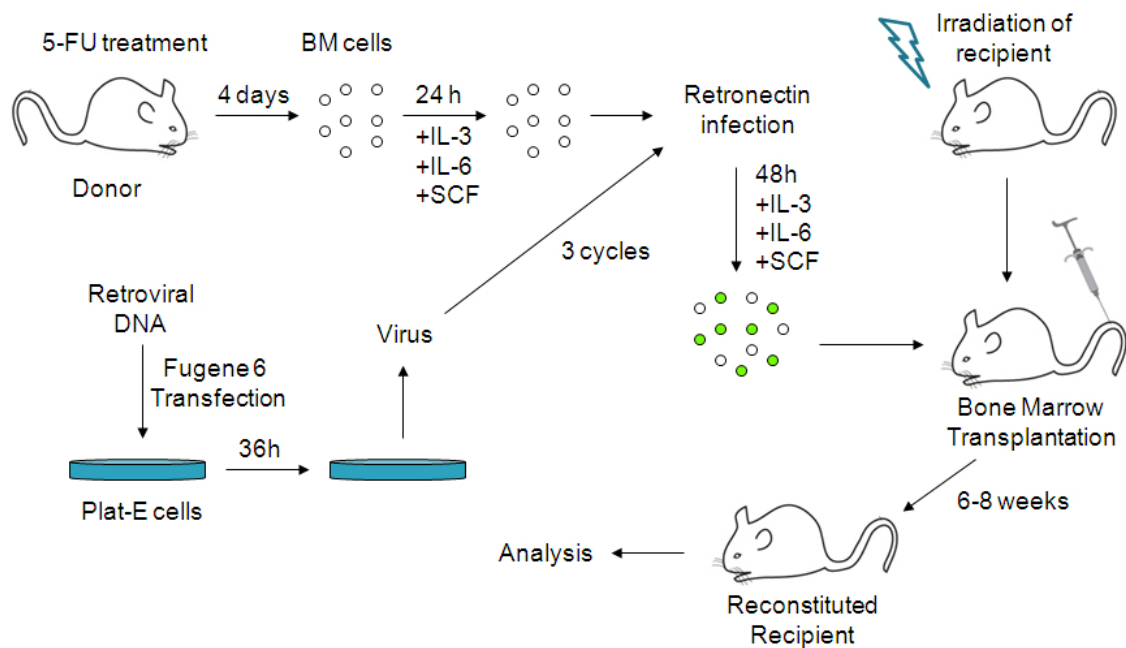


**Figure 2.5:** Generation of bone marrow chimeric mice. Bone marrow cells isolated from 5'-fluorouracil (5-FU) treated C57BL/6J mice were activated with the indicated cytokines for 24 hours, followed by 4 cycles of retroviral infection. Retroviruses harboring the shRNA-IRES-GFP construct targeting the selected genes, were derived from PLAT-E packaging cells. $1.2 \times 10^6$ transduced cells were transplanted into lethally irradiated (9.5 Gy) recipient mice via tail vein injection. Eight weeks after reconstitution, chimeric mice were analysed by Flow cytometry.

To confirm efficient knock-down of the candidate genes *in vivo*, we isolated B220$^+$ B-cells from the spleens of chimeric mice by fluorescent activated cell sorting (FACS) and tested the expression of the respective transcripts by quantitative RT-PCR (Figure 2.6). For all six genes, except for Vps33a, the knock-down was less potent in the isolated splenocytes than in the Ba/F3 cell line. The transcript levels were reduced more than 60% in four cases, namely Ssrp1, Rab5a, Stx7 and Vps33a. However, for Symplekin and Vps16, gene silencing seems to be less efficient *in vivo* because the B220$^+$ B-cells still harbor approximately 60 or 70% of the respective mRNA, when compared to splenocytes isolated from pMIG control mice.



**Figure 2.6:** *In vivo* knock-down efficiency in B220$^+$ splenocytes of bone marrow chimeric mice. Splenocytes isolated from bone marrow chimeras, harboring GFP$^+$ cells expressing shRNAs against the selected genes, were labelled with an APC-conjugated anti-B220 antibody and B220$^+$ GFP$^+$ lymphocytes were sorted by FACS. Total mRNA was isolated and transcript levels of the indicated genes were determined by quantitative RT-PCR. ß-actin was used as internal control. The green bars represent the percentage of remaining transcript after knock-down compared to control B220$^+$ GFP$^+$ cells isolated from pMIG chimeras. The blue bars show the corresponding *in vitro* knock-down efficiency determined in stable BaF/3 cell lines (n = 2; mean values ± SD).

In order to gain an insight into the efficiency and reproducibility of bone marrow infection and reconstitution of recipient mice, we performed two kinds of analysis: First, we calculated how the transfection efficiency of the packaging cell line Plat-E translates into bone marrow infection rates. Since we did not determine the actual viral titer, this relative infection rate serves as an approximation to quantify infection efficiency. The relative infection rate was obtained by dividing the percentage of infected GFP$^+$ bone marrow cells by the percentage of transfected GFP$^+$ Plat-E cells. The transfection efficiency is widely dependent on the cell line, therefore a constant ratio similar to the control situation (pMIG) of about 70 would be expected. For Ssrp1 and Symplekin the relative infection rate is in accordance with the ratio observed in the control situation. In all other cases the value is about 50 (Figure 2.7A). This overall decrease could have several reasons, for example increased apoptosis of bone marrow cells in culture. Moreover, the reduced ratio as observed for Rab5a, Stx7 or Vps33a shRNA transfected bone marrow could already implicate an effect of the knock-down on the cells.
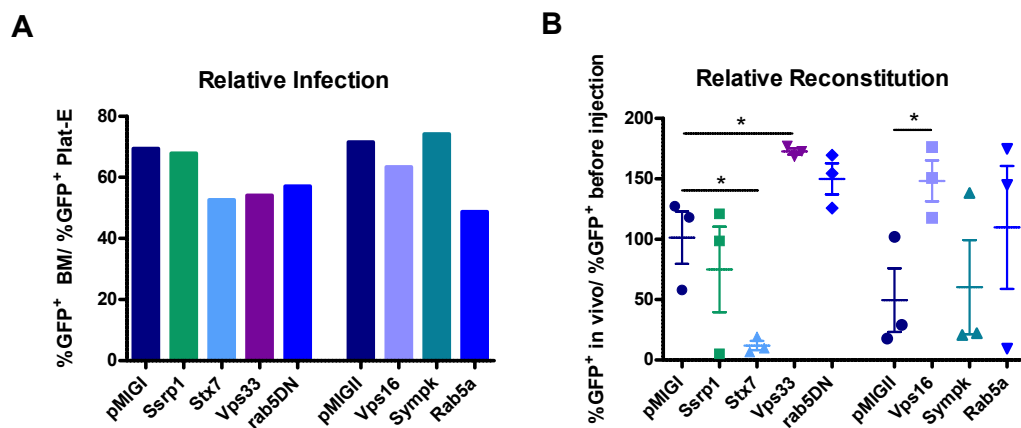


**Figure 2.7:** Relative infection and reconstitution efficiencies. (A) Percentage of infected bone marrow cells was divided by the percentage of transfected Plat-E cells. Bars represent relative infection rate of bone marrow cells expressing shRNAs against the indicated genes. pMIGI and pMIGII correspond to two independent negative controls only expressing GFP derived from two different experiments. (B) Percentage of GFP$^+$ cells after reconstitution *in vivo* divided by the percentage of GFP$^+$ bone marrow cells before transplantation. Each data point represents the value of a single mouse for the indicated genotype, horizontal line indicates mean $\pm$ SEM (n = 3; * P $<$ 0.05).

Since there was a high variability in the percentage of GFP$^+$ cells in the reconstituted mice, we analyzed how this relates to bone marrow infection efficiency. Therefore we divided the percentage of GFP$^+$ after reconstitution *in vivo* by the percentage

of infected bone marrow cells before injection. Considering that a mixed population of infected and uninfected bone marrow cells was injected, the ratio of GFP$^+$ to GFP$^-$ cells should stay the same after the reconstitution and should therefore give a relative reconstitution value of 100. In the first cohort of mice, the pMIGI control mice showed a mean relative reconstitution rate of about 100 (Figure 2.7B), whereas the ratio for Stx7 was significantly decreased in all three mice. This indicates that although the bone marrow cells were properly infected prior to transplantation, the infected cells were not able to contribute to the reconstitution of the recipient to the same extent as uninfected cells. Interestingly, the relative infection value for Stx7 (Figure 2.7A) shows that the infection *in vitro* was less efficient despite a similar Plat-E cell transfection and thus a similar viral titer. Strikingly, all three Vps33a recipients showed a significant increase in the percentage of GFP$^+$ cells after reconstitution compared to control mice. In the second cohort, the pMIGII control mice did not show the expected relative reconstitution rate of 100. Two mice displayed a decreased number of GFP$^+$ cells after reconstitution, whereas one maintained the same ratio as before injection. Although the three mice for each genotype were transplanted with the same bone marrow, a loss or an increase of infected cells after transplantation can be observed in individual mice, indicating that factors independent of the knock-down influence the reconstitution efficiency.

For the analysis of the bone marrow chimeras and the effect of the knock-down on the various blood cell types, we focused on the GFP$^+$ cells and compared the lineage distribution of the experimental knock-down to the pMIG control populations. The choice for this approach is based on the idea that the knock-down of a certain gene in a precursor cell might positively or negatively influence its differentiation capacity and subsequently enhance or inhibit the formation of a certain blood cell lineage. Thus, the abundance of the main hematopoietic lineages was determined in the bone marrow, spleen, thymus and peripheral blood of the recipient mice by flow cytometry eight weeks after reconstitution.

In order to validate this approach, we compared the results of the two independent control cohorts pMIGI and pMIGII, which were generated in independent experiments. Since all the GFP$^+$cells in these mice only harbor the empty retroviral vector and no silencing shRNA, the GFP$^+$ population should contribute equally to all lineages. Chimeric mice were sacrificed eight weeks after the transplantation of GFP$^+$ bone marrow cells and the bone marrow, spleen, thymus and peripheral blood was isolated. After red blood cell lysis, the single cell suspensions of these tissues were stained with fluorescently labelled antibodies and the blood lineage distribution was analyzed by flow cytometry. Figures 2.8 and 2.9 show examples how the gates were set in

thymus and bone marrow samples to analyze the data. First, all viable cells were selected in the forward-side scatter to exclude dead cells and aggregates. Then, these cells were divided into a GFP$^+$ and a GFP$^-$ subset, followed by gating on the population of interest in the forward-side scatter. The gate R1 includes all small cells like lymphocytes and erythroblasts, whereas the R2 gate includes bigger granular cells such as monocytes and granulocytes. Among these cells, the individual sub-populations positive for the indicated markers were analyzed either using a histogram or a dot blot. The analysis in the spleen and the peripheral blood was performed similar to the bone marrow samples. All flow cytometry data were analyzed according to this protocol. To simplify data presentation, the abundance of the individual populations was visualized in bar graphs as percentage of the GFP$^+$ or the GFP$^-$ gate.
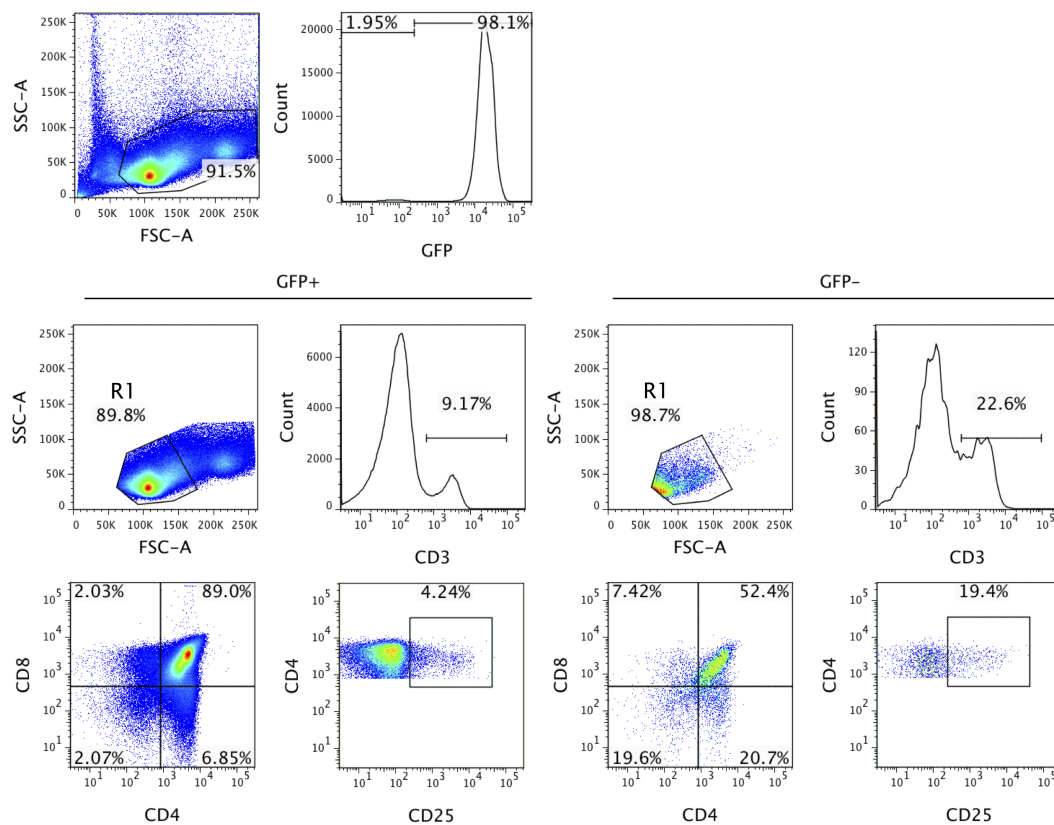


**Figure 2.8:** Representative example of the gating strategy in the thymus to analyze the flow cytometry data. In the first gate, all viable cells were selected, followed by subsequent gating on the GFP$^+$ and GFP$^-$ subsets. The R1 gate was further analyzed for expression of the indicated T-cell markers.
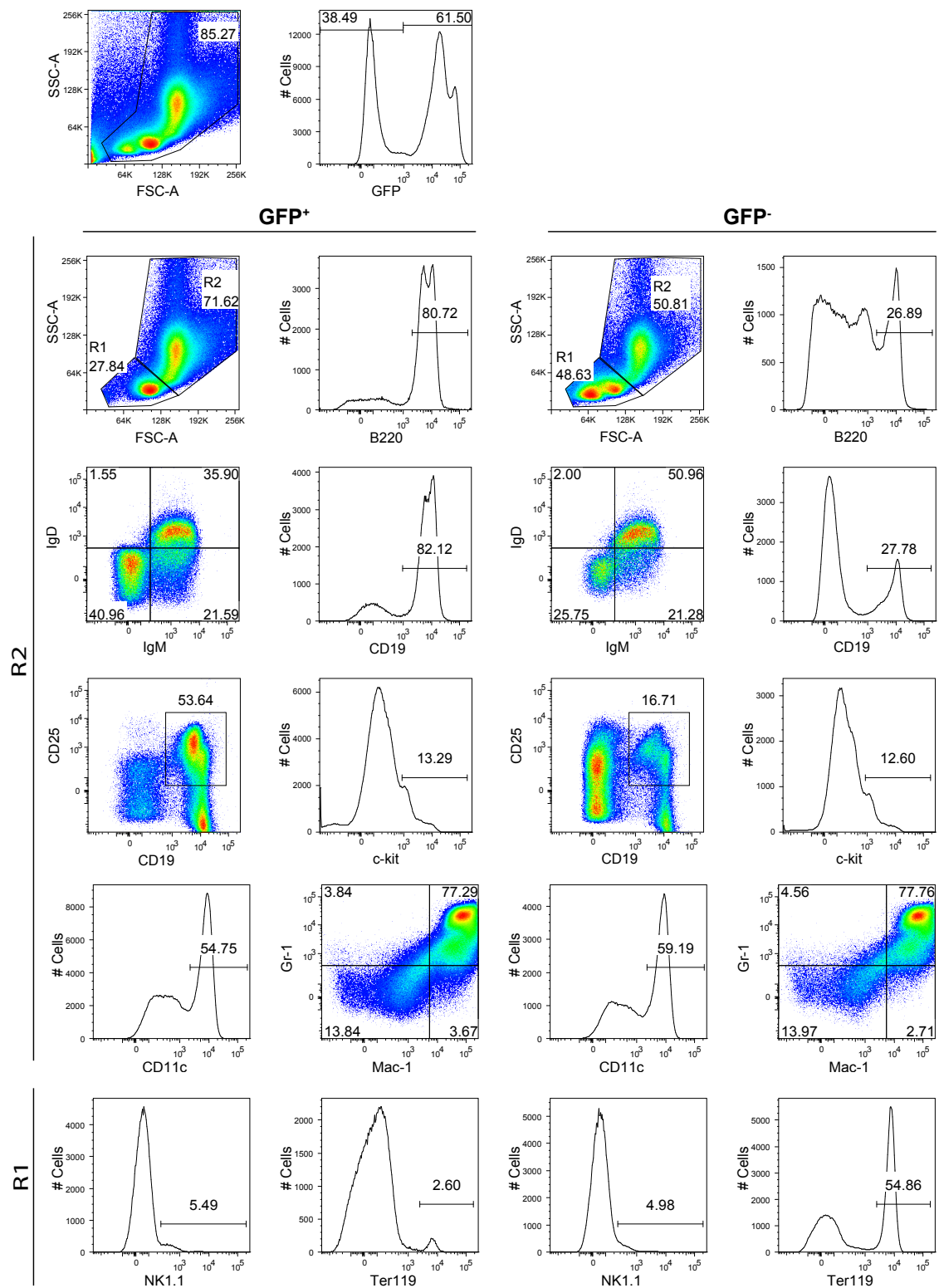
**Figure 2.9:** Representative example of the gating strategy in the bone marrow to analyze the flow cytometry data. In the first gate, all viable cells were selected, followed by subsequent gating on the GFP$^+$ and GFP$^-$ subsets. These cells are divided into the R1 and R2 populations in the forward-side scatter, followed by analysis of the expression of the indicated marker using either a histogram or a dot blot. Gates were set similarly in the spleen and peripheral blood.
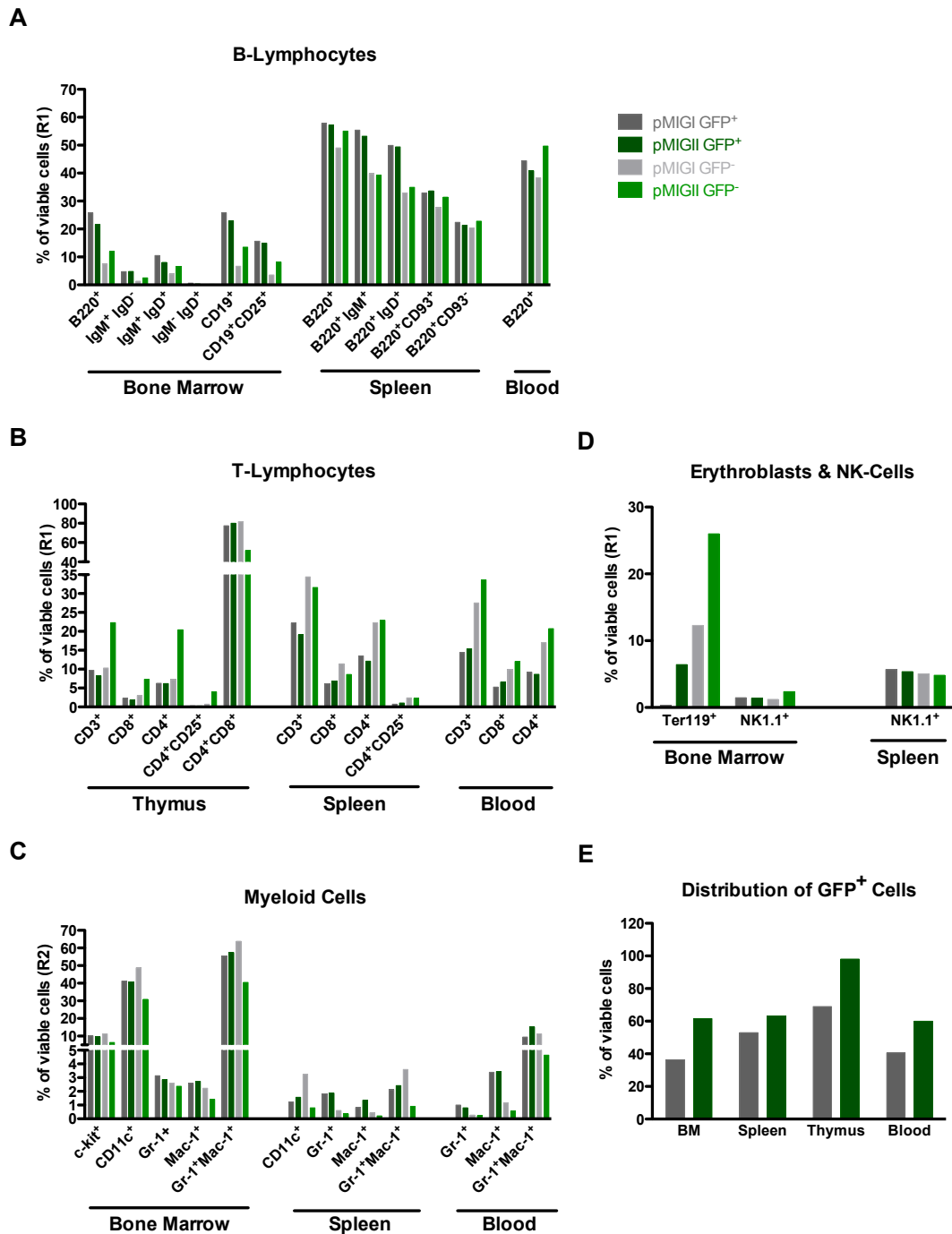
**Figure 2.10:** Lineage contribution of GFP$^+$ cells is similar among pMIG control mice. Flow cytometric analysis of the major blood cell lineages in independent control mice pMIGI and pMIGII 8 weeks after bone marrow transplantation: (A) B-cells, (B) T-cells, (C) myeloid cells and (D) erythroblasts and NK-cells, isolated from bone marrow, spleen, thymus and peripheral blood. Columns represent the percentage of GFP$^+$ (dark grey = pMIGI, dark green = pMIGII) or GFP$^-$ (light grey = pMIGI, light green = pMIGII) cells positive for the indicated markers (n = 1). (E) Distribution of viable GFP$^+$ cells in the indicated tissues (BM = bone marrow).

Considering that the mice were analyzed on three different days and we noticed variances in the data collected separately, probably due to differences in staining and compensation of the cytometer, we only compared results for mice that were examined on the same day. In the control mice, all percentages of GFP$^+$cells were similar in most lineages and no major differences could be observed (Figure 2.10). Of note, the pMIGII control mouse show a higher percentage of GFP$^+$ Gr-1$^+$Mac-1$^+$ cells (15.1%) in the peripheral blood as the pMIGI control mouse (9.47%) (Figure 2.10C). Moreover, there is a difference of more than 6% in the abundance of Ter119$^+$ erythroblasts in the GFP$^+$ compartment of pMIGI and pMIGII control mice. However, the ability of the transplanted GFP$^+$ bone marrow cells to contribute to the erythroblast lineage is generally impaired, a fact that becomes already evident by absence of this population in the forward-side scatter in the R1 gate of the GFP$^+$ subset (Figure 2.9).

On the other hand, another way to analyze the data would be to compare the percentages of GFP$^+$ cells positive for a certain marker to the same population in the GFP$^-$ subset in the same mouse. In the comparison of pMIGI and pMIGII control mice, the ratio of GFP$^+$ to GFP$^-$ cells is in most cases constant throughout a certain lineage (Figure 2.10). Therefore, changes in this ratio due to the knock-down of a certain gene by means of an increase of the GFP$^+$ population that correlates with a decrease in the GFP$^-$ subset, might rule out certain compensatory effects to adjust total cell number.

In summary, the analysis of the control groups showed that the comparison of the GFP$^+$subsets between mice and in regard to the same population in the GFP$^-$ subset in the same mouse is valid to identify if the knock-down of a gene is advantageous or disadvantageous for a cell to contribute to a certain lineage.

## 2.3.1 Reconstitution of hematopoietic lineages with Ssrp1 down-regulated bone marrow cells

Initially, Ssrp1 caught our attention because it is highly expressed in the bone marrow, spleen, thymus and lymph nodes of mice [Hertel et al., 1999] (Figure 2.1), suggesting a potential function in the hematopoietic compartment. As subunit of the FACT complex, Ssrp1 is implicated in various vital cellular processes such as replication, DNA repair and transcription [Formosa, 2008]. Independent from the FACT complex, Ssrp1 also serves as a transcriptional co-activator interacting with other transcription factors such as serum response factor or p63 [Spencer et al., 1999; Zeng et al., 2002a]. Interestingly, gene repression of the *Drosophila* homolog in hemocytes caused besides a severe expansion of plasmatocytes in fly larvae also an increase of crystal cells and promoted the formation of melanotic tumors. However, the function of Ssrp1 in the hematopoietic compartment in mammals has not been addressed so far.

In order to test whether Ssrp1 knock-down also effects proliferation and viability of hematopoietic cells in mice, bone marrow cells expressing a shRNA against Ssrp1 were transplanted into irradiated hosts and the composition of hematopoietic cells was analyzed by flow cytometry 8 weeks after reconstitution. For each mouse the percentage of GFP$^+$ or GFP$^-$ cells contributing to the major blood cell lineages was determined. The mean values of the pooled results of all three mice per genotype are shown as bar graphs in Figure 2.11. The percentage of GFP$^+$ cells accounts for about 40-50% in all analyzed tissues (Figure 2.11E). In the GFP$^+$ subset, the knock-down of Ssrp1 does not result in significantly different percentages of B- , T- or myeloid cells (Figure 2.11A-C). Additionally, the knock-down does not interfere with the reconstitution of the NK-cell or erythroblast compartment (Figure 2.11D). Of note, contribution of GFP$^+$ cells to the erythroblast compartment is markedly reduced compared to the GFP$^-$ subset in both Ssrp1 knock-down and pMIG control chimeras.

In summary this data indicate that Ssrp1 is not essential for the reconstitution and homeostasis of the hematopoietic system, since neither a significant reduction nor increase in the percentage of any blood cell lineage can be observed.
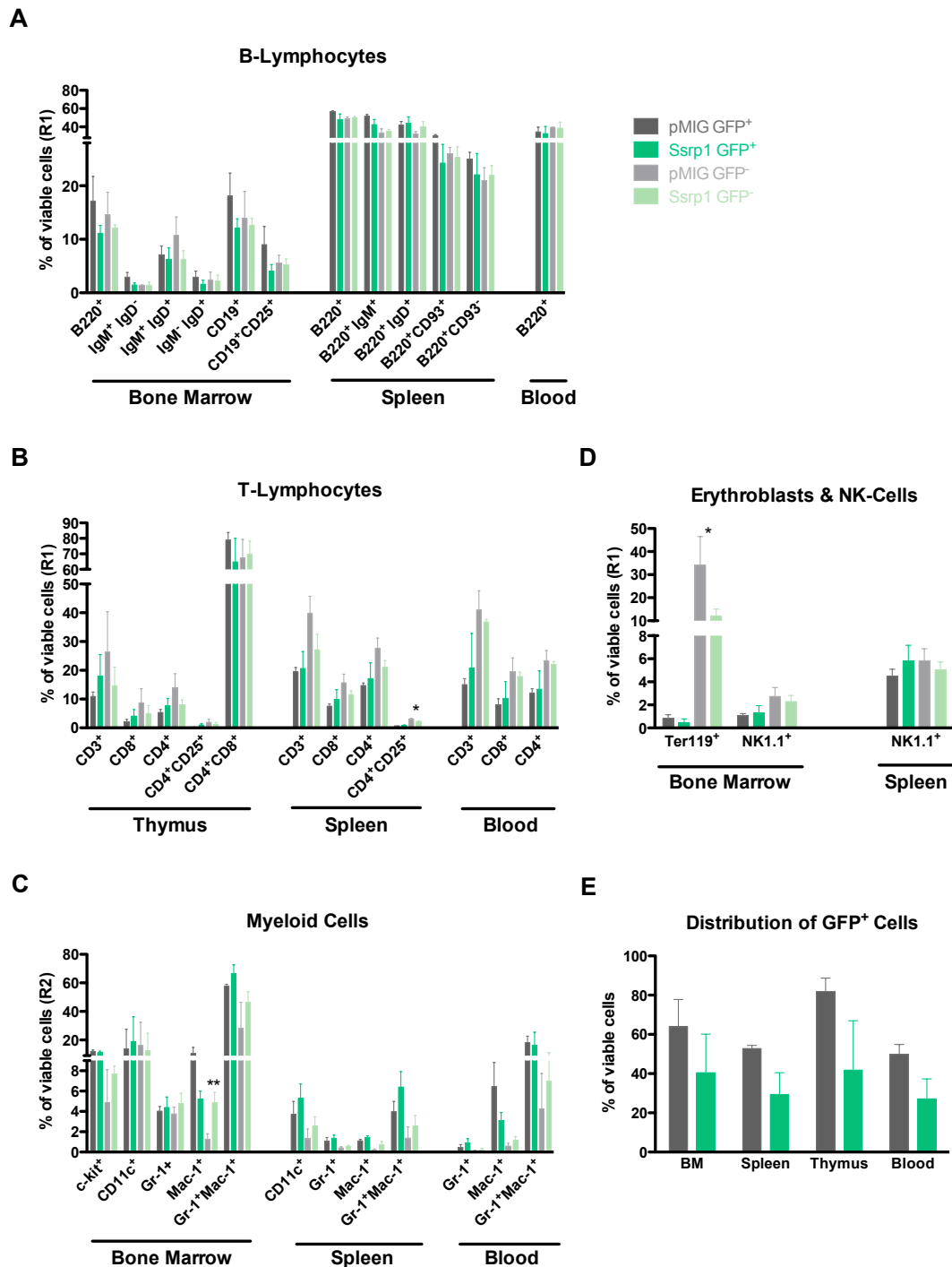
**Figure 2.11:** Comparative flow cytometric analysis of hematopoietic lineages in mice transplanted with Ssrp1 shRNA or empty vector (pMIG) infected bone marrow cells 8 weeks after injection. Percentages of GFP$^+$ (dark grey = pMIG, dark green = Ssrp1) or GFP$^-$ (light grey = pMIG, light green = Ssrp1) cells positive for the indicated lineage markers are shown in bars (mean values $\pm$ SEM, unpaired t test, n = 3 mice per group, * P < 0.05, ** P < 0.01). Individual panels show pooled results for the major blood cell compartments in the indicated tissues: (A) B-cells, (B) T-cells, (C) myeloid cells and (D) erythroblasts and NK-cells. (E) Mean distribution of GFP$^+$ cells in Ssrp1 knock-down (green) and pMIG control (grey) chimeras in the analyzed tissues. BM = bone marrow.

## 2.3.2 Analysis of bone marrow chimeras reconstituted with Symplekin down-regulated bone marrow cells

Symplekin is implicated in the control of polyadenylation-regulated translation, which is important in cell cycle progression and development [Lutz, 2008]. Moreover, Symplekin interacts with various transcription factors, such as the heat shock protein 1 or ZONAB, thereby regulating the expression of stress response genes as well as of cell cycle genes like Cyclin D1 [Xing et al., 2004; Buchert et al., 2009]. The amino acid sequence of the tight junction protein Symplekin is moderately conserved to its *Drosophila* homolog with 35% identical residues (http://www.ebi.ac.uk/ Tools/sss/ncbiblast). Interestingly, knock-down of Symplekin in fly hemocytes resulted in severe overproliferation of plasmatocytes and crystal cells in the developing larvae.

Thus, we analyzed its role in hematopoietic proliferation and homeostasis in mice by the transplantation of bone marrow cells with down-regulated Sympk expression. The lineage distribution of the $GFP^+$ cells, deficient in Sympk expression as well as $GFP^-$ wild-type cells in the bone marrow, spleen, thymus and peripheral blood was analyzed in recipient mice 8 weeks after reconstitution. Flow cytometric analysis showed that down-regulation of Sympk expression has various effects on the B-cell compartment. The percentage of $GFP^+B220^+$ lymphocytes is significantly decreased in the bone marrow, spleen as well as the peripheral blood compared to pMIG control mice. At the same time, the proportion of the $B220^+$ population in the $GFP^-$ subset is elevated in the bone marrow and the spleen compared to pMIG control mice as well as to the $GFP^+B220^+$ subset in Sympk knock-down chimeras, indicating a compensatory effect. Moreover, the percentage of $IgM^+IgD^-$ and $IgM^+IgD^+$ lymphocytes in the $GFP^+B220^+$ compartment is reduced in the bone marrow of Sympk knock-down chimeras. These mice also show a slight but significant decrease in the percentage of $B220^+IgM^+$ and $B220^+IgD^+$ as well as $B220^+CD93^+$ and $B220^+CD93^-$ splenocytes. The knock-down of Sympk further causes a significant reduction of $CD19^+$ B-cells as well $CD19^+CD25^+$ pre-B cells in the bone marrow (Figure 2.12A). In the T-cell compartment, the percentage of $CD3^+$ T-cells in the peripheral blood is significantly lower in Sympk knock-down chimeras than in pMIG control mice. This reduction is accompanied by a decreased proportion of $CD4^+$ helper T-cells in the blood, which show a slight but significant increase in the thymus. On the other hand, T-cell populations in the spleen are unaffected by the knock-down of Sympk (Figure 2.12B).

Interestingly, the bone marrow of Sympk knock-down chimeras harbors a significantly increased percentage of $GFP^+c\text{-}kit^+$ myeloid precursor cells. Moreover, the proportions of $Gr\text{-}1^+Mac\text{-}1^+$ immature myeloid cells is elevated in the bone marrow
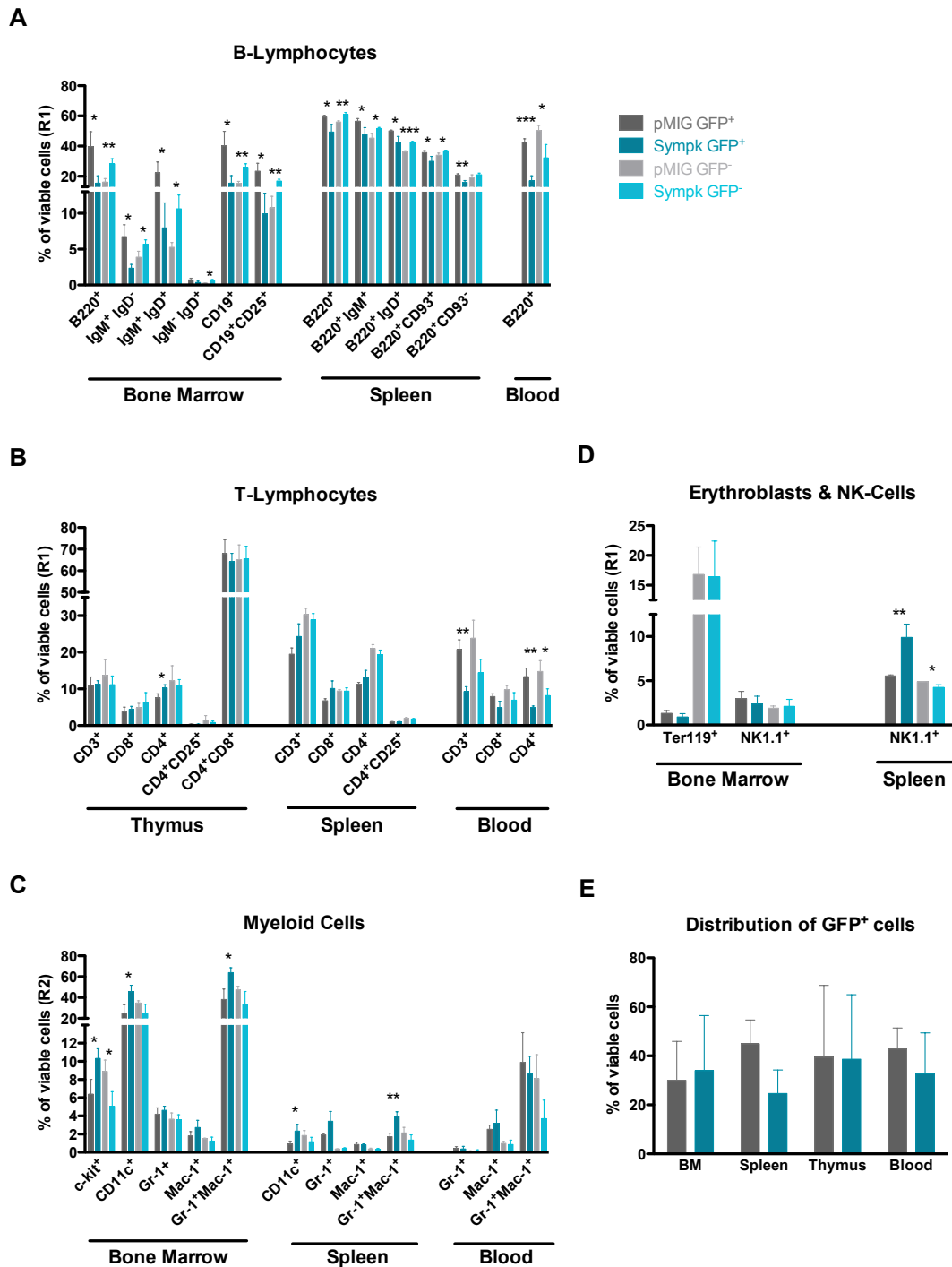
**Figure 2.12:** Flow cytometry data of mice reconstituted with Sympk deficient or control (pMIG) bone marrow 8 weeks after transplantation. Columns show the percentage of infected GFP$^+$ (dark grey = pMIG, dark blue = Sympk) and GFP$^-$ (light grey = pMIG, light blue = Sympk) cells expressing the indicated markers (mean values ±SEM; unpaired two-tailed t test; n = 3; * P < 0.05; ** P < 0.01; *** P < 0.001). Major lineages analyzed in the indicated tissues are clustered in subsequent panels: (A) B-cells, (B) T-cells, (C) myeloid cells and (D) erythroblasts and NK-cells. (E) Mean percentage of viable GFP$^+$ cells (±SEM) in the analyzed tissues are represented as bar graphs. BM = bone marrow.

and spleens of these mice compared to pMIG control chimeras. Additionally, the knock-down of Sympk results in a higher percentage of CD11c$^+$ dendritic cells in the bone marrow as well as the spleen. Interestingly, the ratios of Gr-1$^+$Mac-1$^+$ immature myeloid cells as well as CD11c$^+$ dendritic cells in the GFP$^-$ compartment are similar among Sympk knock-down chimeras and pMIG controls. In contrast, the c-kit$^+$ population shows a significantly decreased proportion in the GFP$^-$ subset of mice harboring Sympk down-regulated bone marrow and compared to pMIG control mice, again suggesting a compensatory effect (Figure 2.12C). Finally, in the spleen the percentage of NK1.1$^+$ natural killer cells is significantly increased in Sympk knock-down chimeras compared to pMIG control mice, while the ratio of this population is normal in the bone marrow (Figure 2.12D).

Taken together, these results indicate that Symplekin down-regulation negatively affects B-lymphocytes, whereas it positively contributes to the repopulation of the myeloid compartment, especially of immature myeloid precursor cells.

### 2.3.3 Repression of Rab5a or the overexpression of a dominant-negative Rab5a mutant show differential effects on bone marrow reconstitution

In the mouse, three isoforms of the *Drosophila* Rab5, namely Rab5a, Rab5b and Rab5c have been identified [Bucci et al., 1995]. The murine Rab5a shows 74% identity at the protein level to the fly Rab5, followed by Rab5c with 73% identity and Rab5b with 71% (http://www.ebi.ac.uk/Tools/sss/ncbiblast). Functionally, all three mammalian isoforms of the small GTPase Rab5 cooperate in the regulation of endocytosis [Bucci et al., 1995]. The fly screen conducted to identify novel conserved factors that regulate hematopoiesis during *Drosophila* development identified Rab5 as negative regulator of plasmatocyte proliferation and homeostasis. Moreover, knock-down of Rab5 in fly hemocytes resulted in an increase of the crystal cell compartment and promoted melanotic tumor formation. Considering that the function of Rab5a might be redundant in the mouse due to compensation by its isoforms Rab5b and Rab5c [Huang et al., 2004], two different approaches were chosen to address the role of the small GTPase in the hematopoietic system: First, a specific shRNA was used for gene silencing. Second, a dominant-negative mutant of Rab5a was overexpressed to interfere with the function of the wild-type protein. In the dominant-negative form, a serine was mutated to an asparagine at residue 34 (Rab5a:S34N) as described previously [Li and Stahl, 1993]. Due to this substitution, the protein has a 100 times higher affinity for GDP than GTP, thereby staying in the inactive GDP-bound state. Furthermore, this mutated form of Rab5a appears to have a more pronounced phenotypical effect on receptor-mediated endocytosis than a siRNA-driven knock-down [Dinneen and Ceresa, 2004; Huang et al., 2004]. To generate the dominant-negative mutant, the coding region of Rab5a was amplified from total cDNA extracted from mouse bone marrow cells and mutated by PCR based site-directed mutagenesis. The construct was then cloned into the same retroviral vector as the short hairpin RNAs (pMIG) for overexpression in bone marrow cells. Hematopoietic cells overexpressing this inactive version of Rab5a or a specific shRNA were again transplanted to lethally-irradiated recipient mice and their contribution to the reconstitution of the hematopoietic system was analyzed by flow cytometry after 8 weeks.

In the B-cell compartment, Rab5a knock-down chimeras show a significantly decreased percentage of $GFP^+B220^+$ lymphocytes in the peripheral blood as well as reduced proportions of $CD19^+CD25^+$ pro-B cells in the bone marrow (Figure 2.13A). However, mice expressing the mutated form of Rab5a display normal ratios of B-

cells in the bone marrow, spleen and blood compared to pMIG control mice (Figure 2.14A). Furthermore, in recipients reconstituted with Rab5a knock-down bone marrow a significantly reduced percentage of peripheral CD4$^+$ T-cell can be observed in the blood, while the ratio of this population in the thymus and the spleen was similar to pMIG control mice (Figure 2.13B). Interestingly, the percentage of CD4$^+$ helper T cells is also significantly reduced in the spleen of Rab5DN over-expressing chimeras. Furthermore, this T-cell population is slightly but not significantly reduced in the peripheral blood (Figure 2.14B).

In the myeloid compartment, different effects of the knock-down of Rab5a and the overexpression on immature myeloid cells can be observed. Mice reconstituted with Rab5a down-regulated bone marrow cells harbor a slight but significant increase of Gr-1$^+$Mac-1$^+$ immature myeloid cell in the spleen compared to pMIG control mice (Figure 2.13C), while this population is significantly elevated in the bone marrow of mice over-expressing the mutant form of Rab5a (Figure 2.14C). Moreover, the NK1.1$^+$ natural killer cells show a significantly increased percentage in the spleen of Rab5a knock-down chimeras (Figure 2.13D), while no significant changes can be observed in the dominant-negative mutant over-expressing chimeras (Figure 2.14D).

The chimeras harboring the Rab5a down-regulated bone marrow transplant display a significantly decreased percentages of Ter119$^+$ erythroblasts in the bone marrow (Figure 2.13D), while this reduction is not observed in the dominant-negative situation (Figure 2.14D). Nevertheless, the GFP$^+$ subset generally contributes only to a minor degree to erythroblasts reconstitution even in the pMIG control mice, thus changes in the GFP$^+$ erythroblast compartment might be highly variable. However, the inability of the GFP$^+$ population to reconstitute Ter119$^+$ erythroblasts might be an explanation why the attempt to reconstitute lethally-irradiated recipient mice with 100% GFP$^+$ bone marrow cells overexpressing the dominant-negative Rab5a failed. These mice died of severe anemia three weeks after transplantation. Importantly, this transplantation experiment was only lethal for mice receiving the Rab5DN over-expressing bone marrow. Control mice reconstituted with 100% GFP$^+$ bone marrow cells harboring the empty pMIG vector were healthy three weeks after transplantation. Furthermore, irradiation control mice that did not receive any bone marrow cells died after 12 days, in approximately 10 days before the recipients of the Rab5a mutant over-expressing bone marrow. Additionally, dominant-negative mutant over-expressing chimeras showed significantly lower numbers of white and red blood cells and platelets in the peripheral blood when compared to the pMIG control mice (Figure 2.15A, B, C). Moreover, we observed a significantly lower thymus and spleen weight in these mice (Figure 2.15D and E).
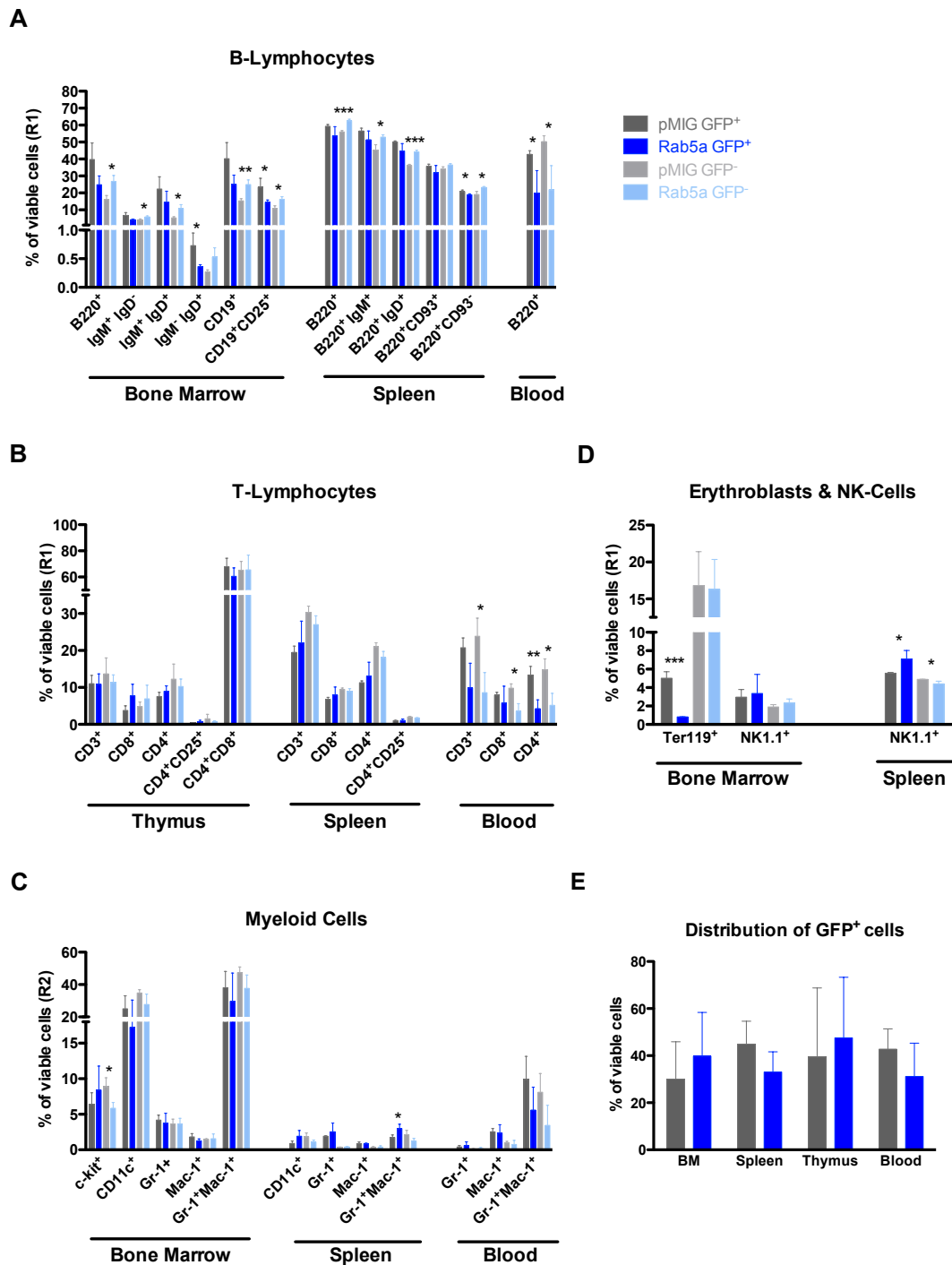
**Figure 2.13:** (A) B-cells, (B) T-cells, (C) myeloid cells and (D) erythroblasts and NK-cells, were analyzed in chimeras reconstituted with Rab5a shRNA knock-down or control (pMIG) bone marrow after 8 weeks. Percentages of transplanted GFP$^+$ (dark grey = pMIG, dark blue = Rab5a) and GFP$^-$ (light grey = pMIG, light blue = Rab5a) cells contributing to the depicted lineages were determined by flow cytometry. Data are shown as mean values $\pm$ SEM (n = 3 mice per group; unpaired two-tailed t test; * P < 0.05; ** P < 0.01; *** P < 0.001). (E) Distribution of GFP$^+$ cells in the analyzed tissues (n = 3). BM = bone marrow.
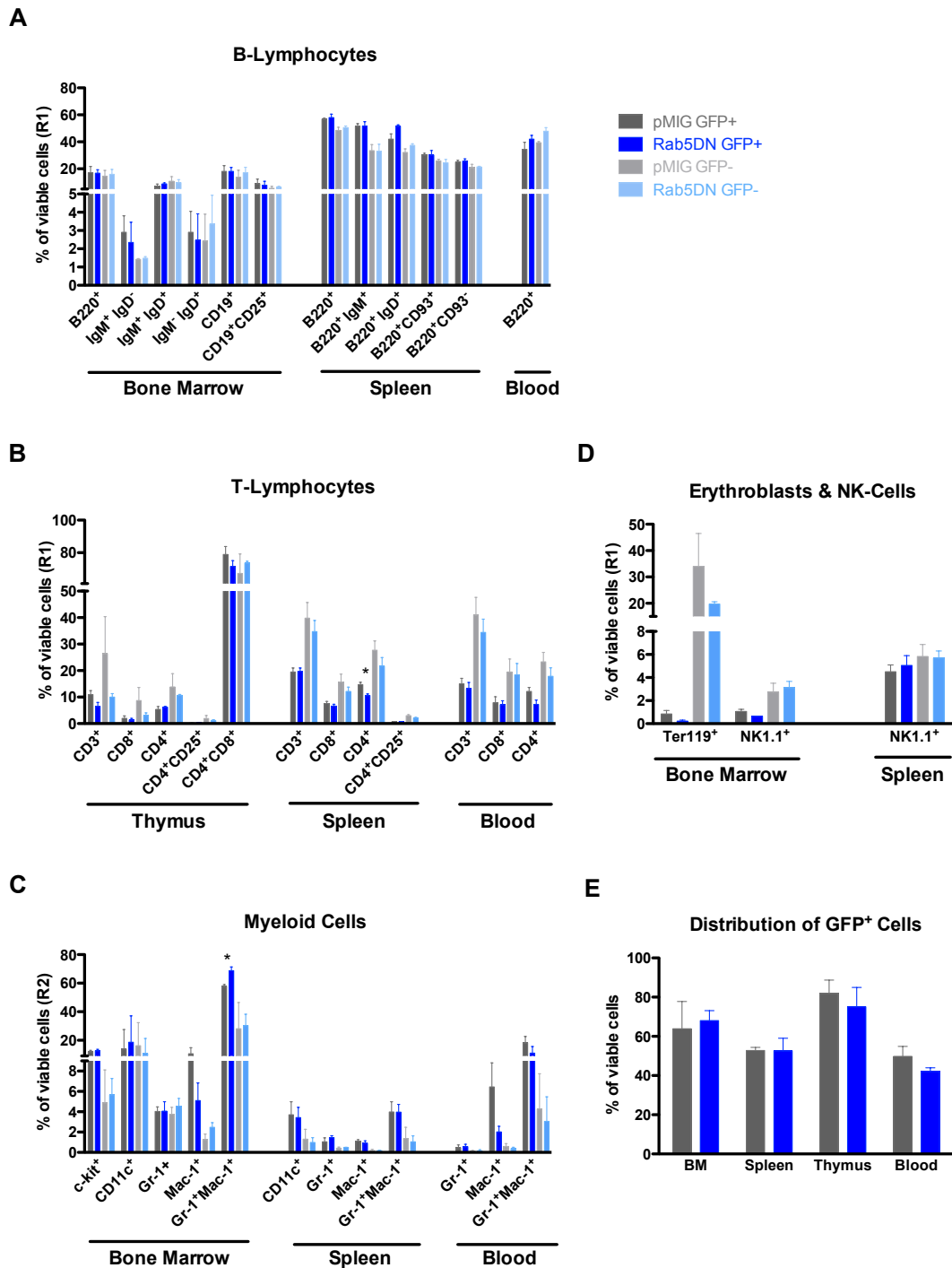
**Figure 2.14:** Flow cytometric analysis of bone marrow chimeras overexpressing a dominant-negative form of Rab5a in comparison with control (pMIG) mice. Major hematopoietic compartments are grouped in separate panels: (A) B-cells, (B) T-cells, (C) myeloid cells and (D) erythroblasts and NK-cells. Columns represent mean values of the percentage of GFP$^+$ (dark grey = pMIG, dark blue = Rab5DN) and GFP$^-$ (light grey = pMIG, light blue = Rab5DN) cells positive for the indicated markers (mean $\pm$ SEM, n = 3 mice per group; unpaired two-tailed t test; * P < 0.05). (E) Distribution of GFP$^+$ cells in the analyzed tissues (n = 3). BM = bone marrow.

Taken together, the knock-down of Rab5a and the interference with its wild-type function by over-expression of a dominant-negative form have different effects on the reconstitution of the various blood cell lineages. This finding is in line with the observation that these two approaches for abrogating the function of Rab5a results in differential phenotypic changes of the endocytic pathway.
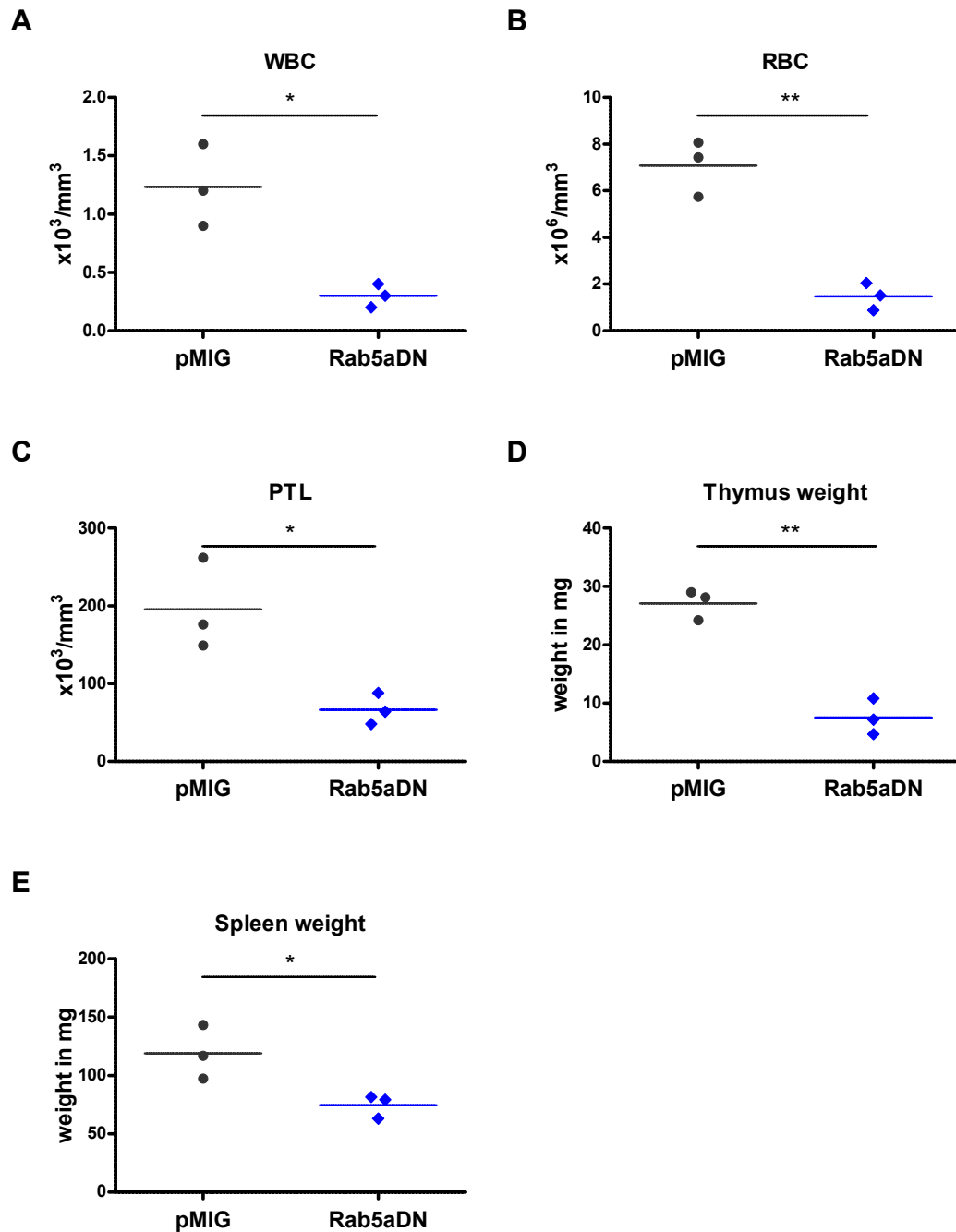
**Figure 2.15:** Bone marrow cells overexpressing a dominant-negative form of Rab5a fail to repopulate lethal-irradiated recipient mice. (A, B, C) Blood cell count of white (WBC) and red blood cells (RBC) as well as platelets (PTL) in recipients of bone marrow overexpressing Rab5aDN or the empty control vector pMIG. (D, E) Comparison of total thymus and spleen weights. Each dot represents result from a single mouse, lines indicate mean values (unpaired t test; n = 3 mice per group; * P < 0.05; ** P < 0.01).

### 2.3.4 Partial suppression of Vps16 has multiple effects on blood lineage reconstitution

Vps16 shares 35% identity with the *Drosophila* Vps16A at the protein level (http://www.ebi.ac.uk/Tools/sss/ncbiblast). Nevertheless, the mammalian homolog is functionally involved in the regulation of membrane fusion of endocytic vesicles as part of multimeric tethering complexes, such as HOPS or CORVET, similar to the *Drosophila* protein [Peplowska et al., 2007]. Moreover, the human HOPS complex was shown to interact with Rab5 and thus regulates endocytosis down-stream of this small GTPase [Rink et al., 2005]. Knock-down of Vps16A in hemocytes of the developing fly larvae resulted in a marked increase in the plasmatocyte population.

The relevance of the murine Vps16 in the hematopoietic system was addressed applying a bone marrow chimeric approach. Lethally-irradiated mice were reconstituted with Vps16 down-regulated bone marrow cells and the blood cell compartment was analyzed eight weeks after reconstitution. Flow cytometric analysis showed that the percentage of various B-cell populations is significantly decreased in the GFP$^+$ subset in the bone marrow, spleen and peripheral blood of Vps16 knock-down chimers. More precisely, the ratios of B220$^+$, IgM$^+$IgD$^-$, IgM$^+$IgD$^+$, IgM$^-$IgD$^+$ as well as of CD19$^+$ and CD19$^+$CD25$^+$ B-cells is reduced in Vps16 down-regulated chimeras compared to pMIG control mice. At the same time, a compensatory increase of the same populations can be observed in the GFP$^-$ subset. Moreover, B220$^+$, B220$^+$IgM$^+$, B220$^+$IgD$^+$ and B220$^+$CD93$^-$ B-cells population are as well slightly but significantly reduced in the spleen of these mice. In the peripheral blood similarly decreased proportions of B220$^+$ B-cells could be observed (Figure 2.16A). In the T-cell compartment, a highly significant reduction in the percentage of CD3$^+$, CD4$^+$ as well as CD8$^+$ T-cells is present in the peripheral blood of Vps16 knock-down chimeras, while the ratios of these populations are normal in the thymus and in the spleen (Figure 2.16B). Interestingly, a reduced percentage of CD4$^+$ T-cells could also be detected in the peripheral blood of chimeras receiving bone marrow cells with down-regulated Rab5a, which functions upstream of Vps16 in the endocytic pathway Rink et al. [2005]. Interestingly, the knock-down of Vps16 further results in a significantly higher percentage of c-kit$^+$ precursor cells in the bone marrow. Moreover, the percentages of GFP$^+$ cells of the myeloid compartment, namely Mac-1$^+$ and Gr-1$^+$ Mac-1$^+$ immature myeloid cells as well as CD11c$^+$ dendritic cells, are significantly increased in the bone marrow, while the ratio of Gr-1$^+$ granulocytic cells is slightly but significantly decreased. Of note, these elevated proportions of myeloid cells in the GFP$^+$ subset were accompanied by a compensatory decrease of the same populations in the GFP$^-$ subset in the Vps16 knock-down chimeras. Furthermore, similarly

elevated proportions of GFP$^+$ myeloid cells, namely CD11c$^+$ dendritic cells as wells as Mac-1$^+$ and Gr-1$^+$ Mac-1$^+$ cells could be detected in the spleen of Vps16 knock-down chimeras compared to pMIG control mice. In the peripheral blood, myeloid populations are similar among Vps16 knock-down and pMIG control chimeras (Figure 2.16C). In the natural killer cell department, a minor but significant decrease of NK1.1$^+$ cells could be observed in the bone marrow while the percentage of this population is significantly increased in the spleen of Vps16 down-regulated bone marrow chimeras (Figure 2.16D).

In summary, the down-regulation of Vps16 promotes the reconstitution of the myeloid lineage as well as of CD11c$^+$ dendritic cells, while resulting in a significant reduction in the percentage of B-cells. This results indicate a possible shift in differentiation in favor of the myeloid lineage.
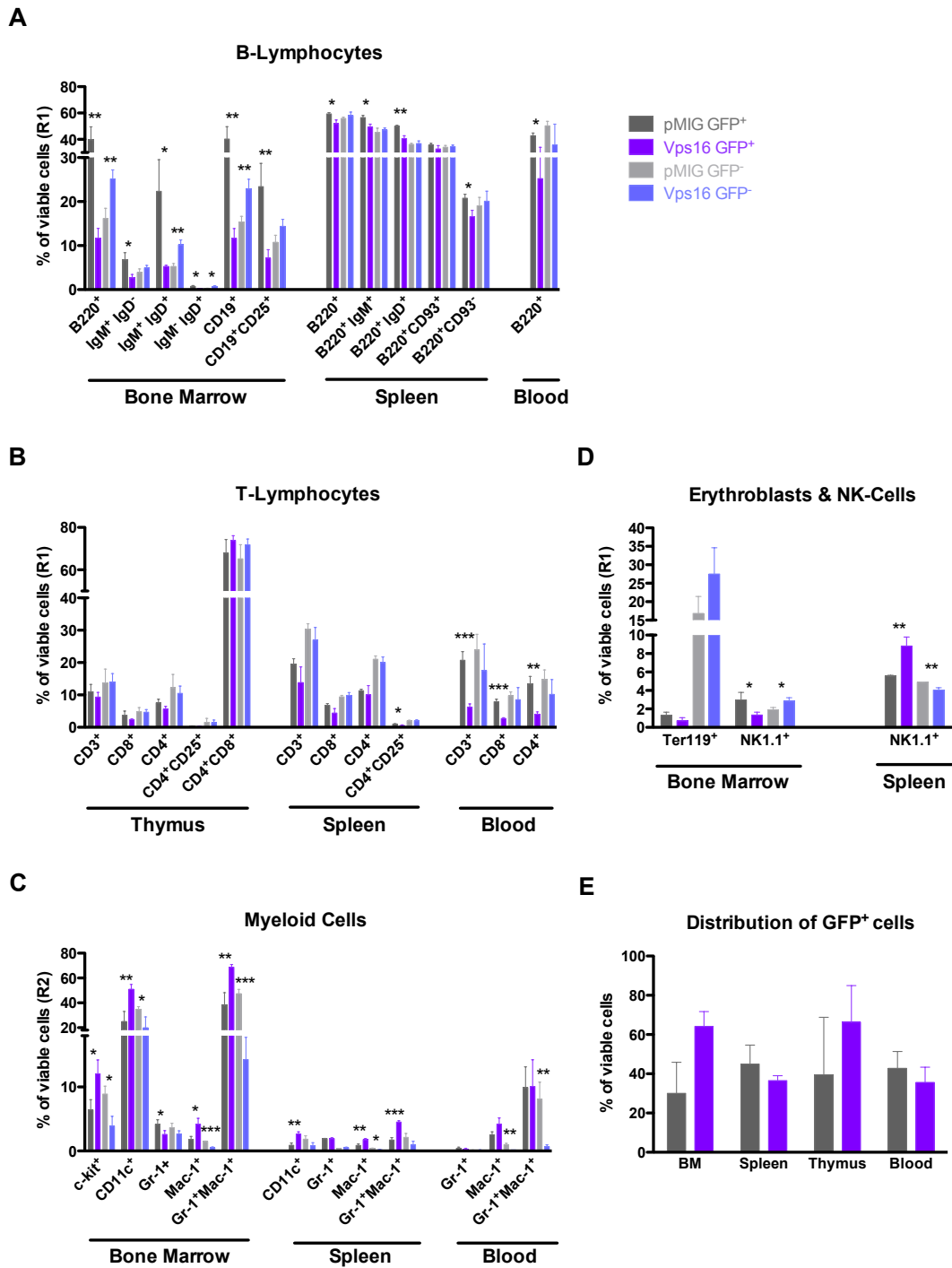
**Figure 2.16:** Comparative flow cytometric analysis of hematopoietic lineages in mice transplanted with Vps16 shRNA or empty vector (pMIG) infected bone marrow 8 weeks after injection. Percentages of GFP$^+$ (dark grey = pMIG, purple = Vps16) and GFP$^-$ (light grey = pMIG, light blue = Vps16) cells positive for the indicated lineage markers are represented as columns (mean values $\pm$ SEM; n = 3 mice per group; unpaired two-tailed t test; * P $<$ 0.05; ** P $<$ 0.01; *** P $<$ 0.001). (E) Distribution of GFP$^+$ cells in the analyzed tissues (n = 3). BM = bone marrow.

### 2.3.5 Reconstitution of lethally irradiated mice with Stx7 down-regulated bone marrow cells

The SNARE protein, Syntaxin 7, is another regulator along the endocytic pathway and mediates homotypic and heterotypic endosome fusion [Nakamura et al., 2000]. Protein alignment analysis revealed an identity of 39% between *Mus musculus* and *Drosophila melanogaster* (http://www.ebi.ac.uk/Tools/sss/ncbiblast). Interestingly, down-regulation of Stx7 expression in hemocytes in *Drosophila* larvae caused not only a severe overproliferation of macrophage-like plasmatocytes, it also induced the formation of melanotic tumors and an increase of the crystal cell population.

In order to address the function of Stx7 in the hematopoietic system, bone marrow reconstitution was analyzed in chimeric mice 8 weeks after transplantation. Interestingly, although the bone marrow used for reconstitution of irradiated hosts contained about 40% infected GFP$^+$ cells, the percentage of GFP$^+$ cells dropped enormously in all three recipients. The proportion of infected cells was reduced to about 2% in the bone marrow of these chimeras eight weeks after transplantation (Figure 2.17E). In contrast, the percentage-wise contribution of the remaining Stx7 knock-down cells to the major hematopoietic lineages is not impaired in these mice compared to pMIG control mice. In detail, the knock-down of Stx7 does not affect the B-cell compartment neither in the bone marrow and spleen nor in the peripheral blood (Figure 2.17A). Similarly in the T-cell compartment, the percentages of the various T-cell populations in the GFP$^+$ subset are similar among Stx7 knock-down chimeras and pMIG control mice (Figure 2.17B). Moreover, the proportion of c-kit$^+$ precursor cells, myeloid cells as well as CD11c$^+$ dendritic cells in the bone marrow are in the same range as in pMIG control chimeras. Interestingly, the percentage of Gr-1$^+$ granulocytes is significantly elevated in the spleens of Stx7 knock-down chimeras, while the peripheral blood harbors normal proportions of this population (Figure 2.17C). The ratios of erythroblasts as well as NK1.1$^+$ natural killer cells are not affected by the knock-down of Stx7 (Figure 2.17D).

Taken together, these results indicate that the down-regulation of Stx7 in bone marrow cells interferes with their ability to repopulate an irradiated recipient mouse, since a general loss of GFP$^+$ cells can be observed in all three recipient mice. Nevertheless, despite the decreased viability of GFP$^+$ cell *in vivo*, the percentage-wise distribution of the remaining GFP$^+$ cells is not overtly affected by the down-regulation of Stx7.
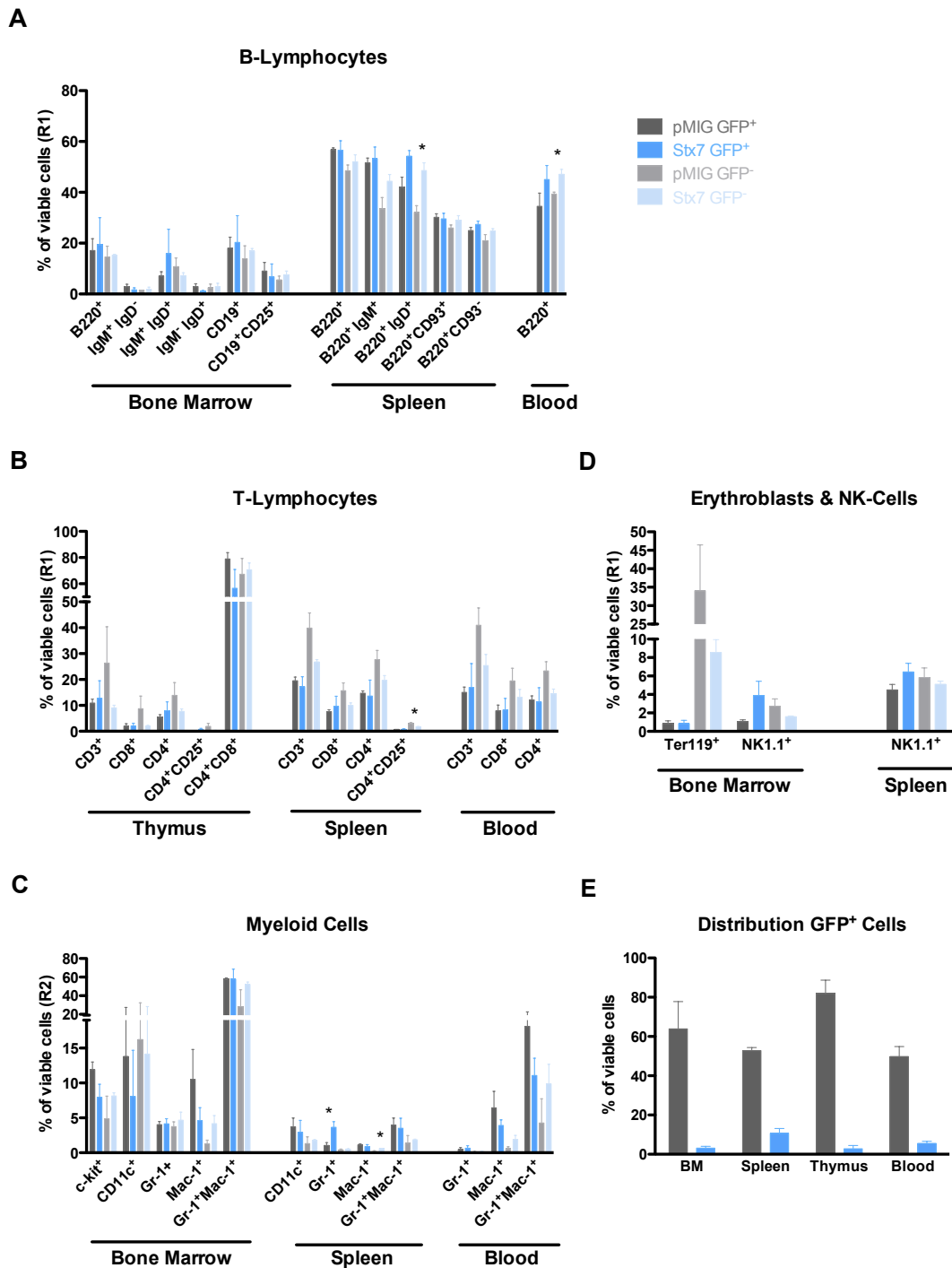
**Figure 2.17:** Flow cytometric analysis of (A) B-cells, (B) T-cells, (C) myeloid cells and (D) erythroblasts and NK-cells, isolated from bone marrow, spleen, thymus and peripheral blood of mice injected with Stx7 down-regulated or control bone marrow. Data are represented as the percentage of GFP$^+$ (dark grey = pMIG, blue = Stx7) or GFP$^-$ (light grey = pMIG, light blue = Stx7) cells positive for the indicated markers (mean values $\pm$ SEM, unpaired t test, n = 3 mice per group, * P < 0.05). (E) Mean distribution of GFP$^+$ cells in Ssrp1 knock-down (blue) and pMIG control (grey) chimeras in the analyzed tissues. BM = bone marrow.

### 2.3.6 Loss of Vps33a expression in bone marrow cells does not interfere with their repopulation capacity

The last candidate gene validated *in vivo* by the chimeric approach is Vps33a, which is, together with Vps16, part of the multimeric tethering complexes HOPS or CORVET, that coordinate Rab and SNARE function and provide specificity to lysosomal or endosomal fusion reactions, respectively [Peplowska et al., 2007]. In mammals, two homologs of Vps33p, namely Vps33a and Vps33b have been identified [Huizing et al., 2001]. Nevertheless, comparative genome analysis revealed that the *Drosophila* Vps33 gene carnation is closer related to Vps33a than Vps33b [Gissen et al., 2005]. At the protein level, the murine Vps33a shows 43% identity to its fruit fly homolog (http://www.ebi.ac.uk/Tools/sss/ncbiblast). The fly screen showed that the knock-down of the *Drosophila* homolog carnation in hemocytes of the developing larvae results in a marked expansion of the plasmatocyte and crystal cell populations.

In order to reveal its relevance in the mammalian hematopoietic system *in vivo*, blood lineage reconstitution was again analyzed in the chimeric transplantation model. Interestingly, all three bone marrow chimeras receiving the transplant with down-regulated Vps33a expression, showed an increase in the total percentage of GFP$^+$ cells from 45% prior to injection up to about 80% in the bone marrow and even more than 90% in the thymus eight weeks after transplantation (Figure 2.18E). However, the overall increase of Vps33a down-regulated cells does not translate into a percentage-wise increase of any major blood cell lineage. More precisely, the percentages of various B-cell lineages in the bone marrow, spleen and peripheral blood are similar among Vps33a knock-down chimeras and pMIG control mice (Figure 2.18A). Additionally, the knock-down does not affect the T-cell compartment, since there are no significant differences in the proportions of any T-lymphocyte population compared to pMIG control mice (Figure 2.18B). The contribution of Vps33a knock-down cells to the myeloid lineage in the bone marrow and spleen as well as the peripheral blood is similar to pMIG control mice (Figure 2.18C). Furthermore, the proportion of NK cells and Ter119$^+$ erythroblast in the bone marrow and the spleen is not impaired by the knock-down of Vps33a (Figure 2.18D).

In summary, these data indicate that the function of Vps33a might be more redundant in the hematopoietic system than of its binding partner Vps16, probably due to compensation by its paralog Vps33b [Gissen et al., 2005].
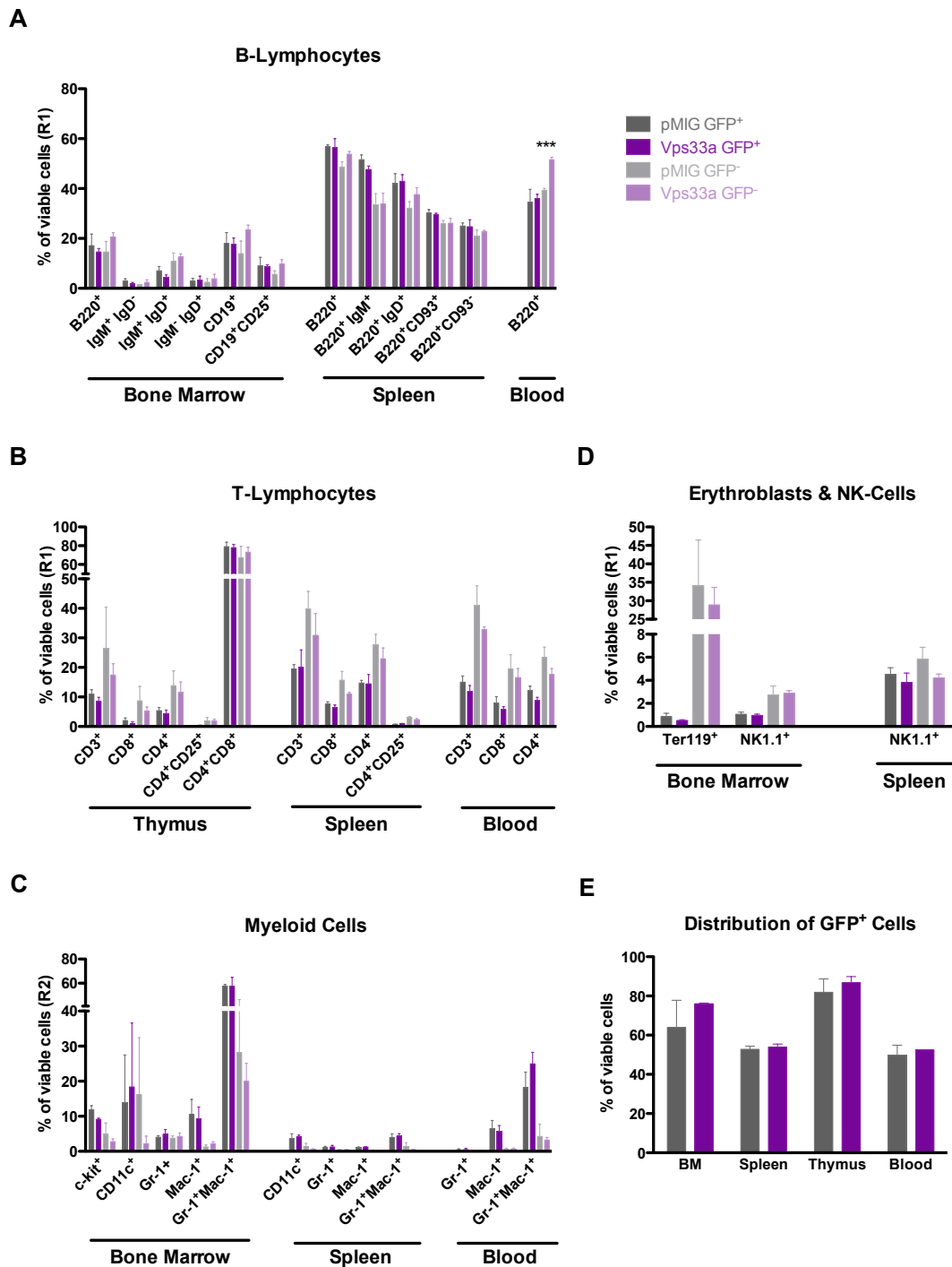
**Figure 2.18:** Flow cytometry analysis of mice reconstituted with Vps33 deficient or control (pMIG) bone marrow 8 weeks after transplantation. Columns show the percentage of infected cells expressing the indicated markers (mean values ±SEM, unpaired t test; n = 3 mice per group, *** P < 0.001). Major lineages analyzed in the stated organs are clustered in subsequent panels: (A) B-cells, (B) T-cells, (C) myeloid cells and (D) erythroblasts & natural killer cells. (E) Mean distribution of GFP+ cells in Vps33a knock-down (purple) and pMIG control (grey) chimeras in the analyzed tissues. BM = bone marrow.

## 2.4 Generation and characterization of a transgenic mouse line overexpressing a dominant-negative form of Rab5a

Considering the strong phenotype observed in *Drosophila* lacking Rab5 expression in plasmatocytes, as well as the interesting functionality of the protein as a small regulatory GTPase involved in endocytosis, we decided to generate a transgenic mouse line conditionally overexpressing the dominant-negative mutant of Rab5a, to study its function in hematopoiesis more precisely. Therefore, we introduced the same serine to asparagine substitution at amino acid residue 34 (S34N) by PCR based site-directed mutagenesis as described previously [Li and Stahl, 1993]. The mutated Rab5a coding region was subcloned into the pIRES-EGFP2 vector (Figure 2.19A), then excised together with the IRES-EGFP sequence and inserted into the pCCALL2 vector [Novak et al., 2000] (Figure 2.19B). Following Cre mediated recombination, the chicken ß-actin promoter and the CMV enhancer control high expression of the transgene together with the GFP reporter via the internal ribosome entry site (IRES).

**A**　　　　　　　　　　　　　　　　**B**
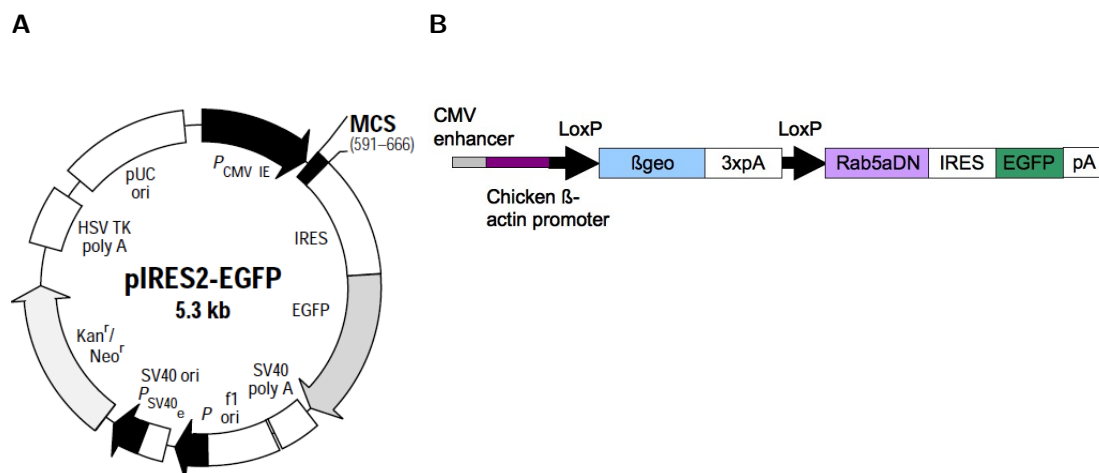


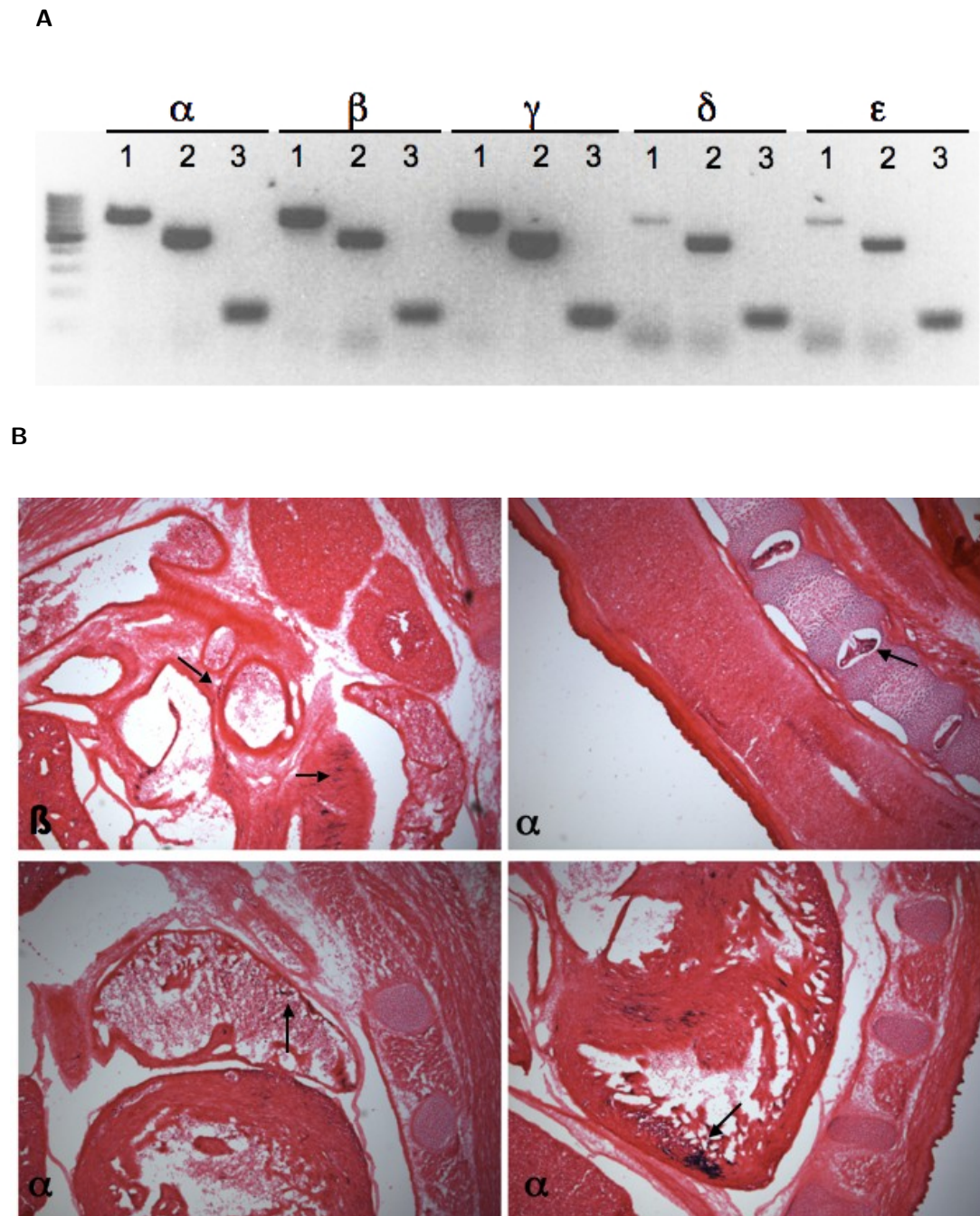**Figure 2.19:** Generation of Rab5aDN transgenic mice. (A) Vector map of pIRES2-EGFP used for subcloning of the Rab5aDN construct to add the IRES-EGFP sequence. (B) Schematic of the linearized pCALL2-Rab5aDN-IRES-EGFP vector used for pronuclear injection.

In total 5 founder lines harboring the transgene were generated by pronuclear injection, hereafter referred to as Rab5aDN lines α, β, γ, δ and ε. The presence of the transgene in the chromosomal DNA of the founder animals was confirmed by PCR (Figure 2.20A). In order to analyze transgene expression in the offspring, we took advantage of lacZ/neomycin fusion gene (ßgeo) [Friedrich and Soriano, 1991] that is inserted in the stop cassette between the two LoxP sites. Thus, prior to Cre-mediated recombination the animals express the enzyme ß-galactosidase, which is able to hydrolyse X-Gal to Galactose and a detectable blue chromophore [Friedrich and Soriano, 1991]. The two male founder mice α and β were crossed to C57BL/6 females and LacZ staining was performed on frozen sections of the embryos isolated on embryonic day E13.5. Unfortunately, only poor LacZ expression could be detected in the striated muscle of the heart, the lung and the spinal cord in the α line and in muscle and connective tissue in the ß line (Figure 2.20B).

Since the LacZ assay is not very sensitive and high expression levels of ß-galactosidase are needed, the mRNA abundance of the transgene was determined by RT-PCR. For this purpose, the α, β and γ founder lines were crossed to Vav-iCre mice, that specifically deletes the stop cassette and induces transgene expression in hematopoietic tissues in the offspring [de Boer et al., 2003]. The resulting mice from this cross, that were either positive for the dominant-negative Rab5a transgene (DN$^+$) or double positive for Rab5aDN and cre (DN$^+$Cre$^+$), were sacrificed at 6 weeks of age and the mRNA expression levels of neomycin (Neo) were analyzed in the bone marrow, spleen and thymus. Thus, only mice carrying the transgene, but not Cre, should be positive for neomycin expression since the ßgeo cassette is lost upon recombination. In the ß line, no expression of neomycin could be detected in any of the analyzed organs. Additionally, the expression in the α line seems to be rather unspecific, since the first two animals express neomycin in the bone marrow, but not in the spleen or thymus, whereas the third DN$^+$mouse shows Neo expression in the thymus but not in the other two tissues. However, the offspring of the γ founder line shows strong expression of neomycin in the bone marrow as well as the thymus in the mouse harboring only the transgene. Importantly, the abundance of neomycin mRNA is significantly reduced in γ mice positive for cre (Figure 2.21).

**A**



**B**



**Figure 2.20:** Characterization of Rab5aDN transgenic lines. (A) Presence of the transgene in genomic DNA of the founder animals was verified by PCR using the following primers: Neo (1), the cloning primers Rab5DN1 and Rab5DN4 (2) and the qPCR primers mRab5a_for and mRab5a_rev (3). For primer sequences see Material and Methods. (B) Male founders of the α and β line were crossed to wildtype C57BL/6 females and the tissue distribution of transgene expression was analyzed by LacZ staining of frozen sections of whole embryos at day E13.5. Arrows indicate areas positive for ß-galactosidase expression.

Taken together, the Rab5aDN transgenic γ line seems to be a promising candidate for further evaluation of the function of Rab5a in the hematopoietic system. We are currently crossing this line to Vav-iCre mice, which leads to conditional overexpression of the dominant-negative mutant in all hematopoietic cells. Afterwards, we will determine if Vav-γRab5aDN mice harbor any hematological abnormalities. Moreover, we hope that these mice will allow us to answer the open questions raised by the results of the Rab5a knock-down and dominant-negative mutant overexpressing bone marrow chimeras.
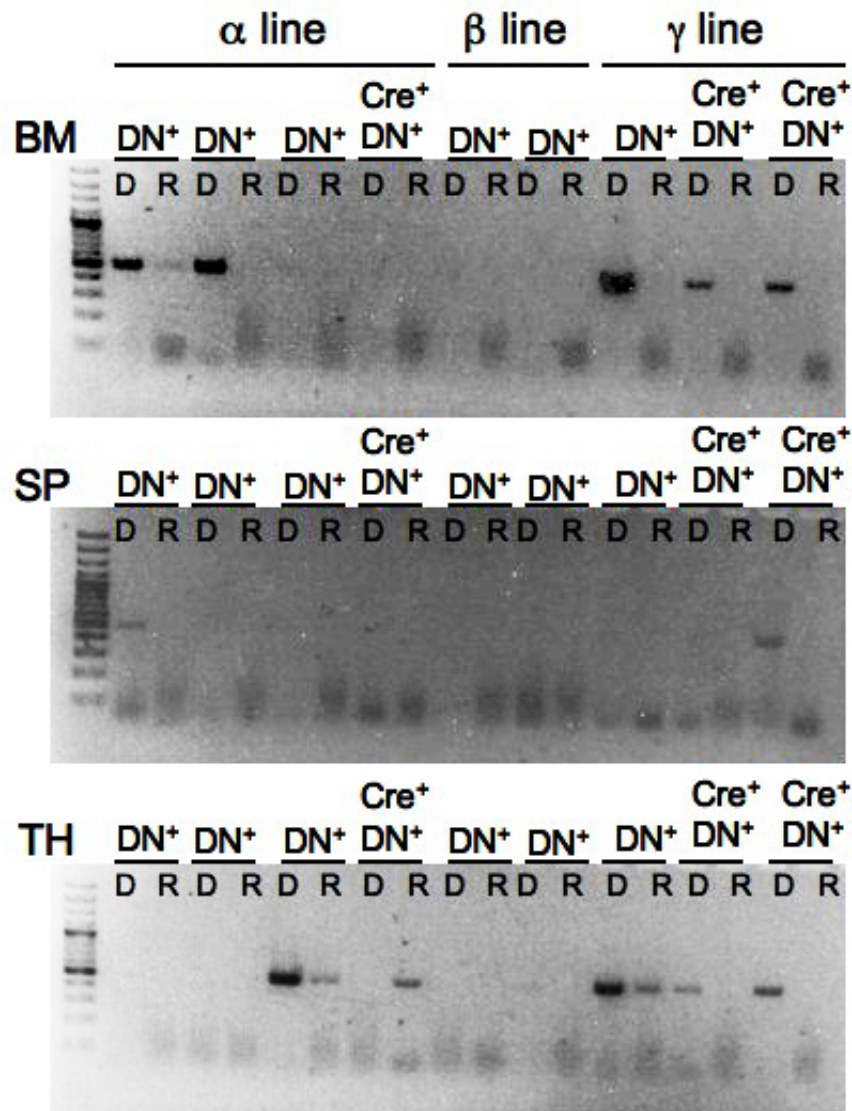
**Figure 2.21:** Expression of the transgene in the offspring of the α, β and γ lines was determined in the bone marrow (BM), spleen (SP) and thymus (TH) of individual mice by RT-PCR using Neo primers. Total RNA was isolated and converted into cDNA (D). Untreated RNA (R) was used to test for contamination of genomic DNA.

## 2.5 Papilin

The knock-down of Papilin in *Drosophila* hemocytes caused one of the most prominent phenotypes in the hematopoiesis screen, namely marked overproliferation of plasmatocytes and melanotic tumor formation in the fly larvae. Papilin is a large extracellular matrix (ECM) glycoprotein [Campbell et al., 1987] with homologs found in nematodes, mice and humans. The Papilin found in *Mus musculus* shows a protein identity of 39% to its *Drosophila* homolog (http://www.ebi.ac.uk/Tools/sss/ncbiblast). Functionally, Papilin is suggested to play a regulatory role in development, organogenesis and angiogenesis by modulating the activity of ADAMTS metalloproteinases [Kramerova et al., 2003]. Since, the precise function of papilin in development is still elusive and more importantly its possible role in the hematopoietic system has never been addressed in mammals so far, a conditional knock-out mouse was generated [Elling et al., unpublished]. Papilin complete knock-out mice (Papilin KO) are viable and do not display any obvious defects.

In order to test whether the absence of Papilin expression causes any phenotypic effects in the hematopoietic system in adult mice, the major blood cell lineages of 10 week old Papilin KO as well as wildtype littermates were analyzed by flow cytometry. The relative weight of the spleen appears to be slightly increased in Papilin KO mice compared to wild-type or heterozygous littermates, although the difference is not significant. The relative thymus weight is similar among mutant and wildtype mice (Figure 2.22A). Interestingly, the blood cell count revealed a significantly decreased percentage as well as overall number of granulocytes in the peripheral blood of Papilin KO mice (Figure 2.22B, C). The flow cytometric analysis did not show any major differences of the blood cell populations in Papilin KO mice compared to wild-type or heterozygous littermates. A minor increase in the total percentage of CD19$^+$ B-cells can be observed in the bone marrow as well as the lymph nodes (Figure 2.22D). In the myeloid compartment, a slight decrease in the percentage of c-kit$^+$ precursor cells was detected (Figure 2.22E). Of note, one of the three Papilin KO mice showed a more than 4-fold increase in the percentage of Gr-1$^+$ granulocytic cells in the bone marrow. Taken together, these preliminary results indicate a possible role for Papilin in granulocyte differentiation or homeostasis. Further analysis, especially of older mice, which might show a more prominent phenotype, will be necessary to specifically rule out the relevance of Papilin in the hematopoietic compartment.
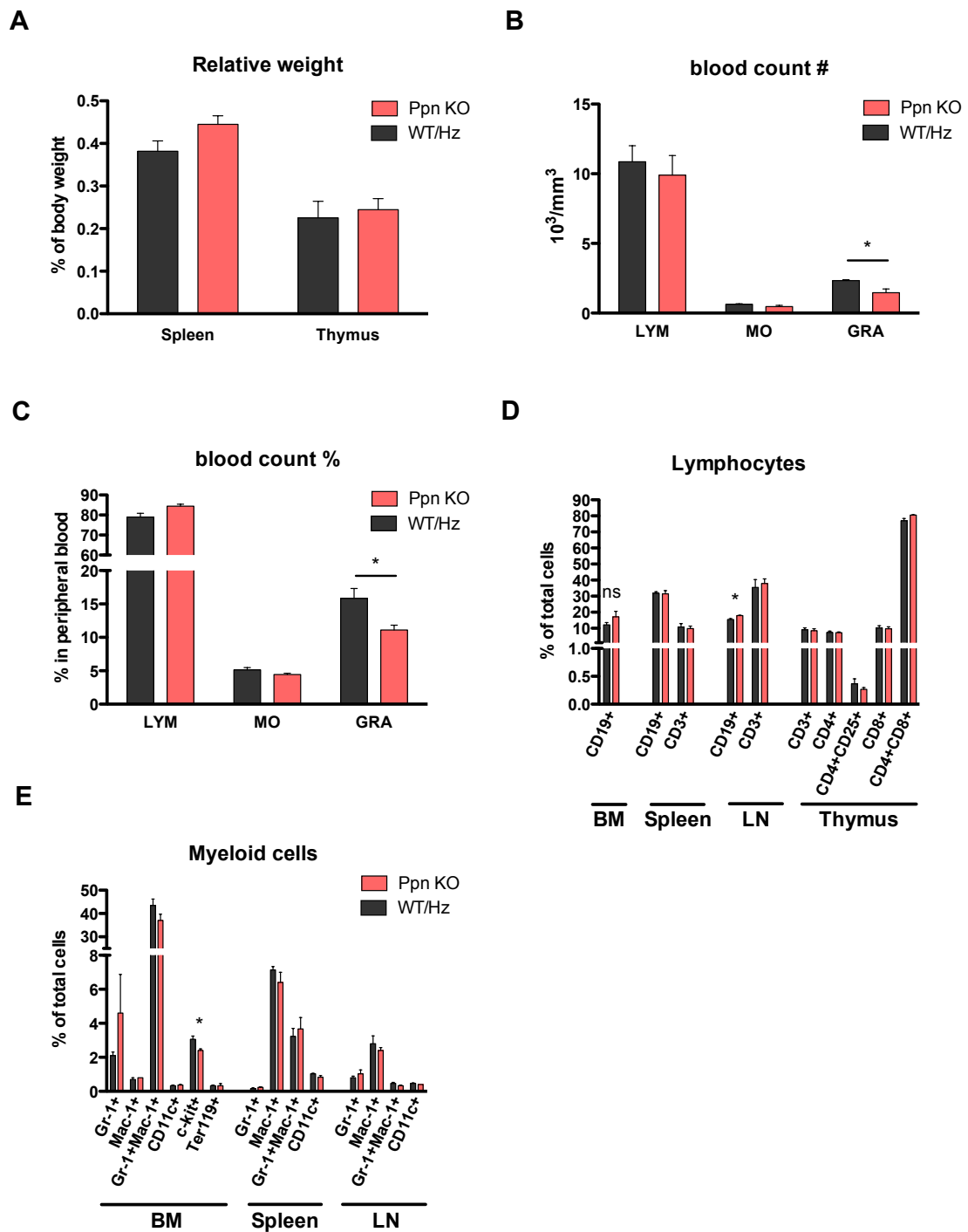
**Figure 2.22:** Analysis of the hematopoietic compartment in Papilin (Ppn) KO mice. (A) Relative weight of spleen and thymus represented as percentage of body weight of 10-week old Papilin KO mice as well as littermate controls (wildtype and heterozygous). (B, C) Blood count of lymphocytes (LYM), monocytes (MO) and granulocytes (GRA) in Papilin KO mice and littermate controls. Data are shown as cell number per $mm^3$ (C) or percentage (D) of peripheral blood. (D, E) Major hematopoietic populations in the bone marrow (BM), spleen, lymph node (LN) and thymus were analyzed by flow cytometry. Data are shown as percentage of total viable cells positive for the indicated marker. Data are shown as mean $\pm$ SEM (t test; n = 3 mice per group; * P < 0.05; ns = not significant).

## Contributions

All the experiments shown here were done by myself, except the following: Ulrich Elling conducted the fly screen and generated the conditional Papilin knock-out mice. Moreover, he supervised the selection of the candidate genes and helped with the isolation of bone marrow cells for the generation of the bone marrow chimeras and dissection of chimeras for flow cytometric analysis.

# 3 Discussion

The genes analyzed here for their role in the hematopoietic system were initially identified in a genome-wide RNAi screen conducted to determine novel regulators of blood cell development as well as homeostasis that are conserved among flies and mammals. The down-regulation of the candidate genes in the fly larvae by RNA interference resulted in fruit fly "leukemia" characterized by massive overproliferation of plasmatocytes as well as the formation of melanotic tumors. Seven of the identified potential tumor suppressor genes were further validated for their importance in blood cell formation in mammals. Functionally, two of the candidates, namely Symplekin and Ssrp1, are implicated in transcriptional regulation, while four other selected genes, specifically Rab5a, Stx7, Vps16 and Vps33a, regulate various crucial steps along the endocytic pathway. The last candidate, Papilin, is proposed to act as a metalloproteinase inhibitor, which suggests a possible association to tumor progression and metastasis.

The generation of bone marrow chimeras allowed us to determine whether bone marrow cells with down-regulated expression of the selected genes are still capable to reconstitute a lethally irradiated host and to what extent these cells contribute to hematopoietic cell lineages. We could show that the down-regulation of two out of six genes, namely Symplekin and Vps16, preferentially promotes the repopulation of the myeloid lineage, leading to an increased percentage of immature or mature myeloid cells in the bone marrow and spleen. Interestingly, knock-down of these two genes was also associated with an increased contribution to the c-kit$^+$ precursor compartment. On the other hand, down-regulation of Vps16 and Sympk, additionally caused a decrease in the proportion of B-cells in the bone marrow, spleen and peripheral blood, while in Rab5a knock-down chimeras B220$^+$ cells were only reduced in the peripheral blood. At the same time, the down-regulation of these two candidate genes had a negative effect on reconstitution of the T-cell compartment, demonstrated by a reduced representation of peripheral T-cells in the blood of Sympk and Vps16 knock-down chimeras. In contrast to this under-representation of various GFP$^+$ B- and T-lymphocyte lineages in these chimeras, the percentage of the third lymphocyte population, namely natural killer cells, is elevated in the spleen compared to pMIG

control mice. On the other hand, the percentage of NK1.1$^+$ natural killer cells was reduced in the bone marrow of Vps16 knock-down chimeras. Moreover, these chimeras harbored an increased percentage of CD11c$^+$ in the bone marrow and the spleen. Together, these results indicate that the knock-down of Symplekin and Vps16 promotes an early lineage shift in favor of myeloid cells. Furthermore, the expansion of c-kit$^+$ cells in Sympk and Vps16 chimeric mice was correlated with an increase in the proportion of immature or mature myeloid cells, arguing against a differentiation block as explanation for the increased c-kit$^+$ precursor population.

Interestingly, the recipient mice reconstituted with Rab5a down-regulated bone marrow cells, showed a similar but much milder reconstitution phenotype than the Symplekin and Vps16 knock-down chimeras. More precisely, the knock-down of Rab5a in the bone marrow transplant resulted in a significantly decreased percentage of B220$^+$ B-cells and CD4$^+$ T-cells in the peripheral blood of recipient mice, while the proportion of NK1.1$^+$ natural killer cells was elevated in the spleen. Moreover, immature myeloid cells were slightly increased in the spleens of these chimeras. However, these results could only be reproduced to some extent in chimeras harboring bone marrow cells that over-express a dominant-negative mutant form of Rab5a. More precisely, these chimeras displayed a decreased percentage of CD4$^+$ T-cells in the spleen, but not in the peripheral blood. Moreover, unlike Rab5a knock-down chimeras Rab5a mutant mice harbored a increased percentage of immature myeloid cells in the bone marrow and not in the spleen. Furthermore, the over-expression of dominant-negative Rab5a had no negative effect on the repopulation of the B-cell compartment. An explanation for these findings might be that these two approaches to interfere with the function of Rab5a have differential effects on receptor-mediated endocytosis. The overexpression of the dominant-negative mutant leads to an accumulation of small vesicles and inhibits endocytosis [Stenmark et al., 1994], while the knock-down of Rab5a alone seems not to interfere with receptor-mediated endocytosis [Huang et al., 2004]. Thus, these data indicate that the phenotypic changes observed in Rab5a knock-down chimeras, especially the negative effect on the B-cell compartment, might be independent of interference with receptor-mediated endocytosis.

Interestingly, the most prominent changes in reconstitution were observed in the bone marrow chimeras harboring the least efficient gene down-regulation, particularly in the case of Vps16 and Symplekin. A recent study applying a similar chimeric approach to identify novel tumor suppressor genes by RNA interference, showed that there is an inverse correlation between shRNA potency and proliferative advantage, due to a negative selection against cells harboring a potent shRNAs *in vivo* [Bric

et al., 2009]. Thus, bone marrow cells harboring a moderate knock-down might be more likely to promote phenotypical changes. Importantly, this effect could as well explain the massive decrease of GFP$^+$ cells in the recipients reconstituted with Stx7 down-regulated bone marrow, since the shRNA against Stx7 appears to confer one of the most potent knock-downs *in vivo.*

Strikingly, all lineages showing an increased percentage upon knock-down of Symplekin, Rab5a or Vps16 belong to innate branch of the immune system, namely myeloid cells or NK-cells. This finding could be explained by the restriction of the *Drosophila* immune system to innate immunity [Reumer et al., 2010]. These results underline the close relationship of fly plasmatocytes to the mammalian myeloid lineage and support an evolutionary link between natural killer cells and fly hemocytes.

Nevertheless, we were not successful in recapitulating the complete severe phenotype observed in fly larvae, namely a myeloproliferative disorder (MPD) or even leukemia in mice. Moreover, the knock-down of three of the candidate genes, namely Ssrp1, Stx7, and Vps33a, in the bone marrow did not reveal any marked phenotypical changes in any of the hematopoietic lineages. This is not surprising considering that for instance acute myeloid leukemias develop as a consequence of at least two types of genetic alterations: One mutation that interferes with normal hematopoietic differentiation and a second hit that confers a proliferative and/or survival advantage [Gilliland et al., 2004; Schindler et al., 2009; Mercher et al., 2009]. Thus, mice harboring only the chromosomal translocation frequently found in human leukemias, mainly develop myeloproliferative disease with a long latency and rare leukemia with low penetrance after six months of age [Ono et al., 2005]. Importantly, introduction of an additional oncogenic lesion promotes full recapitulation of the leukemic phenotype observed in humans [Zuber et al., 2009]. Thus, testing the relevance of the identified genes in an already cancer-prone background, such as the oncogenic E$_\mu$-myc lymphoma mouse model or the AML1/ETO fusion oncoprotein driven myeloid leukemia model [Adams et al., 1985; Yuan et al., 2001], might allow us to determine whether the candidates would promote tumorigenesis. Moreover, the introduction of an internal control by co-transplanting wild-type bone marrow cells expressing a different fluorescent protein such as RFP or dsRed Zuber et al. [2009] or the use of congenic donor and recipient mice, such as CD45.1 and CD45.2 or Thy1.1 and Thy1.2, would allow us to compare only the transplanted hematopoietic cells with down-regulated gene function with wild-type cells in the same mouse. Additionally, this approach would help enable us to exclude secondary effects caused by incomplete deprivation of hematopoietic cells in the recipient and possible antiviral immune responses against the transplant.

Finally, we could detect a significant reduction of peripheral granulocytes in Papilin KO mice as well as a massive increase of Gr-1$^+$ granulocytes in the bone marrow of one of these mice. These data suggest that mature granulocytes might accumulate in the bone marrow leading to a general decrease in the circulation. We also found a decreased percentage of c-kit$^+$ precursor cells in the bone marrow, which could as well explain the reduction of granulocytes in the peripheral blood. Notably, the blood count does not distinguish between mature or immature cells, thus it would be interesting to determine more precisely by flow cytometry which population is affected in the peripheral blood. Taken together, these preliminary results indicate that Papilin might indeed contribute to either myeloid cell differentiation or migration. Further analysis of additional mice will be necessary to elucidate the effects of Papilin down-regulation on the various blood cell compartments.

In summary, the present study indicates that the conserved factors identified to regulate proliferation and homeostasis of blood cells in the fruit fly *Drosophila melanogaster*, to some degree also play a role in hematopoiesis in mice.

# 4 Material and Methods

## 4.1 Antibodies

For flow cytometric analysis, the following antibodies from were used: PE-conjugated Ter119 (Pharmingen #09085B); PE-conjugated CD4 (Pharmingen #553049); PE-conjugated IgD (Pharmingen #558597); APC-conjugated CD117/c-kit (Pharmingen #01909A); APC-conjugated CD11c (Pharmingen #550261); APC-conjugated CD3 (Pharmingen #01089A); biotinylated IgM (Pharmingen #02082D); biotinylated NK1.1 (Pharmingen #01292D); biotinylated CD25 (Pharmingen #01092D); PE-Cy5-conjugated CD19 (Pharmingen #551001); PE-Cy5-conjugated Gr-1 (eBioscience #15-5931-82); PE-Cy5-conjugated CD44 (Pharmingen #553135); PE-Cy7-conjugated B220 (eBioscience #25-0452-82); PE-Cy7-conjugated CD93 (eBioscience #25-5892-82); PE-Cy7-conjugated CD8$\alpha$ (eBioscience #25-0081-81); PE-Cy7-conjugated CD11b/Mac-1 (Pharmingen #552850); APC-Cy7-conjugated B220 (eBioscience #10-0452-81); APC-Cy7-conjugated CD25 (eBioscience #10-0251-81); APC-Cy7-conju-gated CD8$\alpha$ (Pharmingen #557654); and streptavidin-PacBlue (Invitrogen #S11222).

## 4.2 Viral vector and cloning

Three specific small hairpin RNAs (shRNAs) were designed for each gene using the online algorithm "RNAi Oligo Retriever" at RNAi Central (http://katahdin.cshl.org:9331/homepage/siRNA/RNAi.cgi?type=shRNA). The hairpins were generated by PCR amplification of a 97 basepair long single stranded oligonucleotide (Sigma, HPLC purified) using the common primers miR30 FWD and miR30 REV (Table 4.1) and were ligated into the LMP microRNA-adapted retroviral vector (Open Biosystems, Huntsville, AL).

**Table 4.1:** Sequences of PCR primers used for cloning of shRNAs and of the single-stranded oligonucleotides used to amplify the shRNAs.

| Oligo name | Sequence (5' - 3') |
|---|---|
| miR30 FWD | CAGAAGGCTCGAGAAGGTATATTGCTGTTGACAGTGAGCG |
| miR30 REV | CTAAAGTAGCCCCTTGAATTCCGAGGCAGTAGGCA |
| mSsrp1_shOligo1 | TGCTGTTGACAGTGAGCGACCTCGGGATCTGATGAATAAATAGTGAAGCCACAGATGTATTTATTCATCAGATCCCGAGGCTGCCTACTGCCTCGGA |
| mSsrp1_shOligo2 | TGCTGTTGACAGTGAGCGCGCCCAGAATGTTCTGTCAAAGTAGTGAAGCCACAGATGTACTTTGACAGAACATTCTGGGCATGCCTACTGCCTCGGA |
| mSsrp1_shOligo3 | TGCTGTTGACAGTGAGCGCGGGCTTAAACTGCTCACAAAGTAGTGAAGCCACAGATGTACTTTGTGAGCAGTTTAAGCCCATGCCTACTGCCTCGGA |
| mRab5a_shOligo1 | TGCTGTTGACAGTGAGCGCCCTAATATTGTGATAGCTTTGTAGTGAAGCCACAGATGTACAAAGCTATCACAATATTAGGATGCCTACTGCCTCGGA |
| mRab5a_shOligo2 | TGCTGTTGACAGTGAGCGCTGACAACAGCTTATTATTTATTAGTGAAGCCACAGATGTAATAAATAATAAGCTGTTGTCATTGCCTACTGCCTCGGA |
| mRab5a_shOligo3 | TGCTGTTGACAGTGAGCGCGGCAAGCAAGTCCTAATATTGTAGTGAAGCCACAGATGTACAATATTAGGACTTGCTTGCCTTGCCTACTGCCTCGGA |
| mStx7_shOligo1 | TGCTGTTGACAGTGAGCGCGCTGATATTATGGACATTAATTAGTGAAGCCACAGATGTAATTAATGTCCATAATATCAGCTTGCCTACTGCCTCGGA |
| mStx7_shOligo2 | TGCTGTTGACAGTGAGCGCTGAGAGAGAGTCTTCAATCAGTAGTGAAGCCACAGATGTACTGATTGAAGACTCTCTCTCATTGCCTACTGCCTCGGA |
| mStx7_shOligo3 | TGCTGTTGACAGTGAGCGATCCGACTCATTCATGAGAGAGTAGTGAAGCCACAGATGTACTCTCTCATGAATGAGTCGGAGTGCCTACTGCCTCGGA |

| mVps16_shOligo1 | TGCTGTTGACAGTGAGCGCACTGAGGAACTGTTG GAGAAATAGTGAAGCCACAGATGTATTTCTCCAA CAGTTCCTCAGTATGCCTACTGCCTCGGA |
|---|---|
| mVps16_shOligo2 | TGCTGTTGACAGTGAGCGAGCCATTAAGCTGCTG GAGTATTAGTGAAGCCACAGATGTAATACTCCAG CAGCTTAATGGCCTGCCTACTGCCTCGGA |
| mVps16_shOligo3 | TGCTGTTGACAGTGAGCGCACAGTGTTGCTGCAC CTAAAGTAGTGAAGCCACAGATGTACTTTAGGTG CAGCAACACTGTATGCCTACTGCCTCGGA |
| mSympk_shOligo1 | TGCTGTTGACAGTGAGCGCGCTGAGGAGGTCATG GAATACTAGTGAAGCCACAGATGTAGTATTCCAT GACCTCCTCAGCTTGCCTACTGCCTCGGA |
| mSympk_shOligo2 | TGCTGTTGACAGTGAGCGCCGAGAGTATGTGGAG AAATTTTAGTGAAGCCACAGATGTAAAATTTCTC CACATACTCTCGATGCCTACTGCCTCGGA |
| mSympk_shOligo3 | TGCTGTTGACAGTGAGCGATCAGGCACTCTGGAC AAATATTAGTGAAGCCACAGATGTAATATTTGTC CAGAGTGCCTGAGTGCCTACTGCCTCGGA |
| mVps33a_shOligo1 | TGCTGTTGACAGTGAGCGAACTGATAAGGTCAAC AGTTACTAGTGAAGCCACAGATGTAGTAACTGTT GACCTTATCAGTGTGCCTACTGCCTCGGA |
| mVps33a_shOligo2 | TGCTGTTGACAGTGAGCGCGCTGAGAATGTACTC AGTGAGTAGTGAAGCCACAGATGTACTCACTGAG TACATTCTCAGCATGCCTACTGCCTCGGA |
| mVps33a_shOligo3 | TGCTGTTGACAGTGAGCGCGCACATACTGACCTT GAACAATAGTGAAGCCACAGATGTATTGTTCAAG GTCAGTATGTGCTTGCCTACTGCCTCGGA |

## 4.3 Packaging cell line and retroviral production

Ecotropic Platinum-E (Plat-E) retroviral packaging cells (THP Medical Products, Vienna, Austria) were grown under standard conditions (37°C, 5 $CO_2$) in growth medium (DMEM, 10% FCS, 100 U/ml penicillin, 100 µg/ml streptomycin) containing 10 µg/ml blasticidin and 1 µg/ml puromycin. One day before transfection, $6x10^6$ cells were plated onto a 10cm dish in growth medium without antibiotics. After 24 hours cell were transfected with 9 µg DNA using Fugene 6 (Roche Diagnostics GmbH,

Vienna, Austria) according to manufacturers protocol. Transfection efficiency was analyzed by flow cytometry for GFP-expressing cells. Viral particles in the supernatant were collected 36h, 48h, 56h and 64h after transfection and sterile-filtered through a 45 μm syringe filter.

## 4.4 Bone Marrow Chimeras

Male 6 to 8 weeks old C57BL/6J wildtype mice were injected with 2.5mg 5-fluorouracil in PBS intraperitoneally (i.p.). Four days after injection, bone marrow cells were isolated from the fore- and hindlimbs by flushing the long bones (humerus, tibia and femur) with a syringe with PBS containing 4% FCS. After red blood cell lysis with ACK buffer, cells were prestimulated overnight in growth medium (DMEM, 10% FCS, 100 U/ml penicillin, 100 μg/ml streptomycin, 1% L-Glutamine) supplemented with 50 ng/ml recombinant mouse IL-6 (rmIL-6) and 50 ng/ml rmSCF, as well as 20 ng/ml rmIL-3 (PeproTech Austria, Vienna) at a density of $1x10^6$ cells/ml. For the first infection, $1x10^7$ cells were seeded onto RetroNectin-coated plates (Takara, Japan), that were preincubated with viral supernatant for 4 hours at 37°C, in cytokine containing growth medium. The second, third and fourth infection was performed after 8h, 16h or 48h, respectively, by adding fresh sterile-filtered viral supernatant supplemented with the cytokine mix on top of the cells. 12h to 16h after the last infection, bone marrow cells were washed three times with PBS, counted and infection efficiency was determined by flow cytometry. Subsequently, $1.2x10^6$ cells were transplanted into lethally gamma-irradiated (10Gy), 6 week old C57BL/6J mice via tail-vein injection (3 mice per genotype). After injection, mice were treated with 10mg/ml Enrofloxacin (Baytril, Bayer) in the drinking water for 7 days, to prevent infection. Six to eight weeks after reconstitution, mice were sacrificed and the major blood cell lineages were analyzed by flow cytometry.

## 4.5 Flow Cytometry

Bone marrow chimeras were sacrificed by carbon dioxide asphyxiation and peripheral blood, bone marrow, spleen and thymus were isolated. After red blood cell lysis, single cell suspensions were incubated for 15 min with 2.5 μg/ml mouse Fc block (PD Pharmingen) in PBS containing 4% FCS on ice. Cells were washed once, 200 μl primary antibody mix per sample was added and incubated on ice for 30 min in the dark. First antibody was washed out, followed by incubation with secondary antibody for 30 min at 4°C covered from light. Stained cells were washed three

times and samples were analyzed with a PD LSRFortessa cell analyzer using the BD FACSDiva software.

## 4.6 Generation of a dominant-negative mouse line

The full length murine Rab5a was amplified and muted by two step PCR-based mutagenesis using the primers Rab5DN_1, Rab5DN_2, Rab5DN_3 and Rab5DN_4 (Table 4.2) and inserted into the pIRES2-EGFP expression vector. The coding region of the Rab5aDN transgene was then excised together with the IRES-EGFP sequence and ligated into the pCALL2 vector. Insertion of the correct sequence was confirmed by sequencing. The vector was then linearized, the DNA was gel purified using the Elutrap Electroelution System (Whatman) and injected into male pronuclei of single-cell (FVB/N) embryos. Viable eggs were subsequently transferred to pseudo-pregnant B6CBAF1 recipients.

## 4.7 LacZ staining

Male six week old founder mice of the Rab5DN transgenic line α and β were crossed to wildtype C57BL/6 females. Whole embryos were isolated at day E13.5 of pregnancy and fixed in 2% paraformaldehyde in 1xPBS for 2h on ice. Embryos were cryoprotected in 20% sucrose in 1x PBS overnight at 4°C and embedded into Tissue-Tek OCT (Sakura) over dry ice. Blocks were cryosectioned at 10 μm, placed onto adhesion microscope slides (Super Frost Ultra Plus, Menzel), and dried for 2 h at room temperature before storage at -20°C. After re-hydration in 1xPBS , slides were stained in Bluo-Gal staining solution (1.0 mg/ml X-gal, 20 mM potassium ferrocyanide ($K_4(Fe(CN)_6)$), and 20 mM potassium ferricyanide ($K_3(Fe(CN)_6)$), 2 mM $MgCl_2$, 0.01% sodium deoxycholate, 0.02% Nonidet-P40 in 1xPBS) overnight at 37°C, protected from light. Afterwards slides were rinsed in PBS, counterstained with eosin and mounted with coverslips. Slides were analyzed with a Zeiss Axioskop 2 Plus upright microscope.

## 4.8 qRT-PCR

Total RNA was extracted from bone marrow cells, splenocytes, thymocytes or BaF/3 cells, respectively, using the RNeasy Mini Kit (Qiagen, Kat.No.: 74104). 3,3 μg of total RNA was converted to cDNA using Ready to go Beads (GE Healthcare, Cat. No. 27-9264-01) and random hexamers as primer. For quantitative (q)RT-PCR

analysis, 10ng of cDNA (diluted 1:10 with dH$_2$O) was mixed with iQ SYBR Green Real-Time PCR Supermix (BioRad) and the primers depicted in Table 4.2. Samples were analyzed as duplicates in a BioRad iG5 Multicolor real-time PCR Detection System.

## 4.9  Blood count

Mice were sacrificed and 20 µl of freshly collected blood was mixed with 5 µl of 0.5M EDTA (pH 8.0) to prevent blood clotting. Samples were analyzed twice with a Scil Vet abc animal blood counter.

**Table 4.2:** Sequences of used PCR primers and of the single-stranded oligonucleotides used to amplify the shRNAs.

| Oligo name | Sequence (5' - 3') |
|---|---|
| mVps16_for | ACTGTTACACTGCGAACTGG |
| mVps16_rev | CTCAGTAGAGCAATGGGACC |
| mStx7NEW_for | CGGAAGTTCACGTTCAACAG |
| mStx7NEW_rev | CCTTTCAGTCCCCATACGAT |
| NEWmVps33a_for | CGTGTTTGATAACCTCTTGCTG |
| NEWmVps33a_rev | TCTTGGGTGCAAACTTCTCTG |
| mSsrp1_for | GAAACGGGAACAGCTCAAAAG |
| mSsrp1_rev | GCATTAAGCCACAGCATGTAC |
| mRab5a_for | TGGTCAAGAACGGTATCATAGC |
| mRab5a_rev | GCCTTTGAAGTTCTTTAACCCAG |
| mSympk_for | CAGCTTCGAGAGTATGTGGAG |
| mSympk_rev | TGCTTCACTGTTTCCTCTGTC |
| mActb_F | CTTTGCAGCTCCTTCGTTG |
| mActb_R | CGATGGAGGGGAATACAGC |
| Rab5DN_1(BglII)_F | GAAGATCTGGACTTCTTTAAAATTTGGACATGG |
| Rab5DN_2(34N)_R | CGAAGAACCAGGCTATTTTTGCCAACAGCAG |
| Rab5DN_3(34N)_F | CTGCTGTTGGCAAAAATAGCCTGGTTCTTCG |
| Rab5DN_4(EcoRI)_R2 | GGAATTCCGGAGCTCAGTTACTACAACACTGG |
| Neo_forward | GTGGAGAGGCTATTCGGCTATGACT |
| Neo_reverse | CTTGAGCCTGGCGAACAGTTCGGCT |

# 5 Acknowledgements

Upon finishing this thesis, I would like to use this opportunity to thank all the people that helped along the way during my studies and enabled me to finish this thesis.

First, I want to thank Josef Penninger for offering my the opportunity to work on this interesting project in his laboratory and for thoroughly correcting this thesis. Moreover, special thanks goes to Ulrich Elling, who supervised my work and taught me many new things. I also want to thank all the members of the Penninger group for turning this year into a unique experience and always being helpful when needed.

Without any doubt, my endless gratefulness goes to my family who constantly supported me. First, I want to thank my sister Anna for having an open ear for my troubles and always offering good advice. Moreover, I want to thank my uncle Rudi for being like a father, when I needed one, and my aunt Christa, for always giving me the feeling that she is there for me no matter what happens. I am also grateful that my "Omi" is still able to supply me with the best "Kärntner Nudel" and always showing me that she is proud of her granddaughter. Last, I want to thank my father for his financial support thereby enabling me to study in Vienna.

At this point, I also want to especially thank Geri, who became my best friend in the course of studies. I am grateful because he showed me how to take life easier and because he believed in me in moments when I got hopeless. Finally, I also want to thank all my other friends for helping me to relax and get my mind of studying and work, while spending legendary nights out with me.

# Bibliography

Adams, J., Harris, A., Pinkert, C., Corcoran, L., Alexander, W., Cory, S., Palmiter, R., and Brinster, R. (1985). The c-myc oncogene driven by immunoglobulin enhancers induces lymphoid malignancy in transgenic mice. *Nature*, 318:533–538.

Adams, M., Celniker, S., Holt, R., Evans, C., Gocayne, J., Amanatides, P., Scherer, S., Li, P., Hoskins, R., and Galle, R. (2000). The genome sequence of drosophila melanogaster. *Science*, 287(5461):2185.

Agaisse, H., Petersen, U., Boutros, M., Mathey-Prevot, B., and Perrimon, N. (2003). Signaling role of hemocytes in drosophila jak/stat-dependent response to septic injury. *Developmental cell*, 5(3):441–450.

Alfonso, T. B. and Jones, B. W. (2002). gcm2 promotes glial cell differentiation and is required with glial cells missing for macrophage development in drosophila. *Developmental Biology*, 248(2):369–83.

Antonin, W., Holroyd, C., Fasshauer, D., Pabst, S., von Mollard, G., and Jahn, R. (2000). A snare complex mediating fusion of late endosomes defines conserved properties of snare structure and function. *The EMBO Journal*, 19(23):6453–6464.

Barnard, D., Ryan, K., Manley, J., and Richter, J. (2004). Symplekin and xgld-2 are required for cpeb-mediated cytoplasmic polyadenylation. *Cell*, 119(5):641–651.

Barton, G. M. and Kagan, J. C. (2009). A cell biological view of toll-like receptor function: regulation through compartmentalization. *Nature Reviews Immunology*, 9(8):535–42.

Belotserkovskaya, R., Oh, S., Bondarenko, V. A., Orphanides, G., Studitsky, V. M., and Reinberg, D. (2003). Fact facilitates transcription-dependent nucleosome alteration. *Science*, 301:1090–1093.

Belotserkovskaya, R. and Reinberg, D. (2004). Facts about fact and transcript elongation through chromatin. *Current Opinion in Genetics & Current Opinion in Genetics & Development*, (14):139–146.

Birk, D. M., Barbato, J., Mureebe, L., and Chaer, R. A. (2008). Current insights on the biology and clinical aspects of vegf regulation. *Vasc Endovascular Surg*, 42(6):517–30.

Biswas, D., Imbalzano, A., Eriksson, P., Yu, Y., and Stillman, D. (2004). Role for nhp6, gcn5, and the swi/snf complex in stimulating formation of the tata-binding protein-tfiia-dna complex. *Molecular and cellular biology*, 24(18):8312.

Bresnick, E., Lee, H., Fujiwara, T., Johnson, K., and Keles, S. (2010). Gata switches as developmental drivers. *Journal of Biological Chemistry*, 285(41):31087.

Bric, A., Miething, C., Bialucha, C. U., Scuoppo, C., Zender, L., Krasnitz, A., Xuan, Z., Zuber, J., Wigler, M., Hicks, J., Mccombie, R. W., Hemann, M. T., Hannon, G. J., Powers, S., and Lowe, S. W. (2009). Functional identification of tumor-suppressor genes through an in vivo rna interference screen in a mouse lymphoma model. *Cancer Cell*, 16(4):324–335.

Bucci, C., Lütcke, A., Steele-Mortimer, O., Olkkonen, V., Dupree, P., Chiariello, M., Bruni, C., Simons, K., and Zerial, M. (1995). Co-operative regulation of endocytosis by three rab5 isoforms. *FEBS letters*, 366(1):65–71.

Buchert, M., Darido, C., Lagerqvist, E., Sedello, A., Cazevieille, C., Buchholz, F., Bourgaux, J., Pannequin, J., Joubert, D., and Hollande, F. (2009). The symplekin/zonab complex inhibits intestinal cell differentiation by the repression of aml1/runx1. *Gastroenterology*, 137(1):156–164.

Calvo, O. and Manley, J. L. (2003). Strange bedfellows: polyadenylation factors at the promoter. *Genes & Development*, 17(11):1321–7.

Campbell, A., Fessler, L., Salo, T., and Fessler, J. (1987). Papilin: a drosophila proteoglycan-like sulfated glycoprotein from basement membranes. *Journal of Biological Chemistry*, 262(36):17605.

Cao, S., Bendall, H., Hicks, G., Nashabi, A., Sakano, H., Shinkai, Y., Gariglio, M., Oltz, E., and Ruley, H. (2003). The high-mobility-group box protein ssrp1/t160 is essential for cell viability in day 3.5 mouse embryos. *Molecular and cellular biology*, 23(15):5301.

Cho, N., Keyes, L., Johnson, E., Heller, J., Ryner, L., Karim, F., and Krasnow, M. (2002). Developmental control of blood cell migration by the drosophila vegf pathway. *Cell*, 108(6):865–876.

Christoforidis, S., McBride, H., Burgoyne, R., and Zerial, M. (1999a). The rab5 effector eea1 is a core component of endosome docking. *Nature*, 397(6720):621–625.

Christoforidis, S., Miaczynska, M., Ashman, K., Wilm, M., Zhao, L., Yip, S., Waterfield, M., Backer, J., and Zerial, M. (1999b). Phosphatidylinositol-3-oh kinases are rab5 effectors. *Nat Cell Biol*, 1(4):249–252.

Conner, S. D. and Schmid, S. L. (2003). Regulated portals of entry into the cell. *Nature*, 422(6927):37–44.

Daga, A., Karlovich, C., Dumstrei, K., and Banerjee, U. (1996). Patterning of cells in the drosophila eye by lozenge, which shares homologous domains with aml1. *Genes & Development*, 10(10):1194.

de Boer, J., Williams, A., Skavdis, G., Harker, N., Coles, M., Tolaini, M., Norton, T., Williams, K., Roderick, K., Potocnik, A. J., and Kioussis, D. (2003). Transgenic mice with hematopoietic and lymphoid specific expression of cre. *Eur J Immunol*, 33(2):314–25.

Dietzl, G., Chen, D., Schnorrer, F., Su, K.-C., Barinova, Y., Fellner, M., Gasser, B., Kinsey, K., Oppel, S., Scheiblauer, S., Couto, A., Marra, V., Keleman, K., and Dickson, B. J. (2007). A genome-wide transgenic rnai library for conditional gene inactivation in drosophila. *Nature*, 448(7150):151–156.

Dimarcq, J. L., Imler, J. L., Lanot, R., Ezekowitz, R. A., Hoffmann, J. A., Janeway, C. A., and Lagueux, M. (1997). Treatment of l(2)mbn drosophila tumorous blood cells with the steroid hormone ecdysone amplifies the inducibility of antimicrobial peptide gene expression. *Insect Biochem Mol Biol*, 27(10):877–86.

Dingli, D. and Pacheco, J. (2010). Modeling the architecture and dynamics of hematopoiesis. *WIREs Syst Biol Med*, 2(2):235–244.

Dinneen, J. and Ceresa, B. (2004). Expression of dominant negative rab5 in hela cells regulates endocytic trafficking distal from the plasma membrane. *Experimental cell research*, 294(2):509–522.

Duvic, B., Hoffmann, J., Meister, M., and Royet, J. (2002). Notch signaling controls lineage specification during drosophila larval hematopoiesis. *Current Biology*, 12(22):1923–1927.

Dzierzak, E. and Speck, N. A. (2008). Of lineage and legacy: the development of mammalian hematopoietic stem cells. *Nat Immunol*, 9(2):129–136.

Elagib, K., Racke, F., Mogass, M., and Khetawat..., R. (2003). Runx1 and gata-1 coexpression and cooperation in megakaryocytic differentiation. *Blood*.

Evans, C., Hartenstein, V., and Banerjee, U. (2003). Thicker than blood:: Conserved mechanisms in drosophila and vertebrate hematopoiesis. *Developmental cell*, 5(5):673–690.

Evans, C., Sinenko, S., Mandal, L., Martinez-Agosto, J., Hartenstein, V., and Banerjee, U. (2007). Genetic dissection of hematopoiesis using drosophila as a model system. *Advances in Developmental Biology*, 18:259–299.

Fessler, J., Kramerova, I., Kramerov, A., Chen, Y., and Fessler, L. (2004). Papilin, a novel component of basement membranes, in relation to adamts metalloproteases and ecm development. *The International Journal of Biochemistry & Cell Biology*, 36(6):1079–1084.

Fire, A., Xu, S., Montgomery, M., Kostas, S., Driver, S., and Mello, C. (1998). Potent and specific genetic interference by double-stranded rna in caenorhabditis elegans. *Nature*, 391(6669):806–811.

Formosa, T. (2008). Fact and the reorganized nucleosome. *Mol. BioSyst.*, 4(11):1085.

Fortini, M., Skupski, M., Boguski, M., and Hariharan, I. (2000). A survey of human disease gene counterparts in the drosophila genome. *The Journal of Cell Biology*, 150(2):F23.

Fossett, N., Hyman, K., Gajewski, K., Orkin, S., and Schulz, R. (2003). Combinatorial interactions of serpent, lozenge, and u-shaped regulate crystal cell lineage commitment during drosophila hematopoiesis. *Proceedings of the National Academy of Sciences of the United States of America*, 100(20):11451.

Friedrich, G. and Soriano, P. (1991). Promoter traps in embryonic stem cells: a genetic screen to identify and mutate developmental genes in mice. *Genes Dev*, 5(9):1513–1523.

Gabrilovich, D. I., Chen, H. L., Girgis, K. R., Cunningham, H. T., Meny, G. M., Nadaf, S., Kavanaugh, D., and Carbone, D. P. (1996). Production of vascular endothelial growth factor by human tumors inhibits the functional maturation of dendritic cells. *Nature Medicine*, 2(10):1096–103.

Gerber, H.-P. and Ferrara, N. (2003). The role of vegf in normal and neoplastic hematopoiesis. *J Mol Med*, 81(1):20–31.

Gilliland, D. G., Jordan, C. T., and Felix, C. A. (2004). The molecular basis of leukemia. *Hematology Am Soc Hematol Educ Program*, pages 80–97.

Gissen, P., Johnson, C., Gentle, D., Hurst, L., Doherty, A., O'Kane, C., Kelly, D., and Maher, E. (2005). Comparative evolutionary analysis of vps33 homologues: genetic and functional insights. *Human Molecular Genetics*, 14(10):1261.

Godin, I. and Cumano, A. (2002). The hare and the tortoise: an embryonic haematopoietic race. *Nature Reviews Immunology*, 2(8):593–604.

Goto, A., Kadowaki, T., and Kitagawa, Y. (2003). Drosophila hemolectin gene is expressed in embryonic and larval hemocytes and its knock down causes bleeding defects. *Developmental Biology*, 264(2):582–91.

Gould, G. and Lippincott-Schwartz, J. (2009). New roles for endosomes: from vesicular carriers to multi-purpose platforms. *Nat Rev Mol Cell Biol*, 10(4):287–292.

Haas, A. K., Fuchs, E., Kopajtich, R., and Barr, F. A. (2005). A gtpase-activating protein controls rab5 function in endocytic trafficking. *Nat Cell Biol*, 7(9):887–893.

Hartenstein, V. (2006). Blood cells and blood cell development in the animal kingdom. *Annu. Rev. Cell Dev. Biol.*, 22:677–712.

Hattori, K., Dias, S., Heissig, B., Hackett, N. R., Lyden, D., Tateno, M., Hicklin, D. J., Zhu, Z., Witte, L., Crystal, R. G., Moore, M. A., and Rafii, S. (2001). Vascular endothelial growth factor and angiopoietin-1 stimulate post-natal hematopoiesis by recruitment of vasculogenic and hematopoietic stem cells. *J Exp Med*, 193(9):1005–14.

Hedges, S., Blair, J., Venturi, M., and Shoe, J. (2004). A molecular timescale of eukaryote evolution and the rise of complex multicellular life. *BMC Evolutionary Biology*, 4(1):2.

Hertel, L., Andrea, M. D., Bellomo, G., Santoro, P., Landolfo, S., and Gariglio, M. (1999). The hmg protein t160 colocalizes with dna replication foci and is down-regulated during cell differentiation. *Experimental cell research*, 250(2):313–328.

Holz, A., Bossinger, B., Strasser, T., Janning, W., and Klapper, R. (2003). The two origins of hemocytes in drosophila. *Development*, 130(20):4955.

Horiuchi, H., Lippé, R., McBride, H., Rubino, M., Woodman, P., Stenmark, H., Rybin, V., Wilm, M., Ashman, K., and Mann, M. (1997). A novel rab5 gdp/gtp

exchange factor complexed to rabaptin-5 links nucleotide exchange to effector recruitment and function. *Cell*, 90(6):1149–1159.

Hou, S., Zheng, Z., Chen, X., and Perrimon, N. (2002). The jak/stat pathway in model organisms:: Emerging roles in cell movement. *Developmental cell*, 3(6):765–778.

Huang, F., Khvorova, A., Marshall, W., and Sorkin, A. (2004). Analysis of clathrin-mediated endocytosis of epidermal growth factor receptor by rna interference. *Journal of Biological Chemistry*, 279(16):16657.

Huizing, M., Didier, A., Walenta, J., Anikster, Y., Gahl, W., and Krämer, H. (2001). Molecular cloning and characterization of human vps18, vps 11, vps16, and vps33. *Gene*, 264(2):241–247.

Jiang, S.-Y. and Ramachandran, S. (2006). Comparative and evolutionary analysis of genes encoding small gtpases and their activating proteins in eukaryotic genomes. *Physiological Genomics*, 24(3):235–51.

Jimeno-Gonzalez, S., Gomez-Herreros, F., Alepuz, P. M., and Chavez, S. (2006). A gene-specific requirement for fact during transcription is related to the chromatin organization of the transcribed region. *Molecular and Cellular Biology*, 26(23):8710–8721.

Kavanagh, E., Buchert, M., Tsapara, A., Choquet, A., Balda, M. S., Hollande, F., and Matter, K. (2006). Functional interaction between the zo-1-interacting transcription factor zonab/dbpa and the rna processing factor symplekin. *Journal of Cell Science*, 119(24):5098–5105.

Keller, D. and Lu, H. (2002). p53 serine 392 phosphorylation increases after uv through induction of the assembly of the ck2Â · hspt16Â · ssrp1 complex. *Journal of Biological Chemistry*, 277(51):50206.

Keller, D., Zeng, X., Wang, Y., Zhang, Q., Kapoor, M., Shu, H., Goodman, R., Lozano, G., Zhao, Y., and Lu, H. (2001). A dna damage-induced p53 serine 392 kinase complex contains ck2, hspt16, and ssrp1. *Molecular Cell*, 7(2):283–292.

Kennerdell, J. and Carthew, R. (2000). Heritable gene silencing in drosophila using double-stranded rna. *Nature Biotechnology*, 18(8):896–898.

Keon, B., Schäfer, S., Kuhn, C., Grund, C., and Franke, W. (1996). Symplekin, a novel type of tight junction plaque protein. *The Journal of cell biology*, 134(4):1003–1018.

Kim, B., Krämer, H., Yamamoto, A., Kominami, E., Kohsaka, S., and Akazawa, C. (2001). Molecular characterization of mammalian homologues of class c vps proteins that interact with syntaxin-7. *Journal of Biological Chemistry*, 276(31):29393.

Kolev, N. and Steitz, J. (2005). Symplekin and multiple other polyadenylation factors participate in 3'-end maturation of histone mrnas. *Genes & Development*, 19(21):2583.

Kondo, M., Wagers, A. J., Manz, M. G., Prohaska, S. S., Scherer, D. C., Beilhack, G. F., Shizuru, J. A., and Weissman, I. L. (2003). Biology of hematopoietic stem cells and progenitors: implications for clinical application. *Annu. Rev. Immunol.*, 21:759–806.

Kramerova, I., Kawaguchi, N., Fessler, L., Nelson, R., Chen, Y., Kramerov, A., Kusche-Gullberg, M., Kramer, J., Ackley, B., and Sieron, A. (2000). Papilin in development; a pericellular protein with a homology to the adamts metalloproteinases. *Development*, 127(24):5475.

Kramerova, I. A., Kramerov, A. A., and Fessler, J. H. (2003). Alternative splicing of papilin and the diversity of drosophila extracellular matrix during embryonic morphogenesis. *Dev. Dyn.*, 226(4):634–642.

Krzemien, J., Oyallon, J., Crozatier, M., and Vincent, A. (2010). Hematopoietic progenitors and hemocyte lineages in the drosophila lymph gland. *Developmental Biology*, 346(2):310–319.

Kumano, K., Chiba, S., Kunisato, A., Sata, M., Saito, T., Nakagami-Yamaguchi, E., Yamaguchi, T., Masuda, S., Shimizu, K., Takahashi, T., Ogawa, S., Hamada, Y., and Hirai, H. (2003). Notch1 but not notch2 is essential for generating hematopoietic stem cells from endothelial cells. *Immunity*, 18(5):699–711.

Kumano, K., Chiba, S., Shimizu, K., Yamagata, T., Hosoya, N., Saito, T., Takahashi, T., Hamada, Y., and Hirai, H. (2001). Notch1 inhibits differentiation of hematopoietic cells by sustaining gata-2 expression. *Blood*, 98(12):3283–9.

Kumari, S., Mg, S., and Mayor, S. (2010). Endocytosis unplugged: multiple ways to enter the cell. *Cell Research*, (3):256–275.

Lanot, R., Zachary, D., Holder, F., and Meister, M. (2001). Postembryonic hematopoiesis in drosophila. *Developmental Biology*, 230(2):243–257.

Lebestky, T., Jung, S., and Banerjee, U. (2003). A serrate-expressing signaling center controls drosophila hematopoiesis. *Genes & Development*, 17(3):348.

Lemaitre, B. and Hoffmann, J. (2007). The host defense of drosophila melanogaster. *Annu. Rev. Immunol.*, 25(1):697–743.

Li, G. and Stahl, P. (1993). Structure-function relationship of the small gtpase rab5. *Journal of Biological Chemistry*, 268(32):24475.

Li, Y., Zeng, S. X., Landais, I., and Lu, H. (2007). Human ssrp1 has spt16-dependent and -independent roles in gene transcription. *J Biol Chem*, 282(10):6936–45.

Lindsell, C. E., Shawber, C. J., Boulter, J., and Weinmaster, G. (1995). Jagged: a mammalian ligand that activates notch1. *Cell*, 80(6):909–17.

Lopez-Bigas, N., De, S., and Teichmann, S. A. (2008). Functional protein divergence in the evolution of homo sapiens. *Genome Biol*, 9(2):R33.

Lutz, C. S. (2008). Alternative polyadenylation: a twist on mrna 3' end formation. *ACS Chem Biol*, 3(10):609–17.

Medvinsky, A., Rybtsov, S., and Taoudi, S. (2011). Embryonic origin of the adult hematopoietic system: advances and questions. *Development*, 138(6):1017–31.

Meister, M. (2004). Blood cells of drosophila: cell lineages and role in host defence. *Current opinion in immunology*, 16(1):10–15.

Mercher, T., Raffel, G. D., Moore, S. A., Cornejo, M. G., Baudry-Bluteau, D., Cagnard, N., Jesneck, J. L., Pikman, Y., Cullen, D., Williams, I. R., Akashi, K., Shigematsu, H., Bourquin, J.-P., Giovannini, M., Vainchenker, W., Levine, R. L., Lee, B. H., Bernard, O. A., and Gilliland, D. G. (2009). The ott-mal fusion oncogene activates rbpj-mediated transcription and induces acute megakaryoblastic leukemia in a knockin mouse model. *Journal of Clinical Investigation*, pages 1–13.

Minakhina, S. and Steward, R. (2010). Hematopoietic stem cells in drosophila. *Development*, 137(1):27–31.

Nakamura, N., Hirata, A., Ohsumi, Y., and Wada, Y. (1997). Vam2/vps41p and vam6/vps39p are components of a protein complex on the vacuolar membranes and involved in the vacuolar assembly in the yeast saccharomyces cerevisiae. *J Biol Chem*, 272(17):11344–9.

Nakamura, N., Yamamoto, A., Wada, Y., and Futai, M. (2000). Syntaxin 7 mediates endocytic trafficking to late endosomes. *Journal of Biological Chemistry*, 275(9):6523.

Neely, G. G., Hess, A., Costigan, M., Keene, A. C., Goulas, S., Langeslag, M., Griffin, R. S., Belfer, I., Dai, F., Smith, S. B., Diatchenko, L., Gupta, V., ping Xia, C., Amann, S., Kreitz, S., Heindl-Erdmann, C., Wolz, S., Ly, C. V., Arora, S., Sarangi, R., Dan, D., Novatchkova, M., Rosenzweig, M., Gibson, D. G., Truong, D., Schramek, D., Zoranovic, T., Cronin, S. J. F., Angjeli, B., Brune, K., Dietzl, G., Maixner, W., Meixner, A., Thomas, W., Pospisilik, J. A., Alenius, M., Kress, M., Subramaniam, S., Garrity, P. A., Bellen, H. J., Woolf, C. J., and Penninger, J. M. (2010a). A genome-wide drosophila screen for heat nociception identifies &alpha;2&delta;3 as an evolutionarily conserved pain gene. *Cell*, 143(4):628–638.

Neely, G. G., Kuba, K., Cammarato, A., Isobe, K., Amann, S., Zhang, L., Murata, M., Elmen, L., Gupta, V., Arora, S., Sarangi, R., Dan, D., Fujisawa, S., Usami, T., ping Xia, C., Keene, A. C., Alayari, N. N., Yamakawa, H., Elling, U., Berger, C., Novatchkova, M., Koglgruber, R., Fukuda, K., Nishina, H., Isobe, M., Pospisilik, J. A., Imai, Y., Pfeufer, A., Hicks, A. A., Pramstaller, P. P., Subramaniam, S., Kimura, A., Ocorr, K., Bodmer, R., and Penninger, J. M. (2010b). A global in vivo drosophila rnai screen identifies not3 as a conserved regulator of heart function. *Cell*, 141(1):142–153.

Nielsen, E., Christoforidis, S., Uttenweiler-Joseph, S., Miaczynska, M., Dewitte, F., Wilm, M., Hoflack, B., and Zerial, M. (2000). Rabenosyn-5, a novel rab5 effector, is complexed with hvps45 and recruited to endosomes through a fyve finger domain. *The Journal of cell biology*, 151(3):601.

Novak, A., Guo, C., Yang, W., Nagy, A., and Lobe, C. (2000). Z/eg, a double reporter mouse line that expresses enhanced green fluorescent protein upon cre-mediated excision. *genesis*, 28(3-4):147–155.

Ono, R., Nakajima, H., Ozaki, K., Kumagai, H., Kawashima, T., Taki, T., Kitamura, T., Hayashi, Y., and Nosaka, T. (2005). Dimerization of mll fusion proteins and flt3 activation synergize to induce multiple-lineage leukemogenesis. *Journal of Clinical Investigation*, 115(4):919–929.

Orphanides, G., Wu, W., Lane, W., Hampsey, M., and Reinberg, D. (1999). The chromatin-specific transcription elongation factor fact comprises human spt16 and ssrp1 proteins. *Nature*, 400(6741):284–288.

Palacios, R. and Steinmetz, M. (1985). Il3-dependent mouse clones that express b-220 surface antigen, contain ig genes in germ-line configuration, and generate b lymphocytes in vivo. *Cell*, 41(3):727–734.

Peplowska, K., Markgraf, D. F., Ostrowicz, C. W., Bange, G., and Ungermann, C. (2007). The corvet tethering complex interacts with the yeast rab5 homolog vps21 and is involved in endo-lysosomal biogenesis. *Developmental cell*, 12(5):739–50.

Pospisilik, J. A., Schramek, D., Schnidar, H., Cronin, S. J. F., Nehme, N. T., Zhang, X., Knauf, C., Cani, P. D., Aumayr, K., Todoric, J., Bayer, M., Haschemi, A., Puviindran, V., Tar, K., Orthofer, M., Neely, G. G., Dietzl, G., Manoukian, A., Funovics, M., Prager, G., Wagner, O., Ferrandon, D., Aberger, F., chung Hui, C., Esterbauer, H., and Penninger, J. M. (2010). Drosophila genome-wide obesity screen reveals hedgehog as a determinant of brown versus white adipose cell fate. *Cell*, 140(1):148–160.

Prekeris, R., Yang, B., Oorschot, V., Klumperman, J., and Scheller, R. (1999). Differential roles of syntaxin 7 and syntaxin 8 in endosomal trafficking. *Molecular Biology of the Cell*, 10(11):3891.

Pryor, P. R., Mullock, B. M., Bright, N. A., Lindsay, M. R., Gray, S. R., Richardson, S. C. W., Stewart, A., James, D. E., Piper, R. C., and Luzio, J. P. (2004). Combinatorial snare complexes with vamp7 or vamp8 define different late endocytic fusion events. *EMBO Rep*, 5(6):590–595.

Qiu, P., Pan, P., and Govind, S. (1998). A role for the drosophila toll/cactus pathway in larval hematopoiesis. *Development*, 125(10):1909.

Rehorn, K., Thelen, H., Michelson, A., and Reuter, R. (1996). A molecular aspect of hematopoiesis and endoderm development common to vertebrates and drosophila. *Development*, 122(12):4023.

Renneville, A., Roumier, C., Biggio, V., and Nibourel..., O. (2008). Cooperating gene mutations in acute myeloid leukemia: a review of the literature. *Leukemia*.

Reumer, A., Loy, T. V., and Schoofs, L. (2010). The complexity of drosophila innate immunity. *ISJ*, 7:32–44.

Richardson, S., Winistorfer, S., Poupon, V., Luzio, J., and Piper, R. (2004). Mammalian late vacuole protein sorting orthologues participate in early endosomal fusion and interact with the cytoskeleton. *Molecular Biology of the Cell*, 15(3):1197.

Rink, J., Ghigo, E., Kalaidzidis, Y., and Zerial, M. (2005). Rab conversion as a mechanism of progression from early to late endosomes. *Cell*, 122(5):735–749.

Rizki, T., Rizki, R., and Grell, E. (1980). A mutant affecting the crystal cells in drosophila melanogaster. *Wilhelm Roux's Archives of Developmental Biology*, 188(2):91–99.

Rubin, G., Yandell, M., Wortman, J., Miklos, G. G., Nelson, C., Hariharan, I., Fortini, M., Li, P., Apweiler, R., and Fleischmann, W. (2000). Comparative genomics of the eukaryotes. *Science*, 287(5461):2204.

Schindler, J. W., Buren, D. V., Foudi, A., Krejci, O., Qin, J., Orkin, S. H., and Hock, H. (2009). Tel-aml1 corrupts hematopoietic stem cells to persist in the bone marrow and initiate leukemia. *Stem Cell*, 5(1):43–53.

Sevrioukov, E. A., He, J. P., Moghrabi, N., Sunio, A., and Krämer, H. (1999). A role for the deep orange and carnation eye color genes in lysosomal delivery in drosophila. *Molecular Cell*, 4(4):479–86.

Shirakata, M., Hüppi, K., Usuda, S., Okazaki, K., Yoshida, K., and Sakano, H. (1991). Hmg1-related dna-binding protein isolated with v-(d)-j recombination signal probes. *Mol Cell Biol*, 11(9):4528–36.

Shrestha, R. and Gateff, E. (1982). Ultrastructure and cytochemistry of the cell types in the larval hematopoietic organs and hemolymph of drosophila melanogaster. *Development, Growth & Differentiation*, 24(1):65–82.

Silverman, N. and Maniatis, T. (2001). Nf-Îºb signaling pathways in mammalian and insect innate immunity. *Genes & Development*, 15(18):2321.

Simonsen, A., Lippe, R., Christoforidis, S., Gaullier, J., Brech, A., Callaghan, J., Toh, B., Murphy, C., Zerial, M., and Stenmark, H. (1998). Eea1 links pi (3) k function to rab5 regulation of endosome fusion. *Nature*, 394(6692):494–498.

Sorkin, A. and Zastrow, M. V. (2009). Endocytosis and signalling: intertwining molecular networks. *Nat Rev Mol Cell Biol*, 10(9):609–622.

Spencer, J., Baron, M., and Olson, E. (1999). Cooperative transcriptional activation by serum response factor and the high mobility group protein ssrp1. *Journal of Biological Chemistry*, 274(22):15686.

Stenmark, H. (2009). Rab gtpases as coordinators of vesicle traffic. *Nat Rev Mol Cell Biol*, 10(8):513–25.

Stenmark, H., Parton, R., Steele-Mortimer, O., Lütcke, A., Gruenberg, J., and Zerial, M. (1994). Inhibition of rab5 gtpase activity stimulates membrane fusion in endocytosis. *The EMBO Journal*, 13(6):1287.

Strömberg, S., Agnarsdóttir, M., Magnusson, K., Rexhepaj, E., Bolander, Å., Lundberg, E., Asplund, A., Ryan, D., Rafferty, M., and Gallagher, W. (2009). Selective expression of syntaxin-7 protein in benign melanocytes and malignant melanoma. *Journal of proteome research*, 8(4):1639–1646.

Suzuki, T., Oiso, N., Gautam, R., Novak, E., Panthier, J., Suprabha, P., Vida, T., Swank, R., and Spritz, R. (2003). The mouse organellar biogenesis mutant buff results from a mutation in vps33a, a homologue of yeast vps33 and drosophila carnation. *Proceedings of the National Academy of Sciences of the United States of America*, 100(3):1146.

Takagaki, Y. and Manley, J. (2000). Complex protein interactions within the human polyadenylation machinery identify a novel component. *Molecular and cellular biology*, 20(5):1515.

Tan, B. C.-M., Chien, C.-T., Hirose, S., and Lee, S.-C. (2006). Functional cooperation between fact and mcm helicase facilitates initiation of chromatin dna replication. *EMBO J*, 25(17):3975–3985.

Tavian, M., Biasch, K., Sinka, L., Vallet, J., and Péault, B. (2010). Embryonic origin of human hematopoiesis. *Int. J. Dev. Biol*, 54:1061–1065.

Teng, F., Wang, Y., and Tang, B. (2001). The syntaxins. *Genome Biol*, 2(11).

Tepass, U., Fessler, L., Aziz, A., and Hartenstein, V. (1994). Embryonic origin of hemocytes and their relationship to cell death in drosophila. *Development*, 120(7):1829.

Toney, J., Donahue, B., Kellett, P., Bruhn, S., Essigmann, J., and Lippard, S. (1989). Isolation of cdnas encoding a human protein that binds selectively to dna modified by the anticancer drug cis-diamminedichloroplatinum (ii). *Proceedings of the National Academy of Sciences of the United States of America*, 86(21):8328.

Tsang, A., Visvader, J., Turner, C., and Fujiwara..., Y. (1997). Fog, a multitype zinc finger protein, acts as a cofactor for transcription factor gata-1 in erythroid and megakaryocytic differentiation. *Cell*.

Ullrich, O., Horiuchi, H., Bucci, C., and Zerial, M. (1994). Membrane association of rab5 mediated by gdp-dissociation inhibitor and accompanied by gdp/gtp exchange.

Waltzer, L., Bataillé, L., Peyrefitte, S., and Haenlin, M. (2002). Two isoforms of serpent containing either one or two gata zinc fingers have different roles in drosophila haematopoiesis. *EMBO J*, 21(20):5477–5486.

Waltzer, L., Gobert, V., Osman, D., and Haenlin, M. (2010). Transcription factor interplay during drosophila haematopoiesis. *Int. J. Dev. Biol.*, 54(6-7):1107–1115.

Williams, M. (2007). Drosophila hemopoiesis and cellular immunity. *The journal of immunology*, 178(8):4711.

Wong, E. T. and Tergaonkar, V. (2009). Roles of nf-kappab in health and disease: mechanisms and therapeutic potential. *Clin Sci*, 116(6):451–65.

Wong, S., Xu, Y., Zhang, T., and Hong, W. (1998). Syntaxin 7, a novel syntaxin member associated with the early endosomal compartment. *Journal of Biological Chemistry*, 273(1):375.

Wood, W. and Jacinto, A. (2007). Drosophila melanogaster embryonic haemocytes: masters of multitasking. *Nat Rev Mol Cell Biol*, 8(7):542–551.

Wu, C., Orozco, C., Boyer, J., Leglise, M., Goodale, J., Batalov, S., Hodge, C. L., Haase, J., Janes, J., Huss, J. W., and Su, A. I. (2009). Biogps: an extensible and customizable portal for querying and organizing gene annotation resources. *Genome Biol*, 10(11):R130.

Xing, H., Mayhew, C., Cullen, K., Park-Sarge, O., and Sarge, K. (2004). Hsf1 modulation of hsp70 mrna polyadenylation via interaction with symplekin. *Journal of Biological Chemistry*, 279(11):10551.

Yuan, Y., Zhou, L., Miyamoto, T., Iwasaki, H., Harakawa, N., Hetherington, C., Burel, S., Lagasse, E., Weissman, I., and Akashi, K. (2001). Aml1-eto expression is directly involved in the development of acute myeloid leukemia in the presence of additional mutations. *Proceedings of the National Academy of Sciences of the United States of America*, 98(18):10398.

Zastrow, M. V. and Sorkin, A. (2007). Signaling on the endocytic pathway. *Current opinion in cell biology*, 19(4):436–45.

Zeng, S. X., Dai, M.-S., Keller, D. M., and Lu, H. (2002a). Ssrp1 functions as a co-activator of the transcriptional activator p63. *EMBO J*, 21(20):5487–97.

Zeng, Y., Wagner, E. J., and Cullen, B. R. (2002b). Both natural and designed micro rnas can inhibit the expression of cognate mrnas when expressed in human cells. *Mol Cell*, 9(6):1327–33.

Zuber, J., Radtke, I., Pardee, T. S., Zhao, Z., Rappaport, A. R., Luo, W., Mccurrach, M. E., Yang, M.-M., Dolan, M. E., Kogan, S. C., Downing, J. R., and Lowe, S. W. (2009). Mouse models of human aml accurately predict chemotherapy response. *Genes & Development*, 23(7):877–889.

# Curriculum Vitae

## Personal Information

| | |
|---|---|
| NAME | Marie-Theres Tazreiter |
| ADDRESS | Marktgasse 8-10/1/12 |
| | A-1090 Vienna |
| PHONE | (+43) 650 42 1 42 66 |
| E-MAIL | marie.tazreiter@gmail.com |
| NATIONALITY | Austria |
| DATE OF BIRTH | 31/03/1987 |
| PLACE OF BIRTH | Klagenfurt, Austria |

## Education

| | |
|---|---|
| OCTOBER 2005 - APRIL 2011 | Study of Molecular Biology (Master Degree) University of Vienna, Austria |
| JUNE 2005 | High-school graduation (passed with honors) |
| 1997 - 2005 | High School BG/BRG St. Martin, Villach, Austria |
| 1993 - 1997 | Primary School Hermagor and Villach, Austria |

# Research experience

| | |
|---|---|
| OCT 2010 - MARCH 2011 | Technical Assistant<br>Prof. Dr. Josef Penninger<br>IMBA – Institute of Molecular Biotechnology<br>GmbH Austrian Academy of Science<br>Vienna, Austria |
| OCT 2009 - SEP 2010 | Diploma Thesis<br>Prof. Dr. Josef Penninger<br>IMBA – Institute of Molecular Biotechnology<br>GmbH Austrian Academy of Science<br>Vienna, Austria |
| MARCH 2009 - JUNE 2009 | Internship<br>"The role of PTEN, CK2 and the PI3K/Akt pathway in B cell acute lymphoblastic leukemia"<br>Cancer Biology Unit - João Taborda Barata<br>Instituto de Medicina Molecular<br>Lisbon, Portugal |
| OCT 2008 - FEB 2009 | Internship<br>"The Role of RANK in the Development and Maintenance of Central Tolerance"<br>Prof. Dr. Josef Penninger<br>IMBA – Institute of Molecular Biotechnology<br>GmbH Austrian Academy of Science<br>Vienna, Austria |
| JULY AND AUGUST 2008 | Internship<br>"The $\gamma$-Secretase and Alzheimer Disease - Towards Elucidation of the Protein Structure"<br>Bing K. Jap<br>Lawrence Berkeley National Laboratories<br>Berkeley, California, USA |